The temperature dependence of magnetostriction in a nickel crystal

Hunt, Geoffrey H.

THE TEMPERATURE DEPENDENCE OF MAGNETOSTRICTION IN A NICKEL CRYSTAL

by

GEOFFREY H. HUNT, B.Sc.

An account of work carried out at the Science Laboratories of the Durham Colleges in the University of Durham during the period 1951-1954.

Submitted in candidature for the degree of Doctor of Philosophy of the University of Durham.

PREFACE.

This thesis describes an investigation of the longitudinal magnetostriction of a single crystal of nickel over the temperature range - 180° C. to 360° C. The most important measurement to be made at any temperature was of the saturation magnetostriction, but there is considerable interest in measuring the strain at different stages in the magnetization process, and this has been done at several temperatures.

Measurements have been confined to two ellipsoidal specimens cut from the same crystal of nickel with their major axes along cube edge and cube diagonal crystallographic directions.

Part 1 of the thesis describes the background to the work. The development of the theory of ferromagnetism is outlined, and the subject of magnetostriction introduced. Previous magnetostriction measurements, particularly on single crystals of nickel, are discussed.

Part 2 surveys the apparatus used by previous workers for measuring magnetostriction over a range of temperatures, and discusses the design most suitable for the present investigation. Sections 2.3 to 2.7 describe in detail the apparatus used for the high temperature measurements, and section 2.10 the modifications which were necessary for use below room temperature. The preparation of the specimens from the single crystal is described in section 2.8.

In Part 3 the results are presented, and their significance is discussed in relation to theories of the magnetization process.

ACKNOWLEDGMENTS.

The author wishes to thank Dr. W.D. Corner who suggested the problem, and who continually gave invaluable advice and encouragement while acting as research supervisor.

He is indebted to Professor J.E.P. Wagstaff and the staff of the Physics Department of the Durham Colleges for the facilities and advice received during the course of the work; also to Mr. R. Phillips of the Geology Department for assistance with the X-ray crystallography.

He thanks Dr. R.S. Tebble and Mr. R.F. Pearson of the Physics Department of the University of Leeds for the provision of the nickel crystals, and the Mond Nickel Company for the crystal analysis.

He gratefully acknowledges the following awards:- Durham Colleges Research Studentship (1951), British Association 1949 Trust Research Studentship (1953), Ministry of Education Supplemental Award (1953), and a grant from the Durham Colleges Research Fund for the purchase of equipment.

CONTENTS.

PART 1.

BACKGROUND

1.1 INTRODUCTION.

The first measurements of the change in dimensions of a body when magnetized are those recorded in Joule's paper of 1847. He noted a change in length of an iron rod by using mechanical levers and a microscope, but additional experiments to measure the change in volume of the iron were unsuccessful. The closing years of the nineteenth century saw a large number of independent investigations of the various magnetostriction effects, but the results were difficult to correlate due to the large and diverse effects produced by different heat and strain treatments and by impurities. Various inter-related effects were also found, the most important of which are the Villari effect, being the change in magnetization produced by a longitudinal stress, and the change in Young's modulus with magnetization. Before dealing in detail with magnetostrictive effects, however, it is advisable to review briefly the general theory of ferromagnetism in order that the significance of magnetostrictive measurements may be indicated. The review is not comprehensive, as several modern text-books deal adequately with the subject, and for references to recent work the excellent review articles by Stoner (1948, 1950) may be consulted. It is unfortunate that Stoner's reviews do not cover magneto-strictive and allied effects, although a brief introduction

to the subject is provided by Lee (1953), and a consideration of the energies involved in magnetization and magnetostriction processes is given by Kittel, (1949).

1.2 THEORY OF FERROMAGNETISM.

The present position of the theory of ferromagnetism is generally satisfactory in that the majority of the phenomena which are exhibited by ferromagnetic materials can be explained in a qualitative manner; moreover, the theories developed could probably explain quantitatively most of these phenomena if it were possible to solve rigorously the mathematical theory involved.

All the modern theories of ferromagnetism have their basis in a theory published in 1907 by Weiss. This developed the Langevin (1905) theory of paramagnetism by postulating a molecular field acting on the elementary magnets of the medium and proportional to the intensity of magnetization. Langevin had shown that if the orientation of a molecular dipole of magnetic moment μ in a field H is governed by the Boltzmann distribution law, then the moment per unit volume is

$$I = n\mu L\left(\mu H/kT\right) \qquad (1)$$

where $L(x) = \coth x - 1/x$

and n is the number of molecules per unit volume.

With the addition of the Weiss molecular field qI, equation 1 becomes

$$I = n\mu L(\mu \overline{H+qI}/kT) \qquad (2)$$

where q is a factor of proportionality.

Making the approximation $L(x) = 1/3x$ for small values of x, then equation 2 becomes

$$\chi = I/H = n\mu^2/3k(T-T_c) \qquad (3)$$

where T_c is the Curie temperature $n\mu^2 q/3k$.

For temperatures below T_c, equation 3 cannot hold, and the approximation $L(x) = 1/3x$ must be discarded. The susceptibility χ is then no longer constant, and magnetization is present without applied fields. Equation 2 must therefore be solved for I in terms of T by numerical methods, and it is convenient to use reduced units for magnetization and temperature

$$\zeta = I/n\mu \qquad \tau = T/T_c$$

$n\mu$ being the saturation intensity at absolute zero.

Using these units the Weiss theory predicts a universal law connecting ζ and τ which should apply to all ferromagnetics below the Curie point, provided the values of I considered are in fields such that H is negligible compared with the molecular field qI.

The Weiss theory accounts in a very simple way for two

of the most important characteristics of ferromagnetics. The first of these is the linear relationship between T and $1/\chi$ above the Curie point predicted by equation 3. This relationship is very accurate for high temperatures, but near the Curie point the experimental curve falls away from linearity to a lower critical temperature than is provided by extrapolation of the linear section of the graph.

The second characteristic which is readily accounted for is the relationship between saturation magnetization and temperature below the Curie point which for all ferromagnetics follows fairly closely the law predicted using the reduced units, usually known as the law of corresponding states. However, to obtain agreement with experiment it is always necessary to use saturation magnetization figures, and the postulation of the Weiss internal field does not explain why high magnetic intensities are not always obtained in very small applied fields. To explain the familiar hysteresis loops obtained with ferromagnetics, Weiss was obliged to postulate further the division of the ferromagnetic material into small sections magnetized in different directions, there being a random distribution of directions of magnetization in a properly demagnetized specimen with no applied magnetic field. The small sections were at one time supposed to be microcrystals,

but due to the development of the Bitter pattern technique, it is now known that crystals are usually subdivided into sections magnetized in different directions, these sections being known as domains.

Weiss' theory was thus eminently satisfactory except that it could not explain on the basis of classical physics the rather arbitrary assumption of a molecular field proportional to the intensity of magnetization, upon which the whole theory rested. No satisfactory mechanism for the origin of this field was advanced until 1928 when Heisenberg showed that it could be due to electron exchange forces of a quantum mechanical nature. These forces cannot be described in classical terms, as they are due to the effect of overlapping of the wave functions of electrons in orbits of adjacent atoms. Since the orbital motion is related to the spin alignment of the electrons, these forces appear as spin-spin coupling between atoms, although in point of fact they are not due to the magnetic moments of the electron spins. The fact that electron spins and not orbital electron motion are mainly responsible for ferromagnetism was indicated in 1926 when it was calculated on the basis of quantum mechanics that electron spins would give a gyromagnetic ratio of 2, while orbital electrons gave a ratio of 1. Experimental work had shown ratios of about 1.95, and the difference from 2 is sufficiently significant

to show that orbital motion plays a small part.

A further modification to the Weiss theory was introduced by quantum considerations, namely the replacement of a continuous distribution of orientations by a series of discrete positions. This had the effect of changing slightly the form of the relation between ζ and τ, and if it is assumed that there is only one free spin per atom, good agreement is found with experimental results, although the deviations are still significant.

The Heisenberg exchange forces are most easily expressed in the form of the potential energy due to the interaction of the two atoms,

$$V_{ij} = -2 J_{ij} \underline{S_i} . \underline{S_j} \qquad (4)$$

where J_{ij} is the exchange integral connecting atoms i and j, and $\underline{S_i}$ is the spin angular momentum vector of i, in units of $h/2\pi$. These forces are only of very short range, and for a lattice of atoms it is customary to consider only nearest neighbours, but even with this assumption the calculation of magnetic susceptibilities due to exchange forces is in general impossible. Simplified or ideal cases have to be considered, and two approaches to the problem of the ferromagnetic lattice have been made. Heisenberg's model consists of a lattice of atoms, each atom with its own electron orbits, and assumes that all states having the same resultant

spin for the whole crystal have the same resultant energy. The collective electron model developed in particular by Stoner (1933) assumes that the 3d electrons circulate throughout the lattice, and in order to develop the theory mathematically a particular shape has to be ascribed to the electron bands in the metal. Both these models are clearly very different from an actual ferromagnetic, but they do nevertheless enable certain results to be derived which can be correlated with experimental results. The Heisenberg model must be further developed to account for the fact that the saturation intensity at absolute zero is not an integral number of Bohr magnetons, while the Stoner model allows for non-integral values automatically. Mention should also be made of the fluctuation theory developed by Néel (1932) who considered the effects on the Heisenberg model due to fluctuations in the local intensity of magnetization at points in the lattice. The results are encouraging, and suggest that it is dangerous to consider only interactions between nearest neighbours.

Ferromagnetism depends on the alignment of the magnetic moments in the same direction, and in order that a material should exhibit ferromagnetism the exchange integral J must be positive. It is unfortunately impossible to calculate this integral theoretically, and even if the calculations could be performed for free atoms, their introduction into a lattice

would certainly distort the d electron orbits and make the result invalid. It seems from rough estimations and from calculations of the lattice spacing of the ferromagnetics that the exchange integral is positive only if the atomic separation is greater than $1\frac{1}{2}$ times the diameter of the unfilled shell. By considering various lattices it has been shown, particularly by Weiss (1948), that not all types of lattice can be ferromagnetic, even with positive exchange integrals.

1.3 SINGLE CRYSTALS.

Having surveyed the theories of intrinsic magnetization, it is possible to consider the variation of apparent magnetization with field. Attention will be confined to single crystal specimens, which are naturally to be preferred to polycrystalline for most fundamental investigations. The magnetization curves of a single crystal of nickel are shown in Fig. (1), and the different curves indicate that the magnetization forces are not isotropic. Anisotropy in the crystal is such that the magnetization tends to be directed along the easy [111] axes in the crystal,* and it requires considerably more energy to magnetize along the

* In this thesis, unless otherwise stated, a [111] axis is to be understood as any axis of the type [111], and similarly for other types of axis.

[100] or hard directions. Before considering the anisotropy further, the correlation of the magnetization curve shown with domain theory may be noted. In an unmagnetized nickel crystal the domains may be supposed magnetized each along one of the eight easy directions corresponding to the cube diagonals, the net magnetization in any one direction being zero. In small fields the directions change to that nearest the field direction. Thus for magnetization in the [111], [110], and [100] directions, in small fields the resultant magnetization should be I_s, $I_s\sqrt{2}/\sqrt{3}$, and $I_s/\sqrt{3}$ respectively, where I_s is the saturation magnetization. These values are in reasonable agreement with the sharp bends found in the experimental magnetization curve. Further magnetization is due to rotation of the domain directions towards the direction of the applied field against the anistropy forces.

Anistropy is exhibited by the other ferromagnetic elements; for iron the easy direction is the [100] and the hardest direction the [111], while for cobalt the easy direction is the hexagonal axis.

A theoretical analysis of the second stage of the I-H curve on the basis of the Heisenberg model shows fair agreement with experimental results. Better agreement is possible with the assumption of random distortions in the crystal (see Bitter, 1937, p.236). These distortions

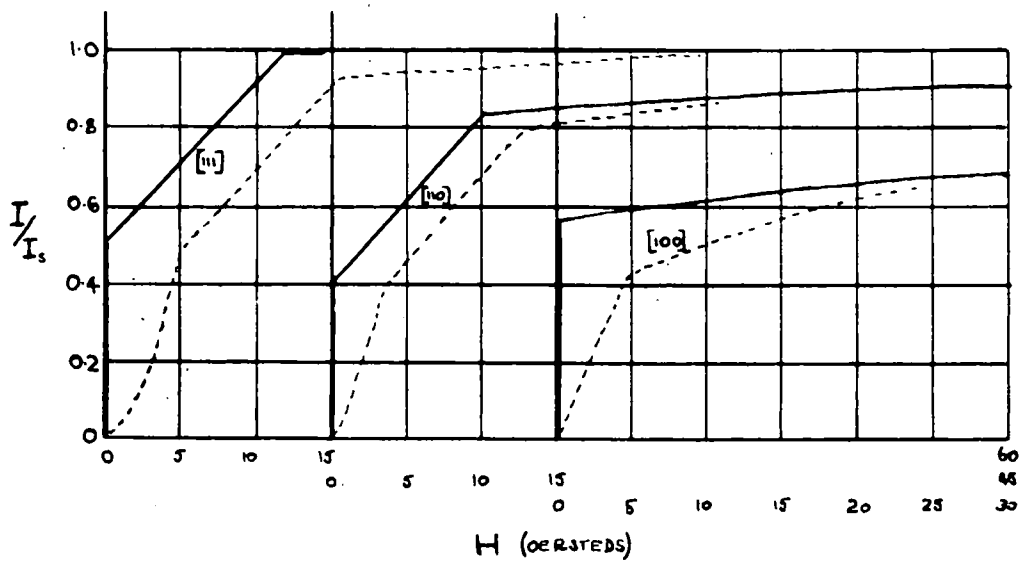

FIG.1. - Magnetization Curves of Randomly Distorted Nickel Crystals. Dotted lines are experimental results by Kaya.

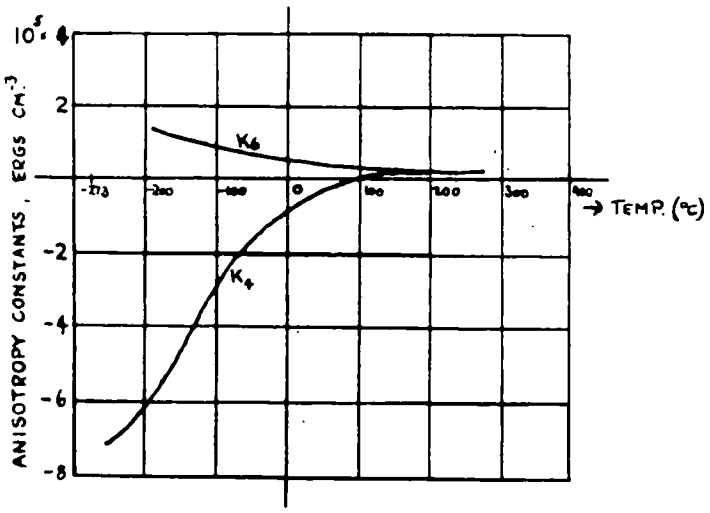

FIG.2. - Dependence of Anisotropy Constants of Nickel on Temperature (Various workers).

prevent saturation being reached in zero field along the easy direction as they form a potential barrier between orientations along the four separate directions of easy magnetization. The point at which saturation is reached is dependent on the strain, and the experimental points fit the theory best for a strain which produces an energy barrier of 6000 ergs per c.c. For directions of magnetization other than the [100], the theory predicts two sharp corners in the magnetization curve, and the agreement with experiment is reasonable, as shown in the figure, the experimental curves being those of Kaya (1928).

As has been shown by Néel (1944) and later by Lawton and Stewart (1948), the shape and orientation of the specimen must have a considerable effect on the magnetization curve. For specimens in which the field is not applied along an axis of symmetry, the problem is very difficult. Solutions have been worked out in a few simple cases, such as spheroids and long rods, with the applied field along the axis of rotation, and the results when compared with experimental results are encouraging.

Analysis of the magnetization curves of single crystals is usually carried out by considering the differences in energy required to magnetize the crystal in different directions. For cubic crystals the anisotropy energy per unit volume may be expressed in terms of the direction

cosines α_1, α_2, and α_3 relative to the cube edges as coordinate axes, and it may be shown by consideration of the symmetry of a cubic lattice that the lowest order terms possible are of the fourth degree. It is usually sufficient to express the energy by the two terms

$$F = K_4 (\alpha_1^2\alpha_2^2 + \alpha_2^2\alpha_3^2 + \alpha_3^2\alpha_1^2) + K_6 \alpha_1^2\alpha_2^2\alpha_3^2 \qquad (5)$$

The temperature dependence of these constants for Nickel is shown in Fig. (2), and it can be seen that K_4 changes sign near 100° C., indicating that the easy direction changes from [111] to [100].

Although the anisotropy has been correlated with different experimental results quite easily, it yet remains obscure in its origin. The Heisenberg exchange energy does not give anisotropy, and classical dipole moment interaction gives values about three orders of magnitude too small. It can only be surmised that spin-orbit coupling produces the anisotropy by effectively coupling the spins of adjacent atoms through the ordinary orbit coupling. The orbits are bound to the lattice directions by means of electrostatic fields and overlapping wave functions, consequently the spins tend to be bound to the crystal structure.

1.4 MAGNETOSTRICTION.

In considering the topic of magnetostriction, it must first be emphasized that this phenomenon is intimately connected with most of the other important aspects of ferromagnetism, for example domain configuration, magnetization curves, anisotropy and thermal effects. It may in fact be linked theoretically with the strain variation of the anisotropy constants, and as is shown very clearly by Kittel, (1949), magnetostriction only occurs because the anisotropy energy depends on the strain in such a way that the stable state of the crystal is deformed with respect to the original crystal lattice.

The Joule magnetostriction, the change in length of a ferromagnetic substance, is usually of the order of a few parts per million, and it normally reaches a limiting value corresponding to the saturation of magnetic intensity. There is also a transverse effect of opposite sign to the longitudinal Joule effect, and a volume effect which is of rather smaller order of magnitude. The smallness of these effects is such that the earlier workers were obliged to use large specimens in order to obtain results of reasonable accuracy, most of the earlier measurements using optical and mechanical lever devices. Modern electrical techniques have allowed greater accuracy to be obtained, in particular with small specimens. The development of experimental technique will be reviewed later.

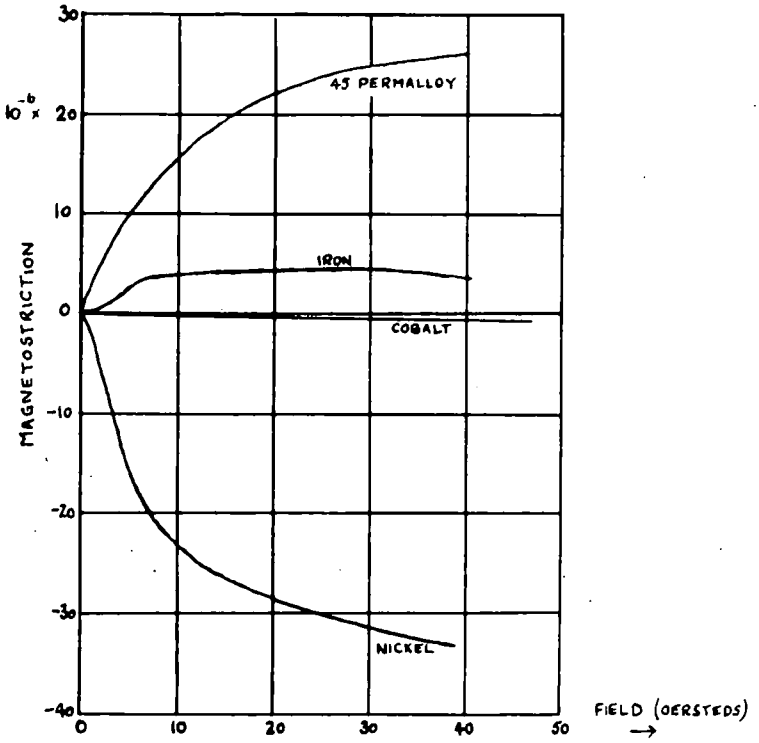

FIG. 3. - Magnetostriction of Polycrystalline Materials in Moderate Fields

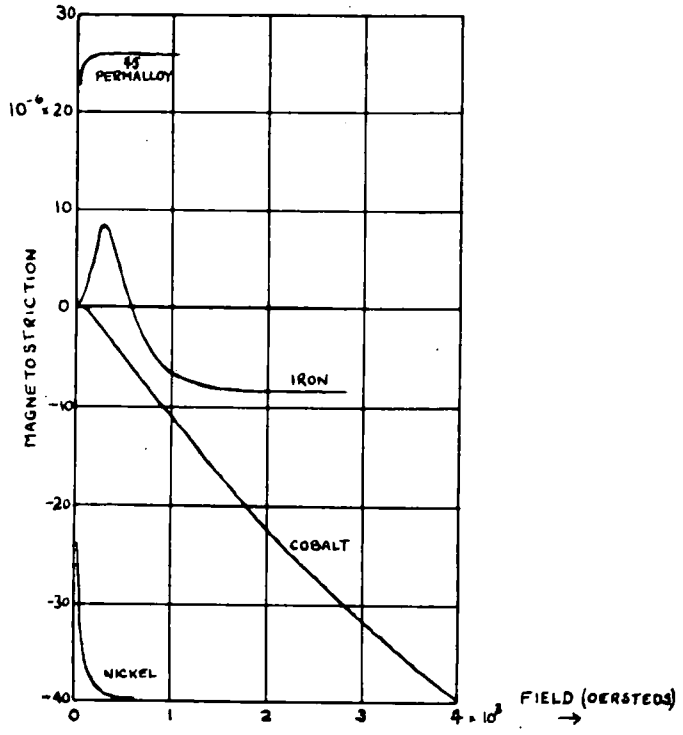

FIG. 4. - Magnetostriction of Polycrystalline Materials in High Fields

The Joule magnetostriction is difficult to account for theoretically since it has completely different characteristics for the three common ferromagnetic metals. Figures (3) and (4) show the effects for polycrystalline materials; the curve for iron at high field strengths is particularly noticeable. Very little change in length occurs at the initial part of the magnetization curve, but when the increase in field causes domain rotation the magnetostrictive effect is large. At high fields corresponding to magnetic saturation there is a small magnetostrictive effect corresponding to the change in intrinsic magnetization.

The curves shown are those for room temperature measurements. Very few experiments have been carried out at other temperatures, but these usually show a progressive decrease of magnetostriction with increasing temperature until at the Curie Point the effect is zero.

The magnetostrictive effects in single crystals are naturally much more suitable for theoretical analysis than those in polycrystalline specimens. The growth of large metallic single crystals is a relatively recent achievement, and it was not until 1925 that Webster carried out magnetostrictive measurements on single crystals of iron. The first experiments on nickel were those reported by Masiyama in 1928, and they showed that the change in length in the direction of the magnetization is always negative, in

contrast to the curves for iron, which showed differences in sign for different crystallographic directions.

Since that time measurements have been made on a range of different alloys, but the results, although of considerable interest in the development of alloys for technical purposes, do not really add a great deal to the knowledge of the fundamental mechanism of magnetostriction.

Shortly after the first measurements of single crystal magnetostriction had been made, an analysis was made by Akulov (1928) of the saturation magnetostriction in cubic crystals. This was later extended (see, e.g. Becker and Döring, 1939) so that the magnetostriction in any direction could be expressed in terms of five constants. The theory does not connect magnetostriction measurements with any other experimentally found values, but merely invokes the laws of crystal symmetry to analyse the results themselves. The change in length per unit length between the undeformed state and the saturation state is found to be

$$\left(\frac{\Delta l}{l}\right)_{SAT} = \lambda = h_1\left(\alpha_1^2\beta_1^2 + \alpha_2^2\beta_2^2 + \alpha_3^2\beta_3^2 - \tfrac{1}{3}\right) + 2h_2\left(\alpha_1\alpha_2\beta_1\beta_2 + \alpha_2\alpha_3\beta_2\beta_3 + \alpha_3\alpha_1\beta_3\beta_1\right)$$

$$+ h_4\left(\alpha_1^4\beta_1^2 + \alpha_2^4\beta_2^2 + \alpha_3^4\beta_3^2 + \frac{2S}{3} - \frac{1}{3}\right)$$

$$+ 2h_5\left(\alpha_1\alpha_2\alpha_3^2\beta_1\beta_2 + \alpha_2\alpha_3\alpha_1^2\beta_2\beta_3 + \alpha_3\alpha_1\alpha_2^2\beta_3\beta_1\right) \qquad (6)$$

$$+ h_3\left(S - \tfrac{1}{3}\right) \text{ for nickel} \qquad + h_3 S \text{ for iron}$$

where the h's are constants for a particular temperature, and

$$s = \alpha_1^2\alpha_2^2 + \alpha_2^2\alpha_3^2 + \alpha_3^2\alpha_1^2$$

The α's are the direction cosines of the magnetization with respect to the crystal axes, the β's the direction cosines of the direction in which the change in length is measured.

The fractional change in volume is then

$$w = 3h_3(s-1/3) \text{ for nickel, and} \qquad (7)$$

$$w = 3h_3 s \text{ for iron} \qquad (7a)$$

Normally h_3 is taken to be zero, corresponding to zero volume change. For a high proportion of the data, it is sufficiently accurate to express λ as a function of h_1 and h_2 only, neglecting the terms containing h_4 and h_5. Then if λ_{100} and λ_{111} are the saturation magnetostriction in the [100] and [111] directions, it follows that

$$\lambda = \frac{3}{2}\lambda_{100}\left(\alpha_1^2\beta_1^2 + \alpha_2^2\beta_2^2 + \alpha_3^2\beta_3^2 - 1/3\right) + 3\lambda_{111}\left(\alpha_1\alpha_2\beta_1\beta_2 + \alpha_2\alpha_3\beta_2\beta_3 + \alpha_3\alpha_1\beta_3\beta_1\right) \qquad (8)$$

since for a demagnetized specimen with randomly orientated domains it may be shown that there is no change in overall dimensions from the undistorted lattice.

These equations fit remarkably well the experimental data found by a number of workers. For example, using Masiyama's data for nickel (1928), the values of the constants were found to be

$$h_1 = -24 \times 10^{-6},\ h_2 = -47 \times 10^{-6},\ h_4 = -51 \times 10^{-6},\ h_5 = 52 \times 10^{-6}$$

it being assumed that h_3 was zero

This analysis is concerned solely with saturation magnetostriction constants. By using the Heisenberg model of a ferromagnetic in which the distribution of domain directions is governed by a probability distribution, it is possible to calculate the magnetostriction in cubic crystals as a function of the magnetization. The theory has been reproduced by Fowler (1936), and only a summary of his treatment will be given here. The length changes are assumed to be due to the rotation of the magnetization direction of domains, each domain being magnetized to saturation and therefore having a deformed lattice structure. The symmetry conditions embodied in equation (8) still hold, so that by consideration only of the number of domains of different orientations corresponding to particular values of the bulk magnetization, the distortion of the whole crystal may be calculated. Using the distribution of domains given by Heisenberg's theory, the following results may be derived for nickel.

In the [111] direction, magnetization proceeds to saturation in very low fields, and the theory shows

$$\frac{\Delta l}{l} = \lambda_{111} \frac{I^2}{I_s^2} \qquad (9)$$

For the [100] direction there is no magnetostriction before the knee of the curve corresponding to $\frac{I}{I_s} = \frac{1}{\sqrt{3}}$. After the knee

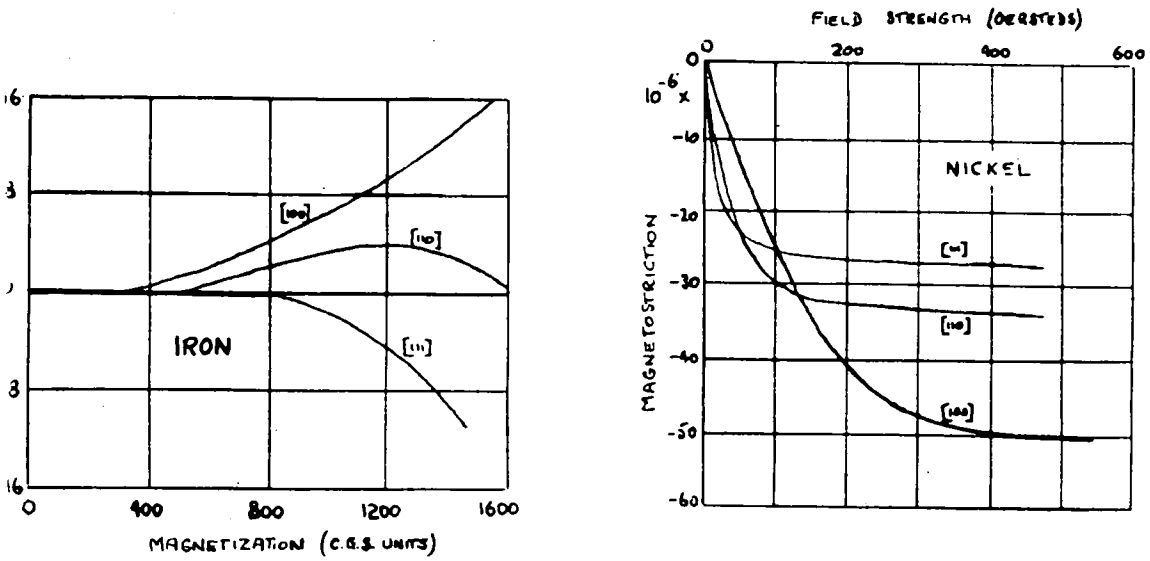

FIG.5. - Longitudinal Magnetostriction of Single Crystals.

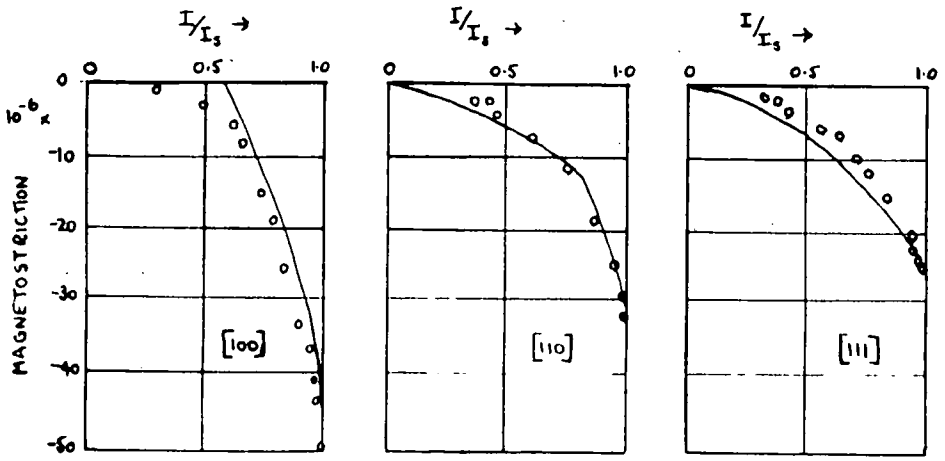

FIG.6. - Magnetostriction of Nickel Crystal calculated from Heisenberg Theory.

$$\frac{\Delta l}{l} = \lambda_{100}\left(\frac{3}{2}\frac{I^2}{I_s^2} - \frac{1}{2}\right) \qquad (10)$$

In the [110] direction there is domain rotation before and after the knee of the curve which corresponds to $\frac{I}{I_s} = \frac{\sqrt{2}}{\sqrt{3}}$. The results derived are

$$\frac{\Delta l}{l} = \frac{3}{4}\lambda_{111}\frac{I^2}{I_s^2} \qquad \left(0 \leqslant \frac{I^2}{I_s^2} \leqslant \frac{2}{3}\right)$$

$$\frac{\Delta l}{l} = \lambda_{100}\left(\frac{3}{4}\frac{I^2}{I_s^2} - \frac{1}{2}\right) + \frac{3}{4}\lambda_{111}\frac{I^2}{I_s^2} \qquad \left(\frac{2}{3} \leqslant \frac{I^2}{I_s^2} \leqslant 1\right) \qquad (11)$$

The experimental results of Masiyama (1928) are best fitted to these equations by putting $\lambda_{111} = -2.7 \times 10^{-5}$, $\lambda_{100} = -5.1 \times 10^{-5}$. The general agreement is then fair, as shown in figure (6), but the sharp changes of gradient predicted by theory are not found, just as they are absent in the I-H curves.

It has been stated already that the h_3 term in equation (6) is usually made zero, corresponding to zero volume change as shown by equations (7) and (7a). This is justifiable in low fields where changes in magnetization and magnetostriction are brought about by domain boundary movements and rotations, but above the point of "technical saturation" there is a volume increase corresponding to the increase in domain magnetization. This volume change is isotropic, and being dependent on the alignment of the spins against thermal forces it is very temperature sensitive. The effect of

applied fields is usually small, since such fields are usually small compared with the Weiss molecular field. The volume change can be observed directly by cooling a specimen through the Curie temperature, when an anomalous coefficient of thermal expansion is found, corresponding to the change in lattice spacing brought about by the formation of spontaneous magnetization.

Mention should be made of the magneto-caloric effect, which is the increase in temperature of ferromagnetic specimens caused by application of magnetic fields, since this also produces a corresponding increase in length of the specimen. The effect has been investigated experimentally by Weiss and Forrer (1926) who used polycrystalline specimens of nickel, and their results show that the maximum temperature increase produced by application of magnetic fields occurs near the Curie temperature. They show that at this temperature (356° C.) an applied field of 3000 oersteds causes an increase in temperature of 0.3° C. At lower temperatures the effect soon falls off; by 345° C. it has dropped to 0.15° C., and by 300° C. to 0.05° C. As a first approximation the temperature increase at a certain temperature is proportional to the applied field.

A further effect which must be taken into account when analysing experimental results is that due to the shape of the specimen. This has not always been allowed for in experimental work, and may account for some of the

discrepancies between the results of different workers. It is due to the change in dimensions of the specimen producing a change in the demagnetizing factor which causes also a change in the energy associated with the demagnetizing field. The effect has been analysed theoretically by a number of workers, and Becker's results for a particular case are given below.

For a prolate spheroid magnetized parallel to its major axis the magnetostriction is increased in the longitudinal effect by an amount:

$$\frac{1}{2} I^2 N \left(\frac{1}{3k} + \frac{a}{2G} \right)$$

in the transverse effect by:

$$\frac{1}{2} I^2 N \left(\frac{1}{3k} - \frac{a}{4G} \right)$$

and in the volume effect by:

$$\frac{1}{2} I^2 N . \frac{1}{k} \qquad (12)$$

where k is the compressibility, G the torsional modulus, N the demagnetizing factor, and a a constant given by

$$a = \frac{3-e^2}{e^2} - \frac{4\pi}{N} \left(\frac{1-e^2}{e^2} \right)$$

e being the eccentricity.

It has recently been shown by Brown (1953) that a uniformly magnetized ellipsoid will not be uniformly strained unless certain additional forces are applied to its surface, but that the mean strain is equal to that calculated by Becker.

Further, non-uniform strain will imply non-uniformity of magnetization of an ellipsoid in a uniform field, although the effect has not been calculated rigorously and is certainly small.

The theories of magnetostriction considered above are all based on various assumptions of crystal and solid-body mechanics, but the fundamental mechanism of the magnetostriction process has not yet been discussed. At the present time there is no adequate theory of this mechanism, although various attempts have been made to correlate magnetostriction phenomena with other magnetization processes. Heisenberg exchange forces by themselves cannot account for linear magnetostriction, since they are isotropic with respect to the crystal lattice, but they may give rise to the volume effect which occurs in high fields. The alternative assumption of dipole interaction, which is anisotropic, except at the absolute zero of temperature, leads to expressions for the magnetostriction constants in terms of the spontaneous magnetization and the rigidity modulus. The results derived are not very satisfying since it is impossible on this basis to give any reason why iron and nickel should exhibit length changes of different signs; and the failure to correlate this theory with experimental results is hardly surprising since the assumption that all the resultant magnetic moment is due to dipole moments at the lattice points is entirely without justification.

According to Becker's calculations (1934), the strain introduced into an undistorted lattice by the magnetization process is

$$\lambda_{100} = \frac{2SI^2}{G} \qquad \lambda_{111} = -\frac{4SI^2}{3G} \tag{13}$$

for a cubic lattice, where G is the rigidity modulus and S is a constant (= 0.4 for a body centered lattice, 0.6 for a face-centered lattice). These values are of similar order to those observed experimentally, but in practice there must be some additional interaction producing magnetostriction. This is now generally thought to be spin-orbit interaction, and Van Vleck (1937) has shown that it may account for magnetic anisotropy.

1.5 PREVIOUS EXPERIMENTAL WORK.

There appears to be no work published on the temperature variation of magnetostriction of Nickel crystals, and in fact the only experiments on single crystals over a range of temperatures are those of Takaki on Iron (1937). It is well to consider some of the other measurements of magnetostriction in order to see that although polycrystalline materials have been extensively studied, the significance of the results obtained is very much open to doubt. It would appear at first sight to be fairly simple to measure

accurately, and with consistency between specimens, the saturation longitudinal magnetostriction of a metal at room temperature. In point of fact, the results obtained, even during the period 1925-1939 when the majority of measurements on pure metals were made, show quite unaccountable variations. Schulze (1931, 1933) gives the saturation value for Nickel as 2.3, 2.5, 2.9 and 3.1 x 10^{-5}. Masumoto (1927) gives 4.7. It seems probable that small amounts of impurity will affect the values found; for example, 1% of iron would produce an error of about 10%. Also, differences in heat treatment might affect the results by causing differences in the strain distribution in the specimens. Experimental errors may account for part of the discrepancies, yet all these factors together do not seem sufficient to make one measured value more than twice another. What then is the cause for the discrepancies? The most plausible reason seems to be the widely different states that may be classified under the heading "demagnetized". These must range from a state in which the domains are randomly orientated to one in which all domains are magnetized parallel to a certain direction, and only the sign of their magnetization differs. In polycrystalline specimens the latter state is of course impossible, and it is reasonable to assume that it is also very improbable for a single crystal, yet it is not difficult to imagine a demagnetized specimen which is quite closely similar to that state. The state which a specimen will

assume when demagnetized will depend on the previous history and the method of demagnetization. The latter is impossible to standardise, since for different shapes of specimen the energy relations governing demagnetization will be different. The previous history of specimens can be standardised, and it would seem advantageous to give details when results are published of the precise treatment to which the specimen has been subjected. It might then be possible, if the magnetostriction results are to be correlated with other experimental results, to prepare further specimens in exactly the same way as those whose magnetostriction data are being used. At the moment, the majority of magnetostriction results are of little value as far as their absolute magnitudes are concerned. This makes experiments on single crystals of the greater value since the directional dependence of magnetostriction provides a useful check on some aspects of the basic theory of ferromagnetism.

TEMPERATURE VARIATION OF MAGNETOSTRICTION OF POLYCRYSTALLINE MATERIAL.

Before considering single crystal results, the temperature variation of the magnetostriction of polycrystalline nickel will be considered. Four sets of results have been published by different workers, and these four sets show significant divergencies. The experiments of Sucksmith (1950), Döring (1936) and Kirkham (1937) have all been made within the last

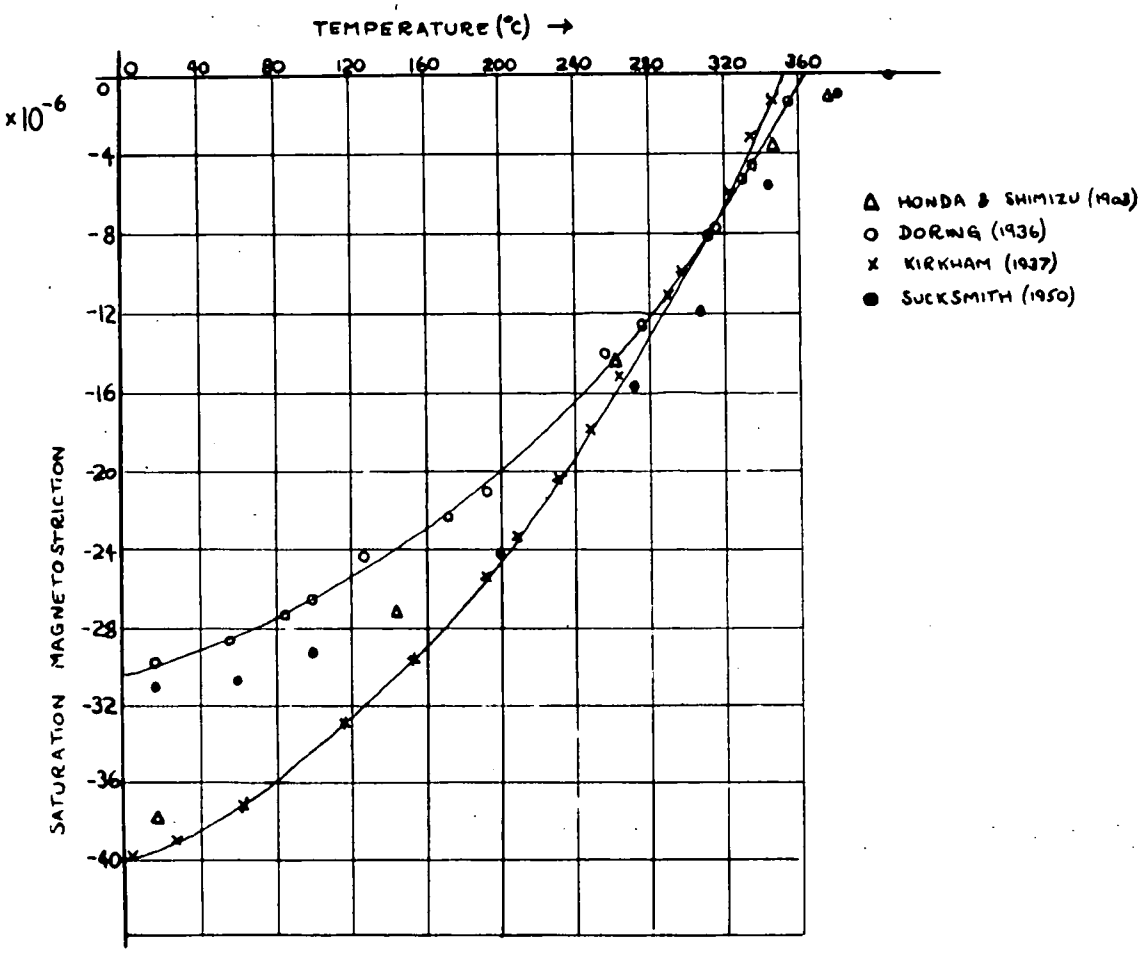

FIG.7. - Saturation Magnetostriction of Polycrystalline Nickel as dependent on Temperature

20 years when it has been possible to obtain extremely pure specimens, hence it is not to be expected that impurities will noticeably affect the magnetostriction in these cases. Both the magnitude and the dependence on temperature of the magnetostriction are widely different, and it is therefore unlikely that absolute calibration of the measuring systems can account for the discrepancies. Döring's curves are most often quoted, for he endeavoured to show that λ is proportional to I_s^2. The graph reproduced in his paper appears to support this, but examination shows that the range over which λ/I_s^2 is constant represents only a 25% variation of λ. The remaining 75% variation to zero magnetostriction at the Curie temperature is compressed into a small section of the graph, and part is conveniently ignored, although calculation from Döring's figures show a significant divergence from the claimed $\lambda - I_s^2$ law.

Kirkham's results show a magnetostriction at 0° C. of 40×10^{-6}, compared with Döring's value of 30×10^{-6}. Again the λ/I_s^2 law is held at the lower temperatures, but nearer the Curie temperature the divergence is not so great as Döring's, and is of opposite sign. Both these workers also measured the intensity of magnetization of their specimens, and found Curie temperatures of about 356° C. by this means. It is therefore surprising that the λ-T curves should cut the temperature axis at 350° C. for Kirkham and about 366° C. for Doring. These discrepancies correspond

to the divergencies of different sign from the $\lambda - I_s^2$ law near the Curie point. It therefore seems advisable to measure λ and I_s together since at the most interesting stage, near the Curie temperature, small errors in the measurement of the temperature can cause large resultant errors in the λ / I_s^2 ratio if λ and I_s are measured separately. Unfortunately it has been found impracticable to incorporate this for the measurements described in this thesis.

Sucksmith's results appear to fall away to a much more constant value near room temperature than the others, and the Curie point would appear to be much higher. He used cylindrical specimens in which the form effect might well be appreciable, yet he made no reference to it.

Honda and Shimizu (1903) find much less curvature in their $\lambda - T$ curve, while near the Curie point their curve approaches the axis much less sharply than found by the other workers. However, since they only give results for 5 different temperatures on a very small graph and without tables, the significance of their results is perhaps doubtful.

Neither of the latter two papers quotes corresponding magnetization figures, so that $\lambda - I_s^2$ curves are impossible to deduce accurately.

The results of work on polycrystalline Nickel may therefore be assessed as follows: λ is proportional to I_s^2

to within a fair degree of accuracy from room temperature to about 200° C, at which temperature λ is about 2/3rds of room temperature value. At higher temperatures the results are not sufficiently consistant to allow any reasonable conclusions to be drawn. The absolute magnitude of the effect varies by over 30% between various workers.

MEASUREMENTS ON SINGLE CRYSTALS OF NICKEL.

There appear to be only two papers describing measurements of the magnetostriction of single crystals of Nickel, and both deal only with room temperature measurements. That of Masiyama (1928) was one of a series dealing with single crystals of the three common ferromagnetic elements and their alloys. The Nickel crystals were in the form of oblate spheroids of major axis 2 cm. and minor axis 0.1 cm., and the measurements were made by an optical lever method. Masiyama summarises his measurements of longitudinal magnetostriction as follows:

(1) Magnetostriction in the plane (100).

In the direction of the tetragonal axis [100], the effect of magnetic elongation is negative for all magnetizing fields; it increases first rapidly and then slowly. As the inclination of the axis [100] increases, the effect of contraction becomes less and at an inclination of 45° or in the direction of the digonal axis [110] attains the minimum. Thus the elongation-orientation curves have a

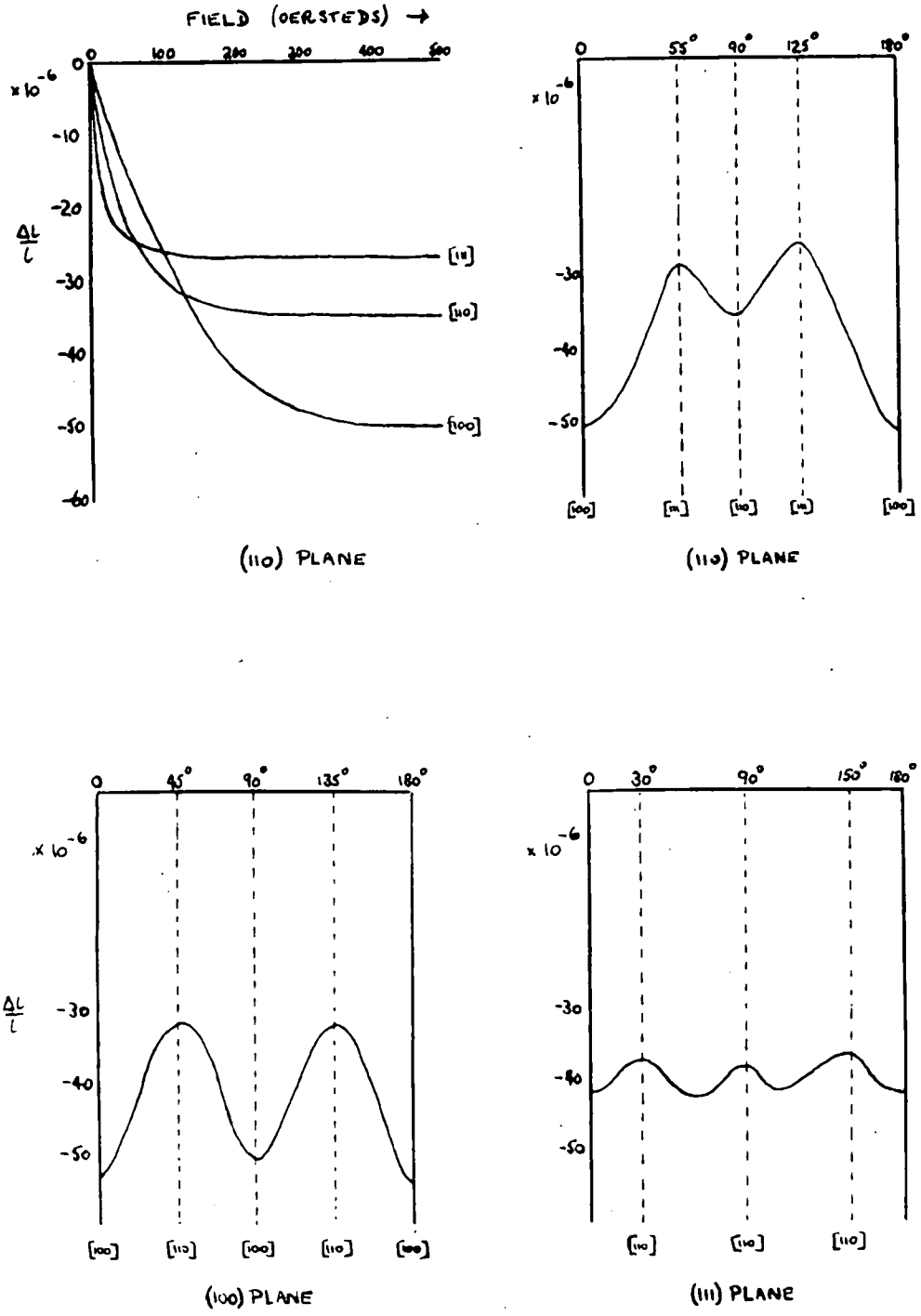

FIG. 8. - Experimental Results by Masiyama of Longitudinal Magnetostriction of Nickel at Room Temperature.

(a) Field dependence in (110) plane.
(b) Saturation in (110), (100) and (111) planes.

period of 90°.

(2) Magnetostriction in the plane (110).

The magnetic contraction in the direction of the axis [100] is the same as in the case of the plane (100). As the inclination of the field to the direction of the axis increases, the contraction decreases, till at 55°, that is in the direction of the trigonal axis [111], it attains a minimum; while with a further increase of the inclination the contraction increases again. The amount of contraction at 90° is, however, less than that at 0°. The elongation-orientation curves have a period of 180°.

(3) Magnetostriction in the plane (111).

The space-lattice in this plane consists of a series of equilateral triangles, and the variation of the elongation-orientation curves is repeated every 60°.

Masiyama's measurements show that the periodicities which could be predicted by lattice geometry are in fact fulfilled. That the absolute values are not to be relied upon is demonstrated by the discrepancies found between saturation values for the [110] and [100] directions using discs cut in different planes.

Becker and Döring (1939), and later Mason (1951) have calculated the values of the five constants in equation (6) which best fit Masiyama's results. These are calculated by methods which involve only differences between saturation magnetostriction in different directions, and therefore the

effect of strains upon the domain configuration of the specimen in the demagnetized state will not affect the results.

Before discussing the values calculated, the experiments of Bozorth and Hamming (1953) may be mentioned. The method adopted was similar to that of Masiyama, namely specimens in the form of discs were used and the saturation magnetostriction was measured in different directions in the plane; the actual measurements were made by using resistance strain gauges. Their results are only recorded in the form of the constants which best fit Becker's five-constant equation, and these constants are calculated by a method similar to that used by Becker and Döring and by Mason. The behaviour of the crystal when magnetized to values less than saturation is not recorded.

The values found by Masiyama and by Bozorth and Hamming are shown in Table 1.

TABLE 1.

SATURATION MAGNETOSTRICTION CONSTANTS OF NICKEL
(AT ROOM TEMPERATURE)

Constant	Masiyama (Direct)	Mason	Becker and Döring.	Bozorth and Hamming
h_1		-40	-24	-69 (3.8)
h_2		-46	-47	-37 (1.9)
h_3		0	0	- 3 (3.1)
h_4		-36	-51	- 8 (5.2)
h_5		+54	+52	+ 8 (3.1)
λ_{100}	-53	-51	-50	-50
λ_{110}	-36	-37	-32	-30
λ_{111}	-27	-19	-20	-23

Masiyama's Results.

Axis	(100) Plane	(110) Plane	(111) Plane	Mean
[100]	-54	-51		-53
[110]	-31	-34	-42	-36
[111]		-27		-27

(All values x 10^{-6})

Column 1 gives the saturation values in the three principal directions as taken directly from Masiyama's figures. Columns 2, 3 and 4 give values of the 5 constants and also the saturation magnetostriction in the three directions as calculated from the constants; for Bozorth and Hamming's results the probable errors are given. Comparison of these last three columns shows a very large diversity in some of the h values; this is a peculiarity caused by the form of the equations which effectively magnifies small differences in the measured values. The significant data for comparison are the λ values. λ_{100} is very good, but λ_{110} and λ_{111} are not so good. In particular λ_{111} is very different from the value taken directly from Masiyama's figures. This may indicate a failure of the Becker equation, but is more likely a result of the non-random distribution of domains in the demagnetized state. Mason and Becker and Döring assumed $h_3 = 0$ in their calculations. Bozorth and Hamming did not, and derived a result not definitely different from zero. The differences between the results obtained by Mason and by Becker and Döring are probably due to the inconsistencies of Masiyama's measurements.

TAKAKI'S EXPERIMENTS.

The experiments carried out by Takaki (1937) on the temperature variation of magnetostriction of single crystals

of Iron were made in order to test Becker's dipole theory of magnetostriction. This theory expresses saturation magnetostriction in terms of the elastic constants of the crystal and the saturation magnetization (see equation 13); the variation of both the latter parameters with temperature being known, the variation of saturation magnetostriction provides a valuable check on Becker's theory. In this respect the results obtained were disappointing, for the variations of the 3 parameters could not be correlated. In other respects, however, the experimental results were very satisfactory. Four specimens in the form of long prolate spheroids were used, and in each case the specimen axis was nearly coincident with one of the prominent crystallographic directions. According to Becker's theory the magnetostriction should be expressible in terms of two parameters and the direction cosines of the lattice (using equation 6 with $h_3 = h_4 = h_5 = 0$), so that at all temperatures Takaki virtually had 4 equations to solve for 2 unknowns. This provided a valuable check on the consistency of the results at any temperature, and the consistency was in fact very good at all temperatures. In all cases the figures used to check Becker's formula were the differences in length between remanence and saturation, since the conditions in the demagnetized state cannot be definitely specified.

The actual magnetostriction measurements are expressed in terms of two constants, C and χ, related to λ_{100} and

λ_{111} by

$$C = \lambda_{100}$$
$$\chi = -2\lambda_{111}$$

χ falls steadily from 0° C. to zero at about 750° C. C falls from 0° C. to 150° C., then rises to 1.2 times its 0° C. value at 500° C, and then falls rapidly to zero at 750° C. Since the elastic moduli are relatively constant over the temperature range considered, the expected variation with temperature was very nearly equal to the variation of the square of the saturation magnetization. The failure of the experimental results to agree with those predicted theoretically shows that Becker's theory is far from adequate.

1.6 THE REFERENCE STATE.

Takaki (1937), by using crystals of iron with mutually perpendicular directions of easy magnetization, was able to state accurately the domain distribution at remanence. He used very long specimens with demagnetizing factors of about 0.003, hence at remanence the tendency for any resultant magnetization perpendicular to the axis of the specimen was very small. With only the six directions of easy magnetization, by making the assumption that the resultant magnetization is directed along the axis of the specimen, it can be readily shown that the domains align themselves in the three

directions closest to the field direction in the proportion of their direction cosines with respect to that direction.

This distribution will not hold in the case of nickel since there are eight directions of easy magnetization. This means that with the assumption of zero intensity of magnetization perpendicular to the specimen axis, there is in general no specifically defined proportion of domains aligned in the four directions nearest the field direction. It might be possible to determine a distribution on the basis of minimum intensity of magnetization both parallel and perpendicular to the axis. For the special cases in which the specimen axis is coincident with the [111] and the [100] axes, the remanent magnetization per unit volume will be, on this assumption, $I_s/3$ and $I_s/\sqrt{3}$ respectively. However, the ratio of possible strain and boundary energy to the energy of the demagnetizing field will be much larger parallel to the axis, and the calculated distribution is a doubtful one.

Experiments carried out by Honda, Masumoto and Shirakwa, show that at temperatures of 200° C. and over there is very little difference between the magnetization curves for the different crystallographic directions in nickel. There is, in fact, more difference between their values of saturation magnetization than between values of magnetization in lower fields. Since the measurements were made with a search coil

and fluxmeter, this may be due to the specimen being incompletely demagnetized. Whatever the discrepancies are due to, there seems even less justification for assuming a particular domain distribution at high temperatures than there is at low.

An alternative state, in fact the one most commonly used, is the demagnetized state. Kaya and Takaki have shown by magnetostriction measurements on iron at room temperature that the demagnetized state is not necessarily that in which the domain magnetizations are directed equally along all the directions of easy magnetization.

The reference state used for measurements described in this thesis was the demagnetized state obtained after successive reversals of the applied field as it was reduced from a value sufficient to saturate the specimen to zero. At room temperature, some measurements were made of the magnetostriction round hysteresis loops of various sizes.

1.7 A NOTE ON THE MEASUREMENT OF LONGITUDINAL MAGNETOSTRICTION.

By using the Becker equation, the saturation magnetostriction in any direction may be expressed in terms of 5 parameters dependent only on temperature.

$$\lambda = h_1\left(\alpha_1^2\beta_1^2 + \alpha_2^2\beta_2^2 + \alpha_3^2\beta_3^2 - 1/3\right) + 2h_2\left(\alpha_1\alpha_2\beta_1\beta_2 + \alpha_2\alpha_3\beta_2\beta_3 + \alpha_3\alpha_1\beta_3\beta_1\right) + h_3(s-1/3) + h_4\left(\alpha_1^4\beta_1^2 + \alpha_2^4\beta_2^2 + \alpha_3^4\beta_3^2 + \frac{2s}{3} - \frac{1}{3}\right) + 2h_5\left(\alpha_1\alpha_2\alpha_3^2\beta_1\beta_2 + \alpha_2\alpha_3\alpha_1^2\beta_2\beta_3 + \alpha_3\alpha_1\alpha_2^2\beta_3\beta_1\right) \quad (6)$$

for Nickel

where the α's and β's are the cosines with respect to the crystallographic axes of the direction of magnetization and the direction in which the change in length is measured, and

$s = \alpha_1^2\alpha_2^2 + \alpha_2^2\alpha_3^2 + \alpha_3^2\alpha_1^2$

If measurements are made with strain gauges, it is relatively easy to measure the strain in directions other than those of the applied field. For measurements at high temperatures, however, strain gauges are difficult to use, and it becomes necessary to transmit the displacement of the free end of the specimen away from the high temperature region. If a solenoid is used to produce the magnetic field, it is very difficult to measure changes in length in directions other than that of the applied field. Putting $\alpha_1 = \beta_1$, $\alpha_2 = \beta_2$, $\alpha_3 = \beta_3$, equation (6) then becomes

$$\lambda = h_1(1-2s) + 2h_2 s + h_3(s-1/3) + h_4(2/3 - 7s/3 + 6r) + 6h_5 r \quad (14)$$

$$= \left(h_1 - 1/3\, h_3 + 2/3\, h_4\right) + s\left(-2h_1 + 2h_2 + h_3 - 7/3\, h_4\right) + 6r\left(h_4 + h_5\right)$$

where $r = \alpha_1^2\alpha_2^2\alpha_3^2$

Thus by measuring the strain in the direction of the applied field, the 5 parameters can no longer be determined since there are only 3 independent parameters in equation (14). Furthermore, the results of Bozorth and Hamming (1953) and of Masiyama (1928) show that at room temperature ($h_4 + h_5$) is not significantly different from zero, even though the values of h_4 and h_5 are very different. r can vary from 0 for a [100] direction to 1/27 for a [111] direction. It is therefore reasonable to neglect the last term of the equation for room temperature measurements.

Hence $$\lambda = h_o + h_s s \qquad (15)$$

where $$h_o = h_1 - \tfrac{1}{3} h_3 + \tfrac{2}{3} h_4$$

$$h_s = -2h_1 + 2h_2 + h_3 - \tfrac{7}{3} h_4$$

Measurements in 2 directions now serve to find the 2 parameters h_o and h_s. The greatest accuracy is obtained by choosing directions with the greatest difference in s; they are the [111] for which s = 1/3, and the [100] for which s = 0. h_o and h_s can then be found from

$$h_o = \lambda_{100} \qquad h_s = 3(\lambda_{111} - \lambda_{100}) \qquad (16)$$

Whether the term in r can reasonably be neglected at other than room temperature is open to some doubt. The term will certainly be small since r cannot be greater than 1/27, and measurements have therefore been confined to 2 specimens with axes along the [100] and [111] directions.

PART 2.

APPARATUS

2.1 APPARATUS OF PREVIOUS WORKERS.

The only previous work on variation of single crystal magnetostriction with temperature is that of Takaki (1937) on iron. His experimental problems were simplified since he was able to use large specimens, and hence the apparatus he used is not strictly comparable with that necessary for the work to be described here. It is nevertheless useful to review briefly the different methods used to measure the temperature variation of magnetostriction of large specimens, and the apparatus used by Honda and Shimizu (1903), Döring (1936), Takaki (1937) and Kirkham (1937) will be considered.

Of these, only Döring did not use a roller and mirror method for the actual displacement measurement; he used a hydraulic device which incorporated a large diameter metal bellows and a fine capillary tube. The various papers do not give many details of accuracy or sensitivity of the apparatus, but Kirkham using a 19 cm. specimen could detect $\Delta l/l$ changes of 1.5×10^{-7}, and the other methods probably gave results of similar accuracy. All four workers used specimens of 19 to 25 cm. long, in each case enclosing them in an electric furnace with non-inductive winding placed in a solenoid. Honda and Shimizu also made provision for cooling below room temperature by pouring liquid air into the apparatus.

The methods used for transmitting the displacement of

the specimen to the measuring device are worthy of note. By using a vertical wire as specimen, and coupling to the end of this a further wire which pressed against the roller, Honda and Shimizu had a very simple arrangement, but it must have been very susceptible to temperature fluctuations. The ellipsoid used as specimen by Kirkham had two small notches in it, and it rested horizontally with these on two knife edges. The knife edges were arranged so that their relative movement rotated the measuring roller.

Döring used a rod of porcelain which was pressed against the free end of the ellipsoid, and a tube of steatite concentric with this rod served to maintain the extensometer at a constant distance from the fixed end of the specimen. Takaki had a similar system using fused quartz rod and tube. Such a method, using materials of low expansion such as quartz, would seem to be the most likely to give accurate results, since there is bound to be a large temperature gradient along the displacement rod.

Sucksmith (1950) used apparatus of rather different type to that of previous workers. He was engaged in measurements of saturation magnetostriction only, and consequently could use a cylindrical specimen. An electromagnet was used to obtain the high fields required, but this presented difficulties since with zero current through the magnet there was a remanent field. The length changes were magnified ten times by a hydraulic bellows, and

then further magnified by the usual roller and mirror method. The total magnification was 5×10^5, and a specimen 1 cm. long was used. The specimen was heated by a furnace wound with nichrome wire.

2.2 GENERAL DESIGN OF APPARATUS.

Using the apparatus described in section 2.1 as a basis for the design of apparatus suitable for single crystal measurements, the following general design was considered suitable.

The specimen, in the form of a prolate spheroid, is mounted at the centre of a solenoid which produces a uniform field over the volume of the specimen. Between the solenoid and the specimen is a heat-producing device which is thermally insulated from the solenoid. Displacement of the free end of the specimen is transmitted to the extensometer by a quartz tube or system of rods. Random fluctuations of the temperature of the specimen produce length changes which are compensated by a non-ferromagnetic metal in thermal contact with the specimen.

The apparatus can be mounted with its axis, i.e. the axis of the specimen and the solenoid, either horizontal or vertical. Vertical mounting has the advantage that the quartz displacement rod can rest on the top of the specimen, and the extensometer on top of the rod, without any forces acting

perpendicular to the axis of the system. The arrangement which is likely to produce the more uniform temperature distribution is difficult to judge, and the distribution probably depends more on detail design of the apparatus than on the axial direction.

Further considerations which governed the general design of the apparatus will now be considered.

The whole scale of dimensions of the apparatus had to be largely determined by the size of single crystal specimen which was to be used. In order that the experimental results should be as accurate as possible, it was desirable to use a large specimen, and the specimen size was therefore determined by the size of the original single crystal ingot. This was obtained from the Department of Physics of the University of Leeds, where it was grown by Mr. R.F. Pearson (see Pearson, 1953), and was in the form of a cylinder a little more than 1 cm. in diameter and about 3 cm. long. From this ingot a specimen could be cut with its axis along any required crystallographic direction, and with a length greater than 1 cm.

An estimate of the probable changes in length which may be produced by magnetization in a single crystal was obtained by assuming that Döring's temperature variation law, $\lambda = kI_s^2$, would hold for single crystals as well as for polycrystalline material. It was therefore likely that length changes would not be greater than those obtainable

at room temperatures unless measurements were made below room temperature, and that the effect would fall to zero at the Curie Point, which for Nickel is approximately 360° C.

The experiments of Masiyama at room temperature show that the saturation longitudinal magnetostriction varies from 20×10^{-6} to 50×10^{-6} according to the crystallographic direction considered. Hence it was reasonable to proceed on the assumption that using a crystal of 1 cm. length or a little more, the maximum displacement of the free end at saturation would be about 50×10^{-6} cm. at room temperature, falling off at higher temperatures.

Present-day practice in the measurement of longitudinal magnetostriction tends towards the use of strain gauges. This method is of particular application where the gauges can be fixed to the specimen itself, but this was unfortunately impossible in the present investigations as the high temperatures envisaged (up to 360° C.) prohibit the use of the adhesives normally employed for bonding the gauge to the specimen, while the use of strain gauges at high temperatures was considered likely to present serious problems. It was therefore necessary to transmit the displacement of the free end of the specimen from the region of the solenoid and the temperature enclosure to a displacement-measuring apparatus outside. The use of a strain gauge under such conditions did not appear to have any advantage

over other types of apparatus employing variations of capacitance and inductance with displacement. As the extensometer could not be placed very far from the rest of the apparatus, and hence a large temperature gradient existed between them, it was felt that the best measuring apparatus would be the one least likely to be affected by temperature changes, and of the three variable parameters mentioned above, the variation of capacitance was chosen.

The displacement to be measured had to be transmitted by rods with the minimum possible coefficient of expansion in order that spurious temperature effects might be minimized. The rods used were of fused silica, which had a mean linear expansion coefficient of 5×10^{-7} $^{o}C.^{-1}$ over the range used. Even with this material, the lengths of rod had to be made as short as possible as the expansion of the silica rods per $^{o}C.$ per cm. is about 1% of the probable maximum displacement to be measured. Hence the solenoid itself had to be as short as was consistent with the production of a uniform field over the length of the specimen.

To maintain the specimen at the required temperatures it was decided to use a heat-conducting liquid which would be pumped continuously past the specimen. This method has three advantages over the alternative of employing an electrical heating element round the specimen, namely:

1) The bulk of material maintained at the high temperature is large, which leads to greater temperature

stability.

2) There are no spurious electro-magnetic effects associated with the heating element.

3) The same system can be adapted for cooling the specimen below room temperature.

The Curie Point of Nickel being near 360° C., the liquid to be used was required to have a boiling point of 400° C. or more if the whole ferromagnetic range was to be investigated. The only materials found which were liquid over the range 0° C. to 400° C. were the silicones, and it was decided that the liquid manufactured by Midland Silicones and known as MS 550 was the most suitable, its boiling point being 405° C. Tests showed that maintaining this liquid at 400° C. for several hours did not affect its properties.

To provide a reasonable bulk of liquid round the specimen, a tube of about 3 cm. diameter was necessary, and round this was needed a vacuum tube to reduce heat loss from the pumping system to a minimum. On the outside of the vacuum tube a stream of water was passed to cool the solenoid, and the solenoid itself surrounded the two tubes. In order to make room for all this, the inside diameter of the solenoid could not be reduced below 7 cm.

In order to give the specimen the necessary mechanical strength, its diameter at the centre could not be made less than 0.2 cm., giving an axial ratio of 5 for a specimen 1 cm. long. At room temperature the saturation intensity of

magnetization is approximately 500 c.g.s. units, and this must produce a demagnetizing field in the specimen of some 350 oersteds. At room temperature the [100] direction of Nickel does not saturate until an effective field of 300 oersteds is applied, necessitating an external field of 650 oersteds. It was therefore decided that the solenoid should be designed to produce a maximum field of 1000 oersteds, sufficient to saturate the crystal under all conditions.

It was found that the minimum length of solenoid which could be used was 20 cm. At this length, it required correcting coils at its ends of 25 cm. diameter in order to produce a uniform field at its centre over a length of 2 cm. Any further reduction in length would not have been possible without reducing the internal diameter of the windings.

It was found necessary to mount the whole apparatus on a galvanometer pillar, since the extensometer is sensitive to vibrations carried through the laboratory floor.

2.3 DESIGN OF EXTENSOMETER.

PRELIMINARY CALCULATIONS.

The displacements to be measured are estimated at a maximum of 50×10^{-6} cm., and it is desirable that such a displacement shall be measurable to an accuracy of at least 1%, i.e. to 5×10^{-7} cm. Displacements somewhat smaller

than this have been measured by means of circuits in which the displacement condenser forms part of a resonant circuit, for example the Whiddington (1920) ultramicrometer. The method here adopted incorporates a bridge network in which two adjacent arms are large condensers, and the other two are formed of the two sides of a differential condenser whose common plate is displaced by changes in length of the specimen.

In the network of Fig. (9), let the capacitances of the condensers have the value shown, and let the input resistance of the valve voltmeter which serves to measure the out-of-balance voltage be R.

Then if a voltage V is applied to the circuit, the voltage across the valve voltmeter is

$$V' = V\left(\frac{C_1}{C_2} - \frac{C_3}{C_4}\right) \Bigg/ \left\{\frac{1}{j\omega C_2 R}\left(1+\frac{C_3}{C_4}\right) + \frac{1}{j\omega C_4 R}\left(1+\frac{C_1}{C_2}\right) + \left(1+\frac{C_1}{C_2}\right)\left(1+\frac{C_3}{C_4}\right)\right\} \qquad (17)$$

Now if C_1 and C_2 are approximately equal, and also C_3 and C_4, and if $R \gg \left|\frac{1}{j\omega C_2}\right| > \left|\frac{1}{j\omega C_4}\right|$

then

$$V' = V\,\frac{C_1/C_2 - C_3/C_4}{\left(1+C_1/C_2\right)\left(1+C_3/C_4\right)}$$

Consider now a change dC_1 in C_1 and dC_2 in C_2.

Then

$$dV' = -V\,\frac{C_1\,dC_2 - C_2\,dC_1}{(C_1+C_2)^2} \qquad (18)$$

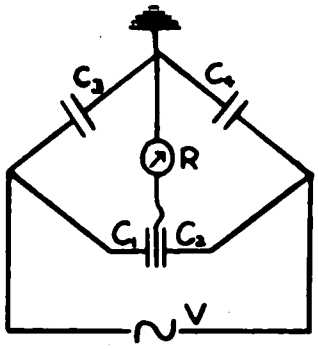

FIG.9. - Capacity Bridge Network.

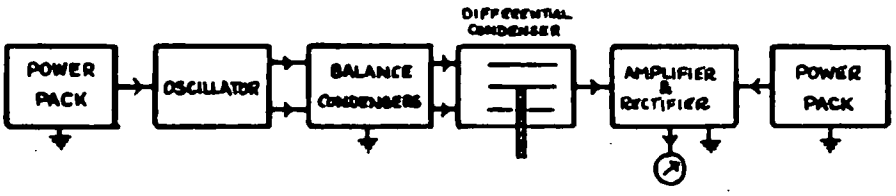

FIG.10. - Block Diagram of Extensometer Circuit

If the separation of the plates of C_1 is t_1, and of C_2 t_2, and if a displacement dt is made to the middle plate,

$$dV' = V dt \cdot \frac{t_1^2 - t_1 t_2 + t_2^2}{t_1 t_2 (t_1 + t_2)} \qquad (19)$$

Before making measurements the bridge is balanced, and although this is best done by making $t_1 = t_2$ and $C_3 = C_4$, this is not possible to arrange accurately. Suppose $t_1 = t + \Delta t$ and $t_2 = t - \Delta t$ then

$$dV' = \frac{V dt}{2t}\left(1 + 4\frac{\Delta t^2}{t^2}\right) \qquad (20)$$

Hence if the bridge is zeroed so that the condensers are within 5% of their maximum value, the output voltage will be

$$dV' = \frac{V dt}{2t} \quad \text{to within 1\%}$$

Taking $dt = 40 \times 10^{-6}$ cm., $t = 10^{-2}$ cm. and $V = 40$ volts, $V' = 80$ millivolts.

If the output is now amplified by about 100, it can be displayed on an ordinary laboratory test meter.

The bridge circuit requires an oscillator providing a peak to peak voltage of about 100, and a valve voltmeter with an amplification of about 100. In the theory given, it was assumed that

$$R \gg \left|\tfrac{1}{j\omega C_3}\right| > \left|\tfrac{1}{j\omega C_4}\right|$$

Now a reasonable value of the input-impedance of a valve voltmeter is 3 MΩ, and with the condenser separation assumed 10^{-2} cm., a capacitance of about 50 pF. is obtained with a plate diameter of 2 inches. Taking $C_1 = C_2 = 50$ pF., $\omega \gg 8 \times 10^3$.

The lowest suitable value for the frequency is therefore about 10^4 cycles per second. At higher frequencies the pick-up effect due to any movement near the test apparatus becomes excessive. With the apparatus built to work at a frequency of 10^4 c/s., movement of the hand within a few inches of the differential condenser causes no noticeable effect. The balancing condensers used are each of 1000 pF.

The oscillator and valve voltmeter are both driven from power packs worked from the laboratory 250 volt A.C. supply, and in order to limit mains voltage fluctuations it was decided to use stabilised power packs. It might have been possible to drive the whole circuit from one power pack, but to avoid any feed-back between the amplifier and the oscillator through the H.T. line, two separate power packs were used. The electronic apparatus, which will now be considered in fuller detail, is therefore assembled as shown diagramatically in Fig. (10).

THE STABILIZED POWER PACKS.

The power packs for rectifying the A.C. mains voltage are of conventional design. They employ a choke

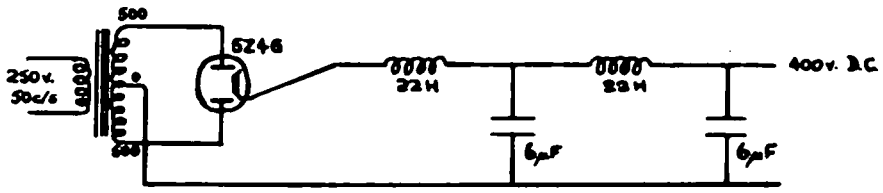

FIG.11. - 400 volt D.C. Power Pack.

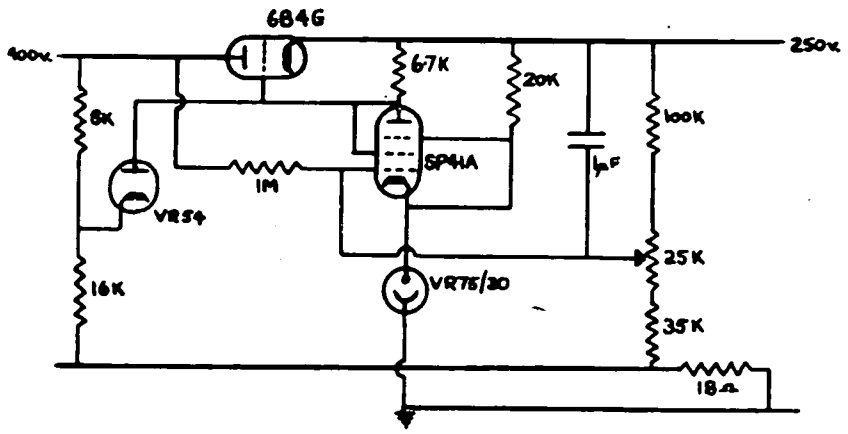

FIG.12. - H.T. Stabilizer.

following the full-wave rectifier since this improves the regulation of the circuit.

The circuit, which is shown in Fig. (11), has the following characteristics:

Maximum ripple, 0.5 volts peak to peak.

With 20 ma. output current, 400 volts output potential.

With 70 ma. output current, 350 volts output potential.

The stabilizer is of the conventional series-parallel type in which the impedance of a triode in series with the load is controlled by a high gain pentode circuit in parallel with the load.

Variations of the output voltage are transmitted to the grid of the SP 41A pentode, which amplifies them and alters the bias on the low-impedance triode 6B4G, thereby opposing any voltage changes. The VR 54 diode is a protecting valve which is designed to cut off the 6B4G if the output voltage rises above a safe value due to failure of the pentode circuit. The VR 75/30 voltage stabilizer provides the reference voltage, and as it is designed to work at about 20 ma. current, which is too large to be passed through the SP 41A, a 20 K resistance is put in parallel with the pentode.

The 18 ohm resistance is intended to compensate for changes in output current by increasing the voltage on the

grid of the pentode when more current is passed. The 1 M resistance is to assist compensation for mains voltage fluctuations by establishing a resistor chain 1M - 25K - 35K which makes the SP 41A grid fall in potential with drop in input voltage. The values of both the 18Ω and the 1 M resistors were determined by tests on the circuit when used with its actual load, i.e. the valve voltmeter or the oscillator. If necessary the output impedance of the power pack and the stabiliser together can be made negative by suitable adjustment of the 18Ω resistor; on test the circuits showed output impedances of about 5 ohms. This is not constant over a large range as the valve characteristics are only linear for variations in the grid potentials of a few volts. Variations of mains voltage of ± 10% produce output variations of less than ± 1%, and long-term stability is better than 0.5 volts in 250 volts output.

In order to verify that the power packs are maintaining their correct output voltages, it was thought desirable to measure the voltages by a potentiometer method which enables fluctuations to be indicated more accurately. The circuit used is that shown in fig. (13).

G is a micro-ammeter which is protected by the 10 K series resistance. The accumulator can be checked against the standard cell, and its voltage backed off to the correct amount by the variable 50 K resistor, using the switch position A. The voltage is then compared with the voltage

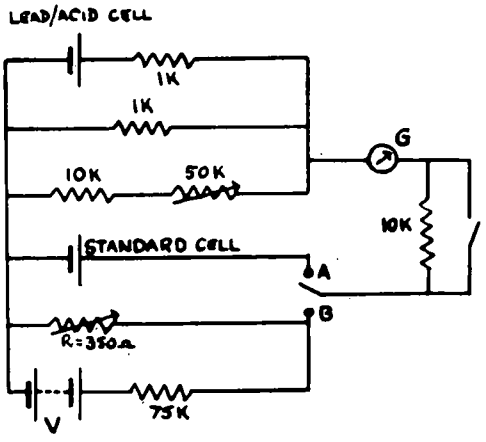

FIG.13. - Bridge for checking H.T. voltage.

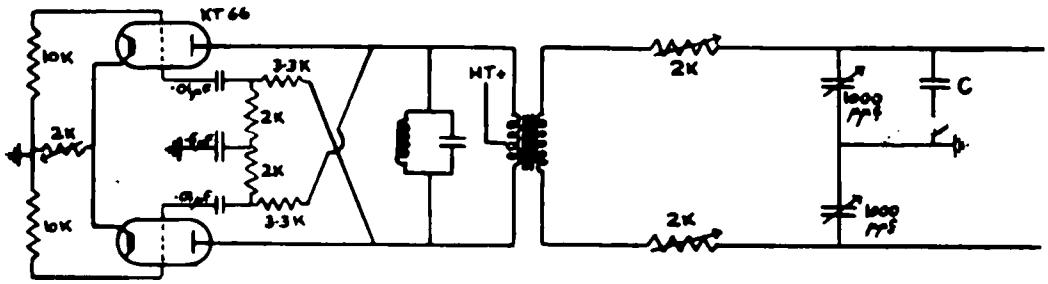

FIG.14. - Oscillator and Balance Circuit

under test (V) by putting the switch to B position and adjusting R, which is made up in steps of 10 ohms. The power pack voltage is normally adjusted for R = 300 ohms with the potentiometer in balance.

THE OSCILLATOR.

It was considered desirable that the input to the valve voltmeter should have one side earthed to reduce spurious pick-up and give generally better stability, and with a Wheatstone bridge network this means that the oscillator output must be equally balanced about earth potential. This made the use of a push-pull oscillator an advantage, and this type of circuit possesses the further merit of providing less distortion than a single-sided type. The design adopted is is shown in fig. (14).

In order to keep the oscillations at a constant frequency, while at the same time dispensing with a buffer stage as is normally used, the tuned circuit forms a much lower impedance section of the anode circuit than the transformer in parallel with it. Since the circuit which the oscillator feeds is of sensibly constant impedance, its effect on the anode circuit of the oscillator is not important. The output transformer has a turns ratio of approximately 4. A high degree of negative feedback is employed which limits the output voltage to a constant value determined by the actual value of the cathode resistor and the potential of

the H.T. line. The valves are KT 66 tetrodes, triode connected.

Tests show that changing the capacitance load by 1% changes the oscillator output by about 1%. Hence the total capacitance load must be kept constant to within 1%.

THE BALANCING CONDENSERS AND PHASE SHIFTER.

The output voltages from the two sides of the oscillator are designed to be equal and 180° out of phase. Due to stray capacitance, inductance and resistance in the circuit, this is not exactly correct, and it has been found necessary to put a resistance in each side of the circuit in order to effect the required phase shift. The balancing condensers are mounted in a screening box which also contains these resistors.

One of the balancing condensers is fitted with a Muirhead slow motion drive which allows the zero to be set with sufficient accuracy.

The circuit is normally used with one of the series resistors zero and one of the condensers at maximum, and the other condenser with the Muirhead drive is kept within 20 pF. of its maximum. This ensures that the extensometer always operates under the same conditions as those used in calibrating it.

The condenser C is of 12 pF., and is used to check that the whole apparatus is working satisfactorily. When it is

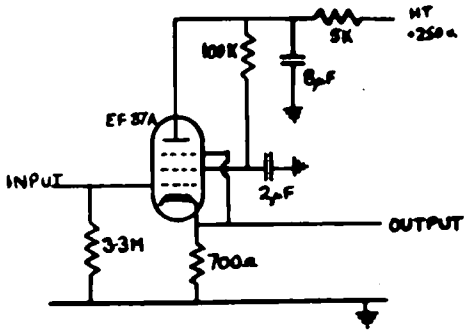

(a) the cathode follower.

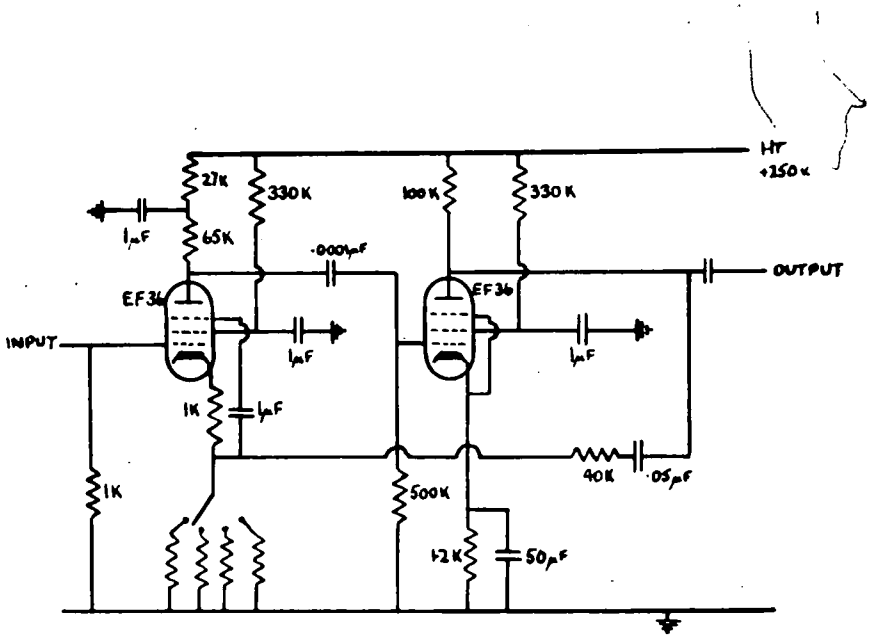

(b) the amplifier

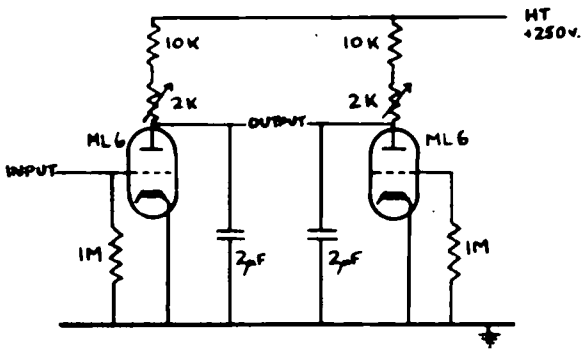

(c) the rectifier

FIG.15. - The amplifier / valve voltmeter.

put into circuit it causes the output meter to register a deflection, which for a given amplification should be constant.

Although the design of the differential condenser belongs strictly to this section, it is thought better to postpone its discussion until the specimen holder has been described, since the two were designed as an integral unit. The condenser has plates of 2 inches diameter, and the separation of each fixed plate from the central moving plate is 0.2 mm.

THE AMPLIFIER AND RECTIFIER.

The first part of the amplifier had to have a high input impedance, and needed to be near to the differential condenser in order that the lengths of screened cable, which would otherwise be necessary to connect the condenser to the amplifier and which would lower the impedance, could be eliminated. For these reasons it was decided to use a cathode follower as the first stage, and this is mounted on a separate chassis within a few centimetres of the condenser.

The design is quite orthodox. The 8 μF condenser and the 5 K dropping resistance act as a decoupling device. The designed amplification of the stage is 0.98, and the input impedance is 3.3 M in parallel with 0.2 pF., which is within the limits determined by the analysis of the Wheatstone bridge network.

The next two stages of the amplifier are resistance-capacitance coupled, and use EF 36 pentodes. Stage 2 is designed to give an amplification of 60, stage 3 of 40, but variable degrees of negative feedback over the two stages limit the total gain to 30, 40, 65, or 120.

The output from the third stage is fed to a rectifying circuit mounted on the same chassis. The rectifying valve is a triode, ML 6, and when no input voltage is applied, its anode potential is balanced against that of a similar triode, so that any fluctuations in H.T. voltage are effectively eliminated. The output voltage is developed across a 10 K resistor, and is then fed onto a test meter of resistance 20,000 ohms per volt. This is normally used on the 12 volt range.

On test the amplifier, valve voltmeter and test-meter gave linear characteristics over an output voltage range of 1.5 to 12 volts. In use, the anode load of the balancing triode is adjusted so that the meter records 2 volts negative with zero input voltage; the system then operates over a linear range.

THE CALIBRATION BEAM.

The extensometer has been calibrated by displacing the moving plate through known distances on a bending beam. The apparatus used is shown in Fig. (16).

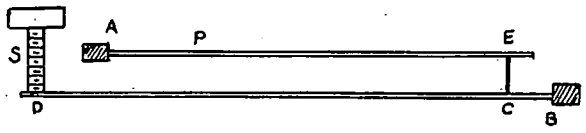

Fig. (16). The Calibration Beam.

AE and BD are two similar beams rigidly clamped to a common framework at A and B. S is a screw operating from the same framework, and rotation of S depresses the beam BD at D. The corresponding movement of the beam at C is transmitted to the beam AE at E, and the differential condenser picks off displacements of AE at a point such as P. Theoretical analysis shows that for two beams of similar material and dimensions, the ratio of movement at P to that at D is

$$\frac{9\,b^2d^2\left(1-{}^{b}/_{3a}\right)\left(1-{}^{d}/_{3c}\right)}{4a^2c^2\left(1-{}^{b^3}/_{c^3}\right)-3a^3b^2\left(1-{}^{3b}/_{a}\right)\left(1-{}^{b}/_{3a}\right)/c}$$

where AE = c, AP = d, BD = a, and BC = b.

The beams were made of steel 1 inch wide and $\frac{1}{8}$ inch thick, and the lengths used for the actual calibration were a = 45.2 cm., b = 2.34 cm., c = 35.7 cm., d = 6.7 cm. Using these figures, the displacement ratio as calculated from the formula is then 1.98×10^{-4}.

S is an 0 B.A. screw having 10 turns per cm., and rotation could be controlled to 1/100 turn, so that

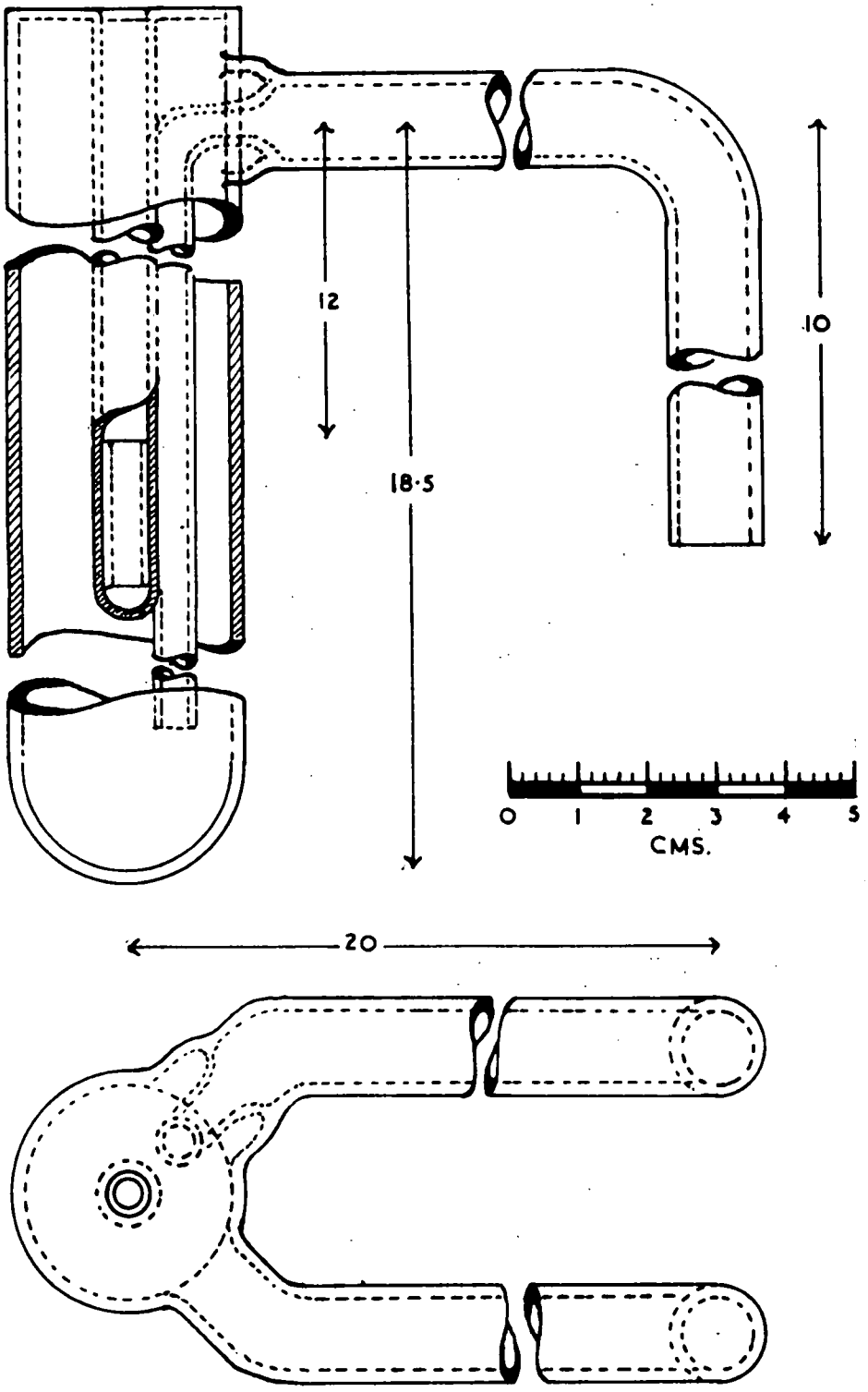

FIG.17. - The Specimen Holder for Magnetostriction Measurements.

displacements of about 2×10^{-7} cm. could be produced. It was felt desirable to check the beam by using the displacement of light fringes, so a lens and mirror system was mounted on the framework and on the beam AE so that Newton's rings could be observed. This showed that there was a significant discrepancy between the calculated and the observed displacements, and the measured ratio was used for calibrating. It is 2.39×10^{-4}, $\pm$ 0.2%. The discrepancy is probably due to the thickness of the beam being of similar magnitude to the length BC, which is not allowed for in the theoretical analysis.

2.4 THE SPECIMEN HOLDER AND THE DIFFERENTIAL CONDENSER.

THE SPECIMEN HOLDER.

The specimen holder is made entirely of fused quartz and is shown in Fig. (17). The specimen is mounted in a metal thimble which is used to compensate for thermal expansion, and this rests in the bottom of the central tube. It is actually supported by the top face of a short length of quartz tube fused to the central tube, this face being ground flat and parallel to the ground face at the top of the holder. The silicone liquid is pumped through the two tubes at the right of the diagram and flows round the space between the central and outside tubes. The holder is designed so that the delivery tubes hang into the pump without making any physical contact, and mechanical vibration of the pump

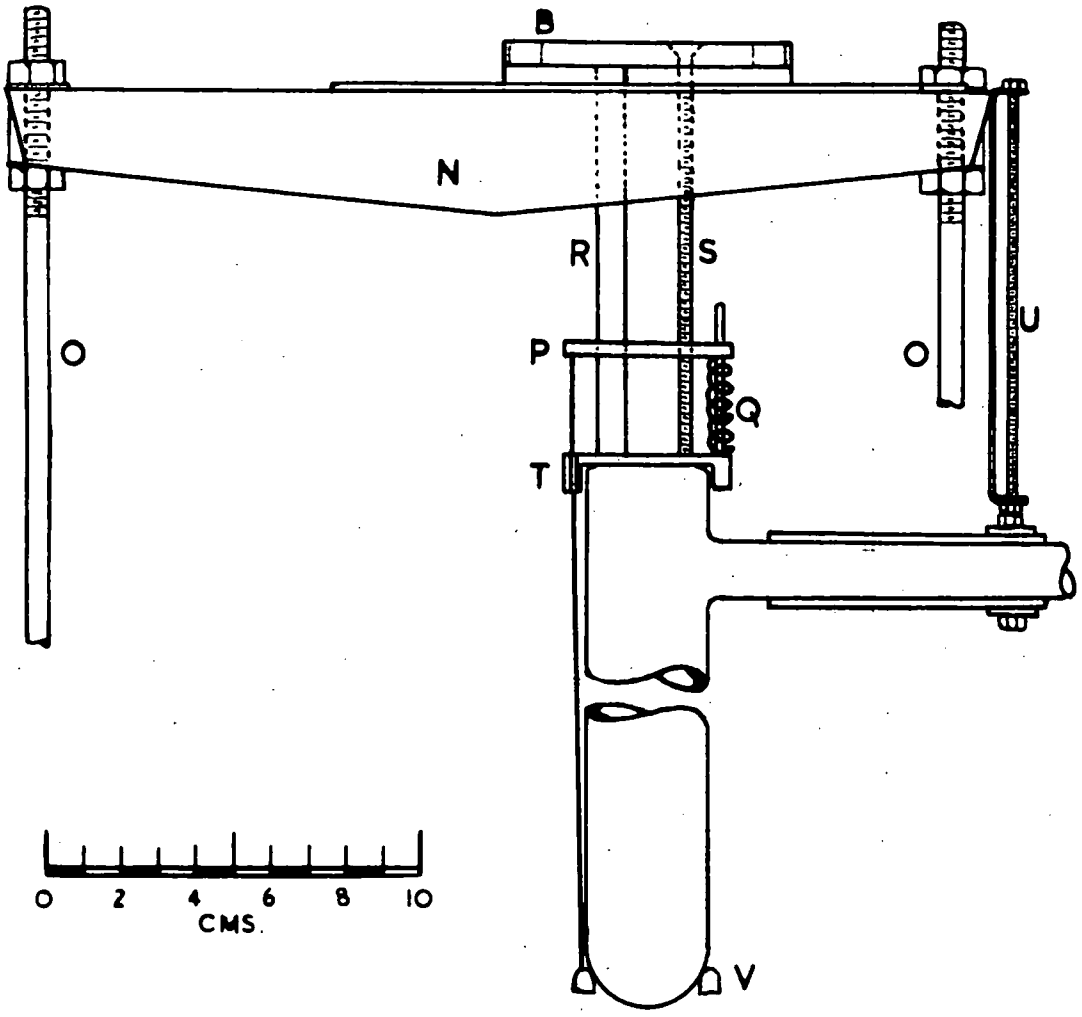

FIG.18. - The Mounting of the Specimen Holder.

is not transmitted to the holder.

The method of mounting the holder is shown in Fig. (18). The two rods R are made of fused quartz and rest against the ground upper face of the holder. Their upper ends are pressed against the brass plate B, which is actually made of two sections fastened together as shown. By this means it is possible to allow the legs of the condenser to bear onto the brass at the same height as the quartz bears onto the brass, and thermal expansion of B is effectively eliminated. The whole system is made rigid by the three screwed brass rods S which are fixed to the collar T and to the plate B. Three springs Q stand vertically on T, and a second ring P rests on these springs. From P there are three wires which pull vertically upward on the ring V, and by tightening the screws S the holder is forced into tight contact with the rods R, and the latter with B. The springs Q are introduced to allow for thermal expansion of the rods and the wires.

The plate B is mounted on a mu-metal disc mounted on the aluminium frame N, which is in turn supported by three vertical brass rods O mounted on the wooden base of the solenoid. The rods are screwed to allow the holder to be rigidly held in position and to be adjusted over a vertical range of about one inch.

It was originally intended that the holder should be supported by this system only, but incorporating three rods R.

However, it was found in practice that due to the weight of the side tubes of the holder when filled with the silicone liquid, it was impossible to keep the holder in correct vertical alignment while maintaining a reasonable amount of spring in the system. It was therefore necessary to support the holder by a further aluminium plate U attached to N, and this counteracted the weight of the side tubes. Although this aluminium expands thermally, the distortion introduced thereby is very small and is negligible along the vertical axis of the system.

The method of mounting adopted provides a continuous length of quartz from the specimen to the differential condenser. Displacement of the top of the specimen is carried to the moving plate of the condenser by a quartz rod, so that all thermal expansions are reduced to a minimum. It has been found desirable in practice to put an aluminium shield round R, S and P, and extending from B to T. This reduces any chance of temperature difference between R and the transmission rod.

THE TEMPERATURE COMPENSATOR.

To minimize the effect of changes in length of the specimen due to thermal expansion while under test, it is mounted in a metal tube with which it is in good thermal contact, and which compensates for length changes by expanding in the reverse direction to the specimen. This

principle has been used many times before, and at room temperatures it is only necessary to use one metal to compensate for expansion. Since the specimen is heated to temperatures greater than 300° C., however, it becomes necessary to find a compensating metal whose coefficient of expansion varies with temperature in a similar way to that of nickel. As an approximation, the length of a piece of metal at a temperature t° C. can be expressed as $l = l_0(1 + \alpha t + \beta t^2)$. Nickel is a particularly unfortunate metal to match in this respect since the ratio α/β is higher than for almost any other. This means that not only must a 2-element compensator be used, but that one of the compensating metals must act in the same direction as the nickel, the other in the opposite direction. The metals chosen were copper and aluminium, since both can be obtained in pure form quite easily, neither are ferromagnetic, and α/β for aluminium is appreciably less than for copper. For nickel, α and β may be considered constant for temperatures below about 350° C., and the anisotropy of expansion is small. Above 350° C., anomolous expansion becomes considerable, and expansion can no longer be represented in terms of the two constants.

For unit length of nickel, length a of aluminium and c of copper, compensation is obtained provided

$$\alpha_{Ni} + a\,\alpha_{Al} + c\,\alpha_{Cu} = 0$$

$$\beta_{Ni} + a\,\beta_{Al} + c\,\beta_{Cu} = 0$$

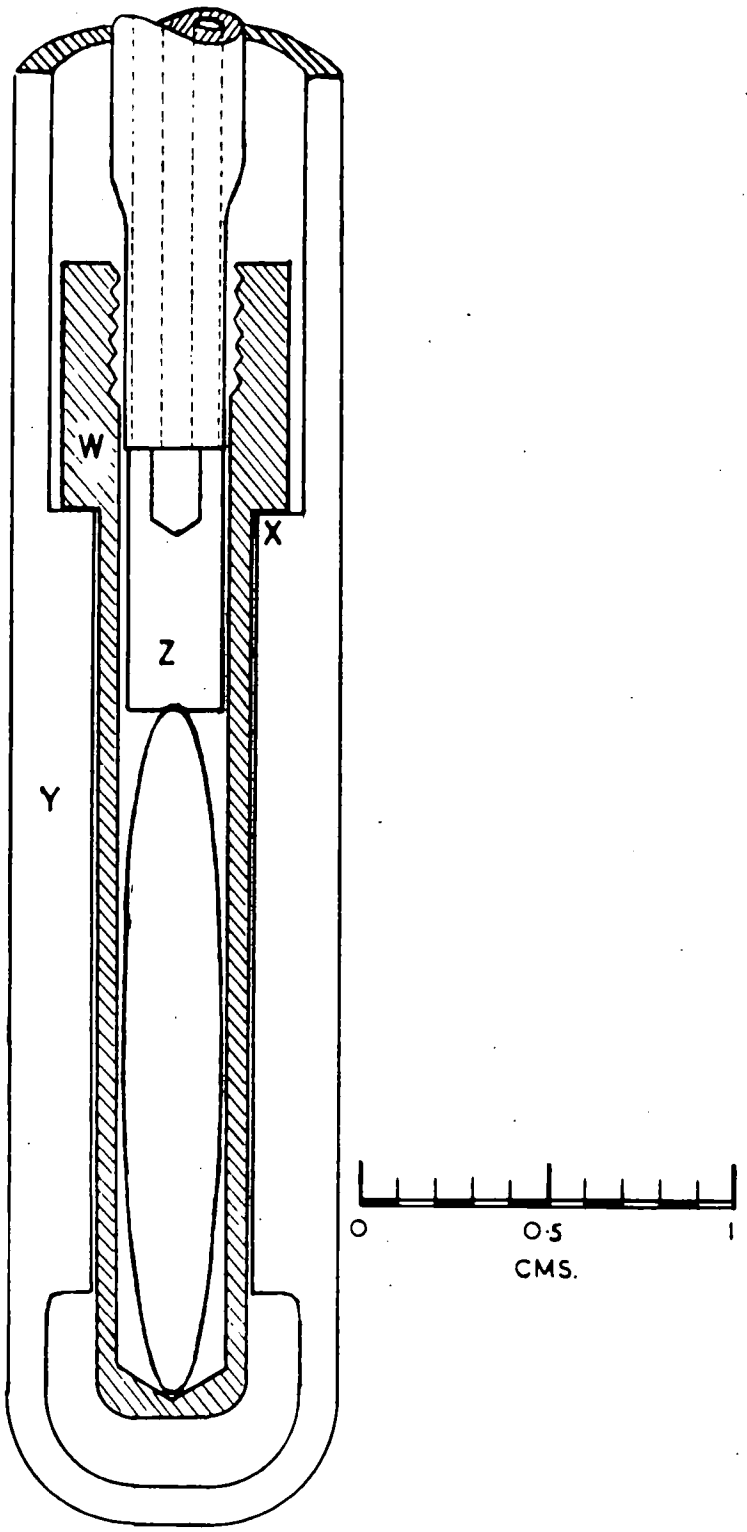

FIG.19. - The Temperature Compensator.

The values of the expansion constants are taken to be:

For aluminium $\alpha = 22.65 \times 10^{-6}$, $\beta = 9.5 \times 10^{-9}$

copper $\alpha = 16.2 \times 10^{-6}$, $\beta = 9.5 \times 10^{-9}$

nickel $\alpha = 12.54 \times 10^{-6}$, $\beta = 8.75 \times 10^{-9}$

Solving for a and c, $a = 0.370$, $c = -1.290$

The copper must therefore act in opposite direction to the nickel and the aluminium. The design adopted is shown in Fig. (19). The cylindrical copper sheath W rests on the ground face of the quartz tube X which is fused to the inside of the central tube Y of the specimen holder. The ellipsoidal nickel specimen rests in the copper, and the aluminium cylinder Z is on top of the nickel. The ellipsoid is maintained vertical as its upper end is held in the small notch in the centre of the lower face of the aluminium. The hole in the upper end of the aluminium is to contain the thermocouple junction which projects from the twin bore tube carrying the thermocouple leads. The primary function of this tube is to transmit the displacements of the specimen to the differential condenser. In calculating the appropriate sizes of the elements forming the compensator, due allowance has to be made for the fact that the ellipsoid is not held at its ends, but at points slightly displaced from them.

The specimen and compensator are immersed in MS 550 silicone liquid in order that temperature gradients may be

reduced to a minimum. This has the additional effect of lubricating the sliding contact between the aluminium cylinder and the wall of the copper tube.

THE DIFFERENTIAL CONDENSER.

The condenser which was used for making magnetostriction measurements was actually the second one constructed for this purpose. It is instructive to consider the first, since several lessons were learned by its behaviour under test. The central moving plate was of brass, 6.5 mm. thick and 3.5 cm. diameter. The fixed plates were also of brass, and were separated by a ring of "Tufnol". Movements were transmitted to the centre plate by a "Tufnol" rod, $\frac{1}{4}$ inch diameter, which was maintained in the correct alignment along the axis of the condenser by means of ball bearings mounted in the two fixed plates. The centre rod was pressed by a helical spring against the body whose displacement was to be measured. This design proved to be unsatisfactory in two respects. Firstly, it was very sensitive to temperature changes. Further, owing to the relative softness of the "Tufnol" rod, it was impossible to set the ball bearings so that displacement of the rod perpendicular to its axis was prohibited. Any such displacement had a large effect on the steadiness and sensitivity of the condenser since it produced a large effective movement of the centre plate relative to the fixed plates. If the bearings were made

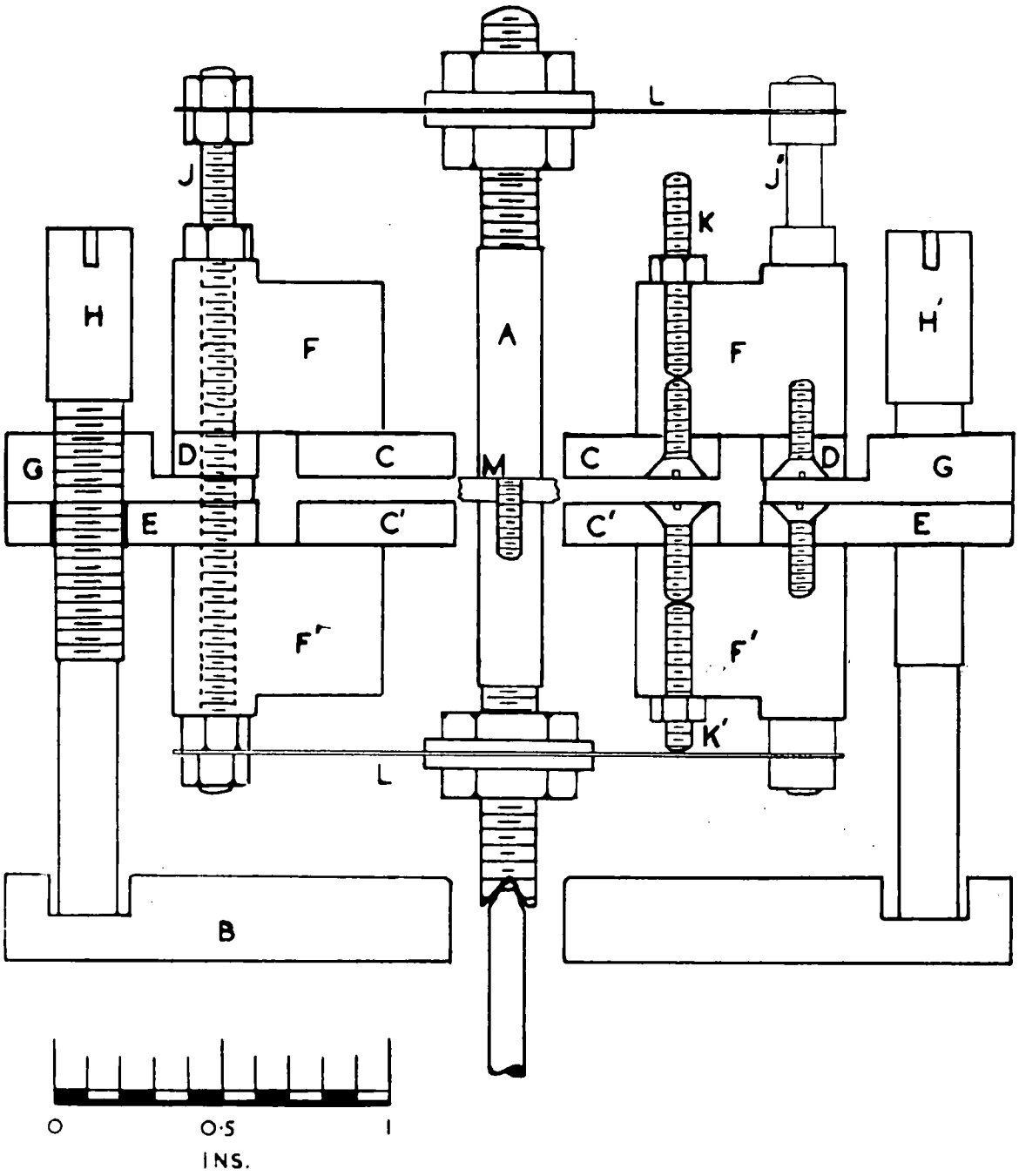

FIG.20. - The Differential Condenser.
(note the 3-fold symmetry, H' and J' are not in the position shown).

tight enough to prohibit this movement, then the rod was prevented from moving freely along its length, and mechanical hysteresis was appreciable.

The arrangement of the second condenser is shown in Fig. (20). To minimize temperature effects, all parts in the condenser whose expansion could cause spurious voltage outputs are made of "Invar". These comprise the central moving plate M, which is not fully shown in the figure, the central rod A on which M is mounted, the three spacers G which maintain the correct distance between the fixed plates C C', and the three screws H which support the whole condenser. Since the plates C C' could not be directly separated by "Invar", they are mounted onto the "Tufnol" blocks F F' which are separated by brass rings D and E as well as the spacers. These brass rings and the plates C C' were machined together while fixed to the blocks so that they should be exactly the same thickness. The spacers are tapped so that a screw H can be screwed into each, and these screws support the whole condenser, allowing it to be raised and lowered by some 8 mm.

In order that the rod A may move freely along its length, it is supported by two flexible plates of steel L, each 0.005 inch thick. These plates are held by the three screws J at a diameter of $1\frac{3}{4}$ inches, and exert very small constraining forces on the rod parallel to its length. It is, however, virtually impossible to displace the rod

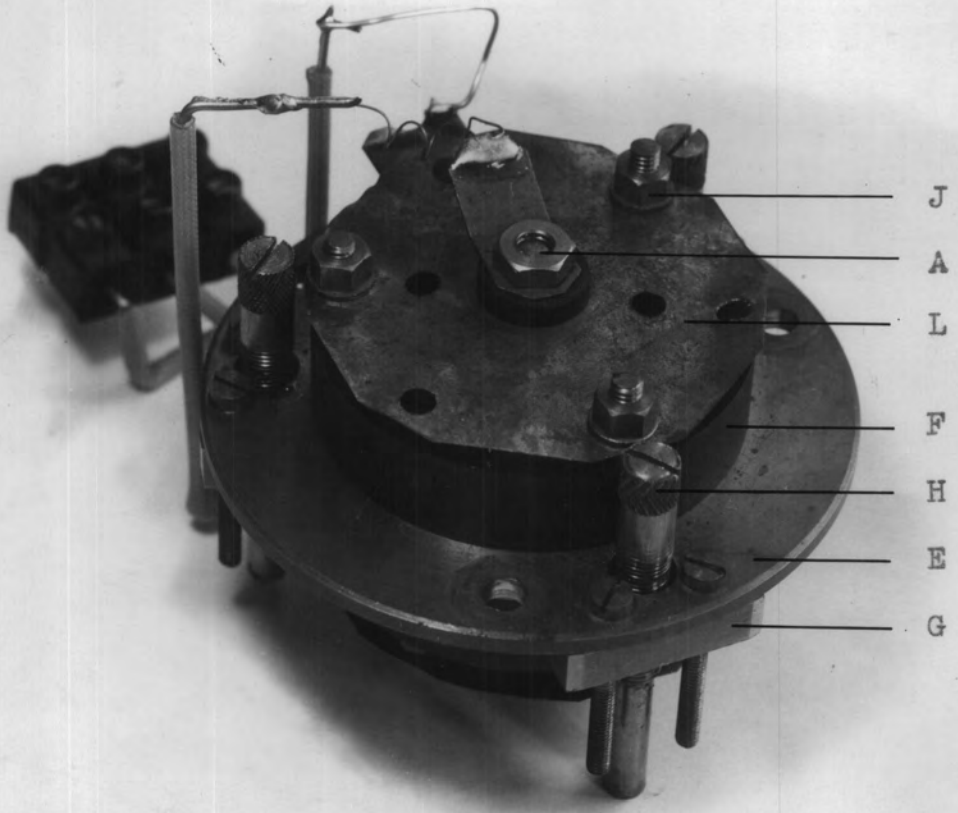

PLATE 1. - The Differential Condenser.

(the lettering corresponds to that in figure 20.)

laterally. In order to preserve the insulation the spring plates do not bear directly on A, but are held off by insulators. There is a slight degree of lateral movement here when the insulators are not screwed tight, and this permits of adjustment so that the central plate may be set parallel to C and C'. The designed separation of the plates is 0.2 mm. on each side. Since it is never possible to set the central plate exactly parallel, nor is it mounted perfectly straight onto the rod A, the separation varies from point to point, resulting in a slight increase of sensitivity above the designed figure.

The leads to C and C' are brought out by screws K and K', while A forms the connection to the moving plate.

The flexible plates L are at earth potential and the plates C and C' are therefore well screened. Owing to changes in length of the "Invar" due to the small field produced by the solenoid near the condenser, it has been necessary to put the condenser in a mu-metal box. This also acts as an electrical and thermal screen.

Three 6B.A. screws are fixed to the brass plate B of Fig. (18) and pass through the ring E of the condenser. On each of the screws a piece of rubber tubing 1 cm. long and 8 mm. diameter is held in compression between the ring E and a 6 B.A. nut. This forces the 3 screws H firmly against the brass plate B. Movement is transmitted to A

by a quartz rod which is ground to conical shape at its upper end, forming a tight fit in the end of A. This rod carries the leads to the thermocouple which is in contact with the temperature compensator. The leads are brought out of the side of the rod through two small holes ground in the side with a fine wheel.

The three "Invar" rods supporting the condenser have screw threads of 40 turns per inch. Tests show that in order to maintain an accuracy of at least 1%, it is necessary that the two balancing condensers should be within 3% of their maximum values. Hence the differential condenser must be adjustable to 3%. This corresponds to a rotation of any one of the three screws of 1/30th of a turn, which it is quite possible to make with a screwdriver. Movements of this order applied to any one of the three screws will not bring the condenser axis out of the vertical an amount sufficient to affect the accuracy.

SOME POSSIBLE ERRORS ASSOCIATED WITH THE CONDENSER.

Due to the method of mounting the central rod of the condenser, there is a restoring force which tends to oppose the displacement of the middle plate. Calculation shows that for a displacement d of the centre of a circular disc of radius a and thickness t made of material of Young's modulus E, a force P is required where

$$P = \frac{t^3 E}{a^2} \cdot d$$

For the two spring steel discs used to support the rod, the necessary thrust is $P = 2.6 \times 10^6$ d dynes, where d is measured in cms. This thrust has two effects. It causes a systematic error in the calibration of the condenser, and an error in the measurement of magnetostriction.

The error of displacement introduced on the calibrating beam is approximately $\Delta d = l^3 P/3EI$

where l is the length AP of section (2.3), and I is the moment of inertia of cross-section of the beam. For the beam used, this becomes $\Delta d = 3.75 \times 10^{-10} P$

$= 10^{-3} d$

so that the error introduced may be neglected for the purposes of the experiments undertaken.

The error introduced into the magnetostriction measuring apparatus will be caused by the change in thrust along the displacement rod and along the specimen holder and its supports, which will cause elastic deformation of the quartz. Since these will act in opposition, the effect cannot be greater than that caused in the displacement rod itself.

Taking the rod to be 20 cm. long and 0.3 cm. diameter, and E for fused quartz as 0.67×10^{12} dynes/cm^2, the contraction caused by an increase in stress will be

$$\Delta d = 4.5 \times 10^{-10} P$$

and using the value of P resulting from a condenser displacement d,

$$\Delta d = 1.1 \times 10^{-3} d$$

The effect may again be neglected.

2.5 DESIGN OF THE SOLENOID.

PRELIMINARY CALCULATIONS.

The solenoid was required to produce a uniform magnetic field of up to 1000 oersteds over a length of 2 cm., and to be not longer than 20 cm. The D.C. generator available can produce up to 3 amps at 300 volts.

Consider a coil of length L cm., internal radius R_1 cm. and external radius R_2 cm., wound with a wire of total radius including insulation r cm.

If the coil is of infinite length, the magnetic field at its centre due to a current I is

$$\frac{4\pi I}{10} \times \frac{1}{2r} \times \text{(number of layers)} \quad \text{oersteds} \qquad (21)$$

For I = 3 amps, then for a field of 1000 oersteds

$$\frac{R_2 - R_1}{r^2} = \frac{10^4}{3\pi}$$

The finest gauge wire suitable for carrying 3 amps is 20 s.w.g. copper. Since large power dissipation in the coil is probable, the temperature may rise appreciably, and it was considered desirable to use glass insulation; the wire chosen was "Lewmexglas" for which r = .061 cm.

$$\therefore R_2 - R_1 = \frac{10^4}{3\pi} (.061)^2 \text{ cm.} = 4 \text{ cm. approx.}$$

To enable all apparatus to be slipped within the solenoid, R_1 may be taken as 3.5 cm., hence R_2 = 7.5 cm.

The total length of wire in the solenoid is

$$\int_{R_1}^{R_2} \frac{L}{2r} \cdot \frac{2\pi R}{2r} \, dR$$

$$= \frac{\pi L}{4r^2}\left(R_2^2 - R_1^2\right) = 9.3 \times 10^3 \, L$$

The resistance per cm. of the wire is 2.58×10^{-4} ohms. Hence the total resistance of the solenoid is 2.4 L ohms, which for L = 20 becomes 48 ohms. This is quite satisfactory since there will be additional resistance due to the supplementary coils mounted at the ends of the solenoid in order to improve the uniformity of field at the centre.

The distortion in field near the centre of the solenoid may now be calculated. The method adopted is as follows. Three points on the axis of the solenoid are considered, A, B and C. They are respectively 10, 10.5 and 11 cms. from one end of the solenoid, the solenoid being symmetrical about its centre. The fields are calculated at these three points, and by a suitable arrangement of the coil windings the fields may be made equal. It is more difficult to calculate the lateral distortion of the field from uniformity, but it is known that for an axially symmetrical system of coils, the uniformity of the field along and perpendicular to the axis is of similar magnitude. Moreover the specimen diameter will not be greater than 1/10th of its length, so that if

the fields at A, B and C are equal there should be a uniform field over the entire body of the specimen.

The calculations are based on the standard formula for the field at a point on the axis of a uniformly wound coil. If this coil has dimensions as shown relative to the point P (Fig. 21), then

$$H = K'\left[f'(l_2, x) - f'(l_1, x)\right] \qquad (22)$$

where $K' = \frac{2\pi n I}{10}$ and $f'(l, x) = l \log_e \left[\frac{x + (x^2 + l^2)^{1/2}}{y + (y^2 + l^2)^{1/2}}\right]$

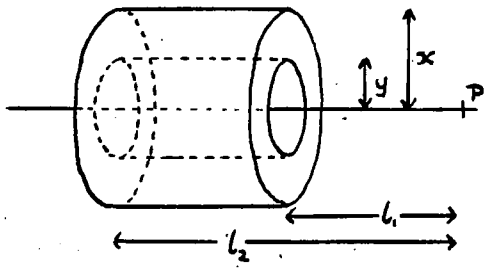

Fig. 21.

H is the field in oersteds, n the winding density in turns/cm^2. I is the current in amps and all dimensions are in cms.

Since it was necessary to use 7-figure logarithm tables, it was decided to use tables to base 10, and then

$$H = K\left[f(l_2, x) - f(l_1, x)\right] \quad \text{where } K = 2.3026 \times \frac{2\pi n I}{10} \qquad (23)$$

$$f(l, x) = l \log_{10} \left[\frac{x + (x^2 + l^2)^{1/2}}{y + (y^2 + l^2)^{1/2}}\right]$$

Under conditions of full current, I = 3, K = 298 oersteds. All field values were worked out without multiplying by K until the final stage.

BASIC DESIGN.

Heddle (1952) states that to arrange a coil having 2n points on the axis with the same field as at the centre, then n supplementary coils are required at each end. He assumes, however, that the widths of these coils are fixed, but if the widths are taken as variables in addition to the depths perpendicular to the axis, then there are two variables per coil, so that to equate the fields at A, B and C requires only one pair of coils.

For the main solenoid, the calculated fields are

$$h_A = 3.03942$$

$$h_B = 3.03738$$

$$h_C = 3.03155$$

The fields denoted by h must be multiplied by K to give the absolute value, H for I = 3 amps being 905 oersteds. This is satisfactory since the compensating coils will add sufficient field to make the actual field approach 1000 oersteds.

$$\frac{h_A - h_B}{h_A - h_C} = 0.258$$

The initial stage in the design of the compensating coils used a trial and error method. Calculations showed that a coil of 10 cm. to 12 cm. outer radius and 3.5 cm. to

5 cm. in length at each end would give the correct negative value of $h_A - h_B$, and various lengths of coil were then tried with a constant outer radius of 11 cm. to find the one giving the best ratio $(h_A - h_B)/(h_A - h_C)$ which should equal 0.258. It was found that a length of 4 cm. gave 0.263. Calculation for various outside diameters, using the same wire and current as in the main solenoid gave the following results (Table 2).

TABLE 2.

For supplementary coils 4 cm. in length at extreme positions. Inside radius 7.5 cm. Varying outside radius.

Outside Radius	h_A	$h_B - h_A$	$h_C - h_A$	Ratio	Total h_A	Error $(h_A - h_B)/h_A$	Resistance (Ohms)
11.0	.57194	.00163	.00624	.263	3.6113	$12.7\ 10^{-5}$	29.6
12.4	.80696	.00187	.00715	.263	3.8464	$4.2\ 10^{-5}$	44.5
13.5	.98920	.00197	.00753	.262	4.0286	$1.5\ 10^{-5}$	57.5
14.2	1.10342	.00200	.00767	.261	4.1428	$0.7\ 10^{-5}$	66.4
15.0	1.23195	.00202	.00785	.258	4.2713	$0.2\ 10^{-5}$	76.8

It can be seen that a uniformity of at least 1 in 10^4 can be obtained with a pair of supplementary coils of outside radius 12.5 cms., and this value was adopted.

In order to make the solenoid as versatile as possible, it was provided with tappings so that different layers of the winding could be energized separately. For different values

of the external diameter of the main coil the corresponding values of ($h_A - h_B$) and ($h_A - h_C$) were calculated, and similar values were found for different values of the diameter of the compensating coils. Hence by drawing graphs of ($h_A - h_B$) and ($h_A - h_C$) against external radius for both coils, and equating the values of $|h_A - h_B|$, the correct diameter of the compensating coils could be found for any number of layers of the main coil.

TABLE 3.

For solenoids 20 cm. long, 3.5 cm. internal radius.

Radius Outside cms.	h_A	$h_A - h_B$	$h_A - h_C$	Ratio
4.5	0.80630	.00036	.00146	.246
6.0	1.95956	.00109	.00439	.248
7.5	3.03942	.00203	.00787	.258

TABLE 4.

For supplementary coils 4 cm. long, 7.5 cm. internal radius.

Radius Outside cms.	h_A	$h_B - h_A$	$h_C - h_A$	Ratio
8.5	0.15693	.00072	.00257	.280
9.5	0.32062	.00117	.00443	.265
11.0	0.57194	.00163	.00624	.263
12.4	0.80696	.00187	.00715	.263
13.5	0.98921	.00197	.00753	.262
14.2	1.10342	.00200	.00767	.261
15.0	1.23195	.00202	.00785	.258

From the graphs drawn from these tables the data for Table 5 was found.

TABLE 5.

Tappings on the main and supplementary coils.

No. of Layers	Radius Outside cms.	End Coil Radius cms.	End Coil Layers	Total Resist-ance ohms.	Total h_a	Total H_a (Oersted) X
4	3.982	7.6	2	5.8	0.41	124
8	4.465	7.9	4	12.2	0.84	250
12	4.946	8.25	6	19.3	1.29	385
18	5.67	8.95	12	33.4	1.95	580
24	6.39	9.95	20	52.2	2.65	787
30	7.11	11.45	33	77.9	3.40	1012
33	7.48	12.5 XX	41	95.4	3.85	1146

X For I = 3 amps.

XX Incomplete compensation.

MECHANICAL DESIGN OF THE SOLENOID.

The former on which the solenoid is wound is made up in three sections, the main coil and the compensating coils. They are all made of brass, the end plates being $\frac{1}{8}$ inch thick and the cylindrical section 1/16th inch. The main former stands vertically on an oak base, and the lower compensating coil is mounted with its lower end flush on the same base. The upper coil is attached at its upper end to the top face of the main coil by three brass plates so that the whole coil is quite rigid.

Between the windings and the formers there is a layer of insulation. On the end plates this takes the form of fibre sheet 1.5 mm. thick; over the cylindrical surface is wound glass tape 0.007 inches thick.

The windings are brought out of the formers through polythene insulators onto a terminal board from which any of the windings may be energised.

THE WINDING OF THE SOLENOID.

The main coil was wound on a winding machine, but automatic feed-in of the wire could not be used as it gave serious non-uniformity of winding at the ends. The different layers were separated by insulation only when tappings were taken out through the end plates, and this insulation took the form of a single winding of glass tape 0.007 inches thick. It was found that this gave a fairly smooth base for further windings, as without insulation any winding defects tended to repeat themselves on successive layers.

TABLE 6.

The main coil windings.

Winding	Layers	Actual		Designed	
		Turns	Resistance	Turns	Resistance
1	4	640	4 ohms	664	4.1 ohms
2	4	622	4.5	664	4.7
3	4	638	5	664	5.1
4	6	933	8	996	8.8
5	6	931	9	996	10.0
6	6	929	10	996	11.0
7	4*	625	7.2	498	6.1

* Designed for 3 layers.

The end coils were wound on a lathe as their large diameter prevented their being mounted on the winding machine. No intermediate insulation was used. It was very difficult to make the windings uniform as any defects at the end plates tended to progress to the centre on successive layers. As a result, the outer windings were fed on without conforming to a strict number of layers.

TABLE 7.

The end coil windings.

Winding	Layers	Top Coil		Bottom Coil		Design	
		Turns	Resistance Ohms	Turns	Resistance ohms	Turns	Resistance ohms
2	2	61	0.8	63	0.8	66	0.85
3	4	118	1.6	122	1.6	132	1.85
4	6	174	2.5	173	2.5	198	2.65
5	8	241	4.0	235	4.0	264	4.4
6	13	358	6.3	358	6.3	429	7.4
7	8	193	4.0	197	4.0	264	5.7

TABLE 8.

Total resistance of windings (In Ohms)

Winding	1	2	3	4	5	6	7
Resistance	4.1	6.2	8.2	13.1	16.7	22.8	15.3
Total Resistance	4.1	10.3	18.5	31.6	48.3	71.1	86.4

ACTUAL PERFORMANCE OF THE SOLENOID.

Tests have been carried out to determine the field distribution in the solenoid. The search coil used was 1.85 cm. in length and had an overall diameter of 1.185 cm.

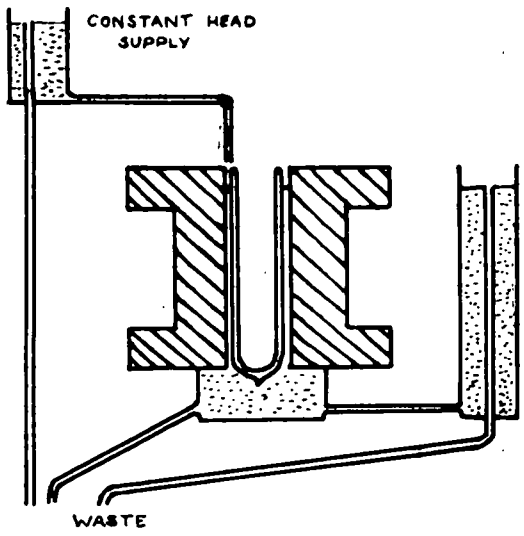

FIG.22. - The Cooling System.

FIG.23. - Distortion of Field along the Axis.

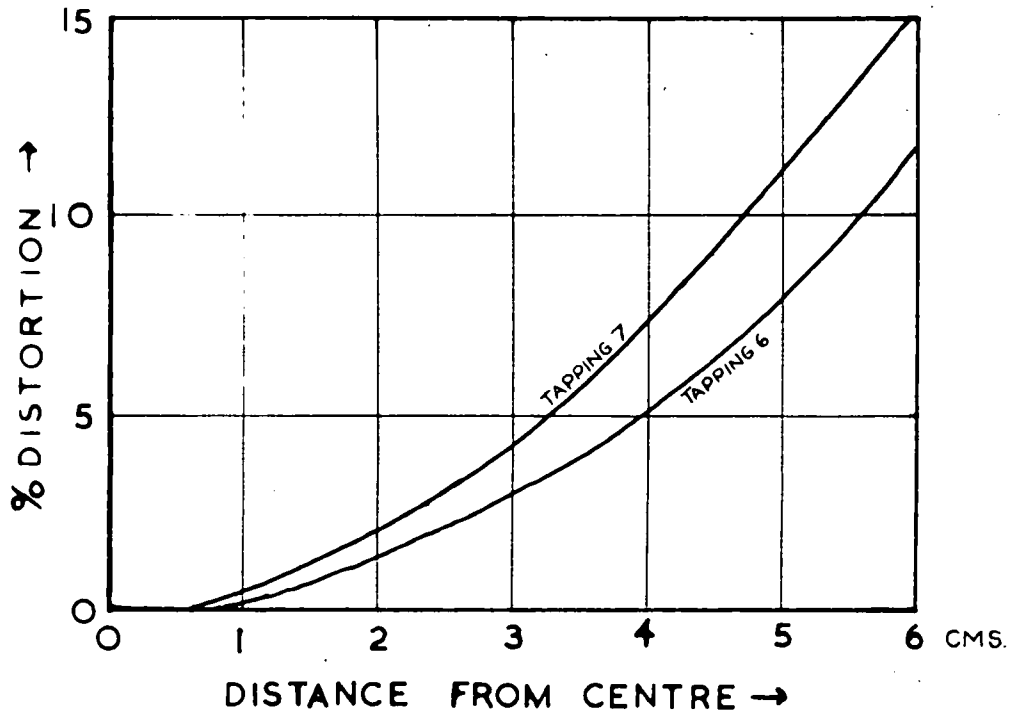

The estimated effective area of the coil was 186 cm.^{2} A Grassot fluxmeter of sensitivity 15,000 Maxwell-turns per division was used in conjunction with the search coil, and the meter deflection was measured with a lamp and scale at 1 metre. Using a long narrow solenoid, this system was calibrated, and the sensitivity found to be 35 oersteds per cm.

TABLE 9.

Field on axis of solenoid in Oersteds/Unit current

Distance from centre	Tapping 6		Tapping 7	
	Field	% Distortion	Field	% Distortion
0	295	0	331	0
0.5 cm.	295	0	331	0
1 "	295	0	331	0
1.5 "	293	0.7	327	1.3
2 "	291	1.3	324	2.3
2.5 "	288	2.3	322	3.0
3 "	285	3.3	320	3.7
3.5 "	281	4.7	315	5.3
4 "	279	5.3	310	7.0

Table 9 shows the results obtained, and the % distortion from the maximum field is shown in Fig. (23). This shows that distortion is negligible when the coil is moved over

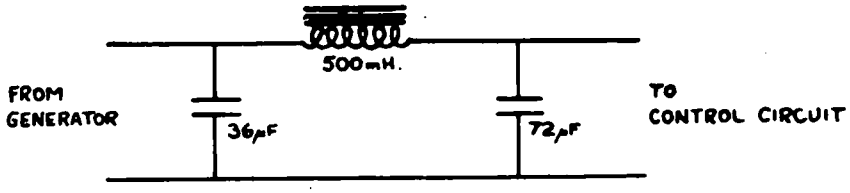

FIG.24. - Smoothing Circuit for Solenoid D.C. Supply.

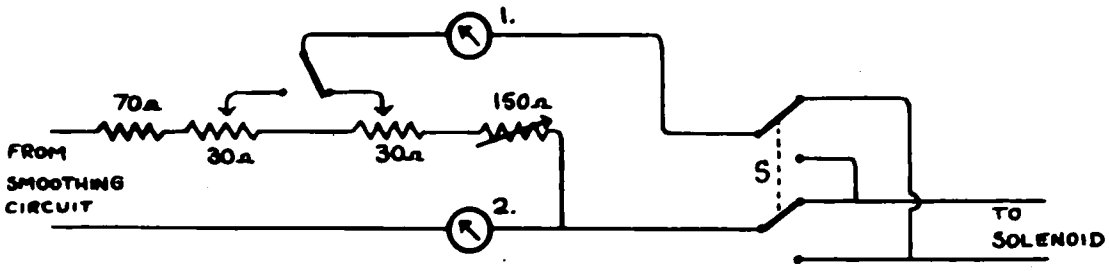

FIG.25. - Control Circuit for Solenoid D.C. Supply.

1.5 cm., which means that the field is uniform over about 3 cm. The actual field is less than the designed field due to the reduction in winding density.

THE D.C. SUPPLY AND CONTROL.

For the present series of experiments the minimum step by which the field needs to be adjusted is about 1 oersted; owing to the demagnetizing effect this produces at low fields a much smaller change of field in the specimen. At room temperatures, in the [111] direction, the effective field change corresponding to this is about 1/20 oersted.

The D.C. generator has a considerable ripple, mainly of frequency 645 c/s., but also containing a component of frequency 41 c/s. This falls as the current from the generator is increased, and normally the current drawn is between 2 and 3 amps in order that the ripple may be maintained at a reasonable amount. The circuit shown in Fig. (24) is used to reduce the ripple as far as practicable.

This smoothing circuit eliminates the 645 c/s ripple almost completely, but when a current of 3 amps is drawn it leaves a residue of about 1 volt R.M.S. at 41 c/s.

To control the current the circuit shown in Fig. (25) is adopted. The intermediate tappings on the solenoid are not normally used.

Meter No. 1 is a 4 inch 500 ma. moving coil meter adapted and re-calibrated for use up to 3 amps, and is used to

measure the current through the solenoid. Meter No. 2 is similar and measures the total current drawn from the generator. Using the control circuit the current through the solenoid is continuously variable from 0 to 3 amps while the current from the generator is maintained between 2 and 3 amps.

The reversing switch S in Fig. (25) allows the current through the solenoid to be reversed. By rapidly changing the switch position while at the same time decreasing the magnitude of the current through the solenoid, the specimen can be demagnetized to the reference state described in section (1.6). A more rapid reversal was attempted by application of the 50 c/s. mains supply to the solenoid through a variable transformer. However, at 50 c/s., it was found that the real component of the impedance of the solenoid was 300 ohms. The increase of 200 ohms above the D.C. resistance was almost certainly due to the eddy currents produced in the brass former by the rapid variations of magnetic flux through it. The high real impedance prevented the passage of sufficient current through the solenoid to magnetize the specimens to saturation, consequently the use of 50 c/s alternating current for demagnetizing the specimens was not possible.

THE COOLING SYSTEM.

In order to maintain the solenoid at a reasonable temperature, a stream of water is passed down the inside

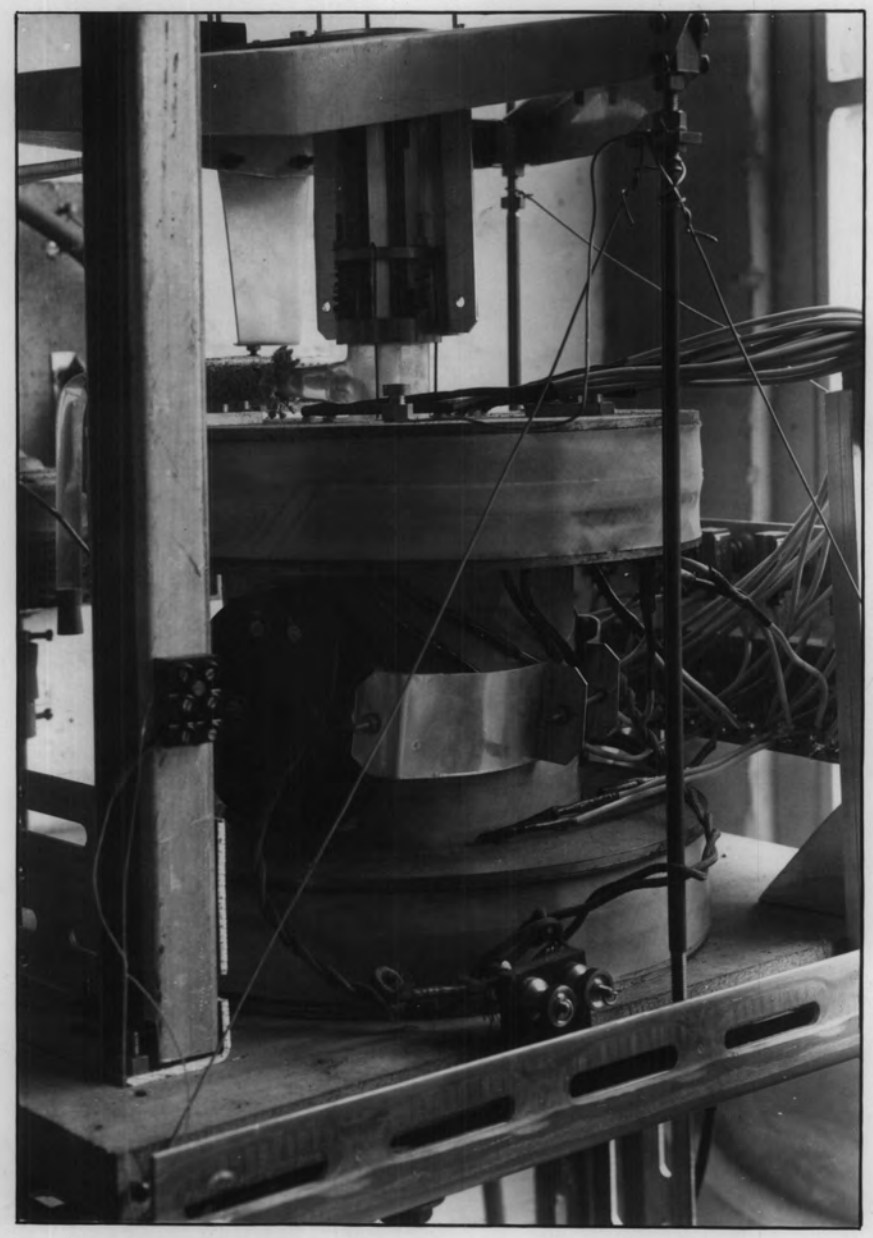

PLATE 2. - The Solenoid.

The specimen holder is in position, and the compensating coils for the horizontal field are mounted on the solenoid.

of the former. A brass reservoir is clamped to the bottom of the inner former and the system kept watertight with a rubber gasket. The reservoir is emptied into the waste system, and water flows in from a constant head device. A special arrangement is made to guard against overflow as shown in Fig. (22), opposite page 76.

The constant head is about 3 feet above the level of water in the solenoid, and this provides a rate of flow of about 30 cc. per second. With 1000 watt heat dissipation this corresponds to a temperature rise of 8° C., although parts of the windings themselves must be hotter than the actual former.

COMPENSATION FOR THE EARTH'S MAGNETIC FIELD.

Measurements were made of the earth's magnetic field at the exact position where the specimen was placed for magnetostriction measurements. The horizontal component H was found by Schuster's method using a tangent galvanometer, and the vertical component V from H with a dip circle. The values found were

$$H = 0.236 \text{ oersteds}$$

$$V = 0.473 \text{ oersteds}$$

Compensation was made for these two fields. For the vertical field this was done by putting an additional current of 13 ma. through the inner winding of the solenoid. For the horizontal field a pair of coils was mounted on the solenoid,

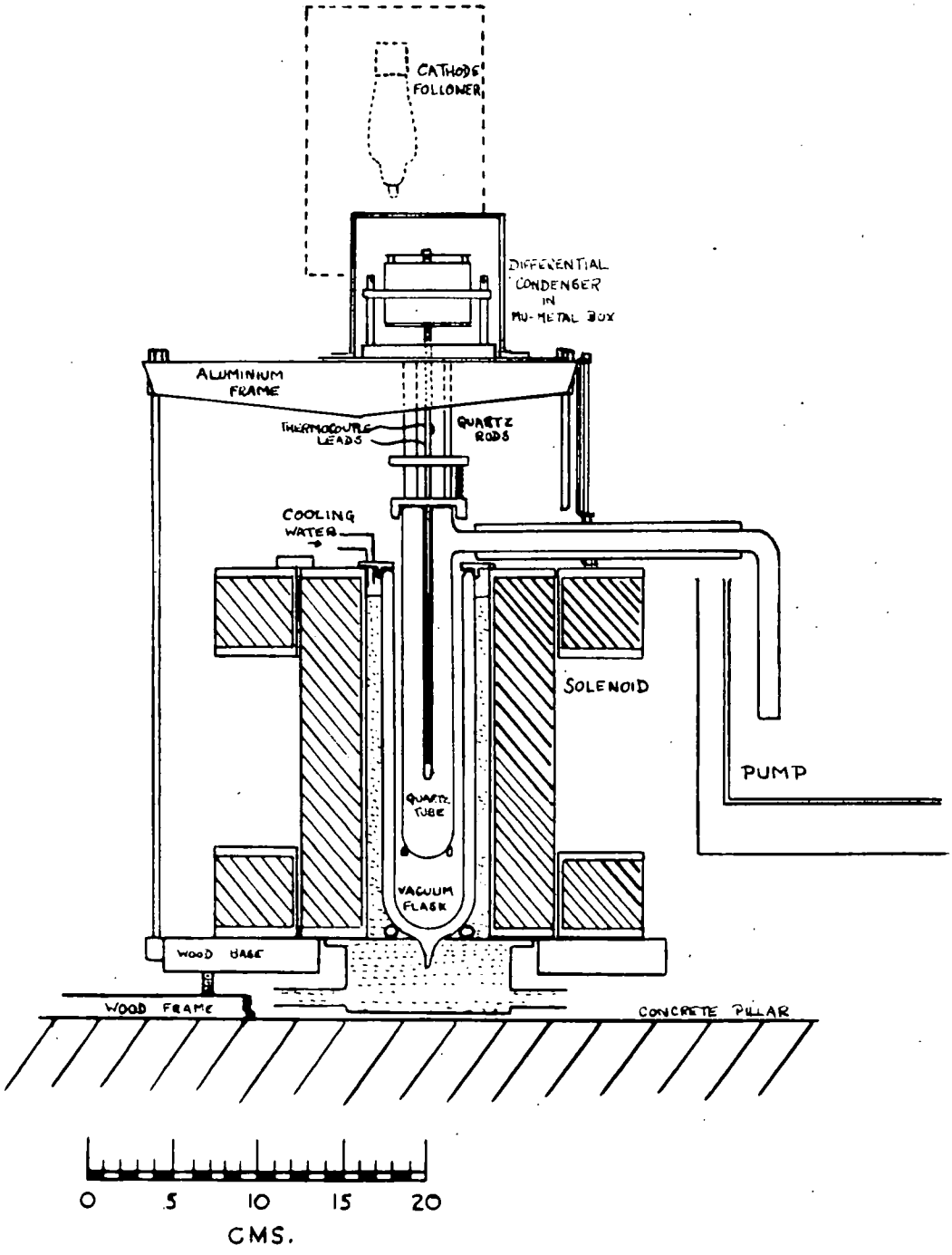

FIG. 26. - General arrangement of apparatus for High Temperature Magnetostriction Measurements.

the centre of each coil being 8 cm. from the centre of the solenoid, and the diameter of each being 18 cm. These give a horizontal field at the centre which is very nearly uniform, there being a 2% variation from the central value at 5 mm. from the centre. With 21 turns on each coil, the current necessary for compensation was found experimentally to be 0.4 amperes.

In practice it was found that even with the most sensitive measurements there was no detectable difference between the results obtained with and without compensation of the earth's magnetic field.

2.6 DESIGN OF THE CIRCULATION SYSTEM AND MEASUREMENT OF TEMPERATURE.

In order that the specimen may be maintained at the desired temperatures, the silicone liquid MS 550 must be pumped continuously through the specimen holder. The latter cannot be allowed to touch the pumping system at any point, or mechanical vibrations of the pump would be transmitted to the specimen and the extensometer. The circulating system constructed used the principle of the syphon, and the pump itself merely maintains a difference of levels between two cups into which dip the two side arms of the specimen holder. The pump is mounted in an aluminium box which is fixed to the wall of the laboratory, and is not connected in any way to

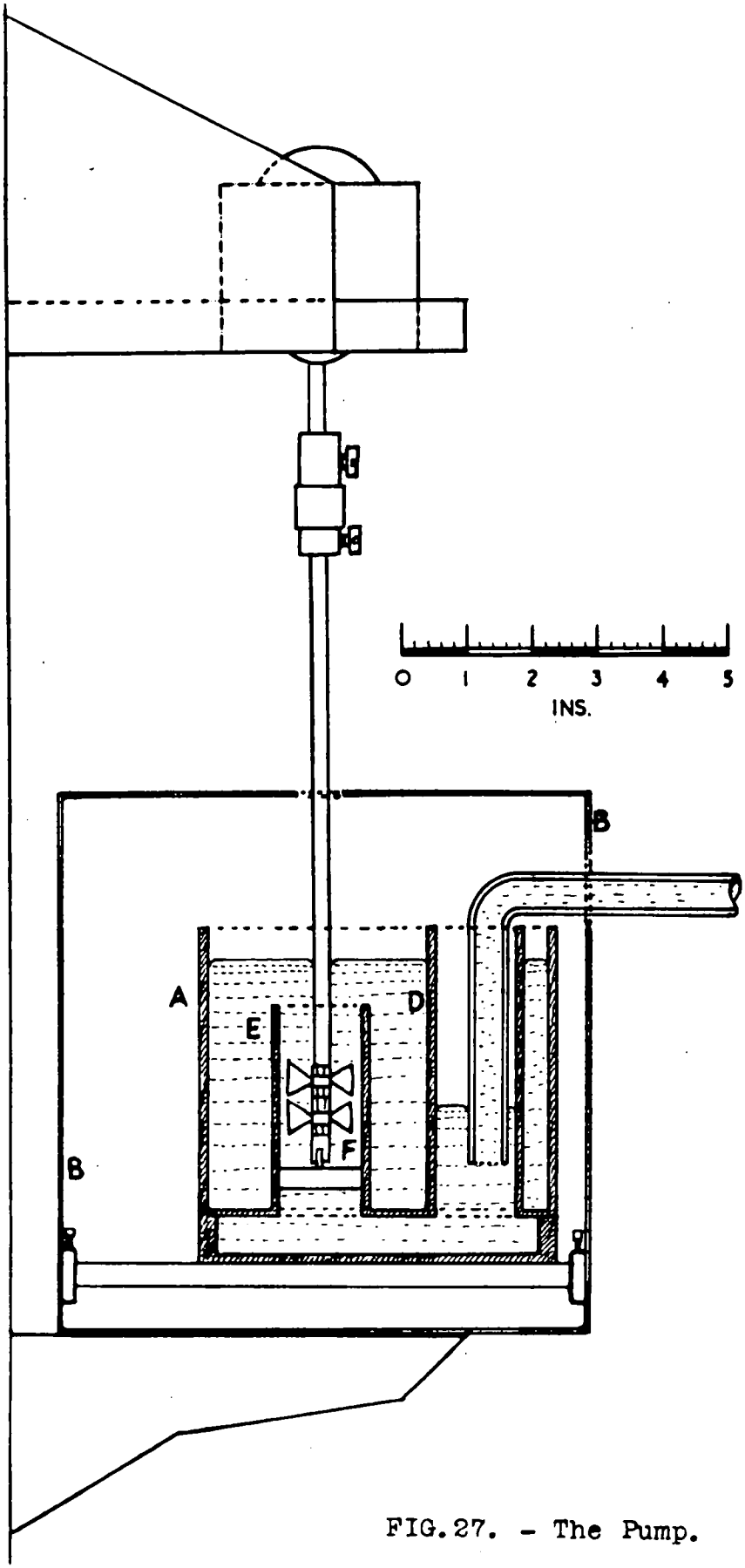

FIG. 27. - The Pump.

the galvanometer pillar on which the measuring apparatus is mounted.

A cross-section through the pump is shown in Fig. (27). A is a heavy brass box with walls of 3/16" and 1/8" brass, which is mounted inside the aluminium box B on two 5/16" rods of Pyrex glass. The brass box contains about 1000 cc. of the MS 550 liquid, and the whole has a thermal capacity of about 800 cals/^{o}C. The box has a false bottom, into which are fitted two vertical brass tubes of 1¼" internal diameter, the tube D being offset from the centre line of the box. By means of the paddle F, which is rotated by a small 20 volt motor, the liquid is pumped up the tube E and the level in D is consequently depressed. One of the side tubes of the specimen holder dips into the liquid in the tube D, the other dips into the liquid in the remainder of the box.

The liquid is heated by a coil of Nichrome wire which is mounted in a Pyrex glass spiral and slips over the tube E. For clarity this is not included in the figure. The 50 c/s alternating current through this wire is supplied by a variable transformer which can give from zero to 250 volts, and at 250 volts the heat generated by the coil is 1000 watts. The pump is thermally insulated from the aluminium box B by glass wool, so that heat loss from the sides is small. Most of the heat loss at temperatures above 200^{o} C. is caused by escaping vapour, for it is impossible to seal the pump

since no part of it must touch the specimen holder tubes. A brass lid prevents most of the vapour from escaping, and the aluminium box also has a lid. With the 1000 watt heating coil, it is possible to heat the liquid in the pump to its boiling point, namely 405° C. The specimen will not reach this temperature due to heat loss along the sides of the holder, but when these tubes are lagged with asbestos tape, the temperature difference between the pump and the specimen is only 20° C. at 350° C.

To allow for thermal expansion of the silicone liquid, a glass tube is taken from the pump to the reservoir of 400 cc. capacity which can be raised or lowered to maintain the correct depth of liquid in the pump. By means of a side tube let into this connecting tube, bubbles of air and vapour can be released, and the amount of liquid in the system increased; this is necessary since a certain amount of vapour is lost at temperatures above 200° C.

It was originally intended to use a temperature controller to maintain the temperature of the system constant. In a pumping system such as this, temperature fluctuations of the specimen may be caused by fluctuations in the pump itself, or variations in the heat loss of the liquid being pumped to the specimen. Long-term effects are not very important, since it requires only a few minutes to make a complete set of magnetostriction measurements at one temperature. Short-term effects in the pump itself are

eliminated by the large heat capacity of the pump and its contents, and the only possible causes of trouble are therefore short-term changes in heat loss from the specimen holder side tubes and from the specimen holder itself. Such changes cannot be effectively countered by using a temperature controller, for even if the pump were of low thermal capacity, the time delay caused by the flow of liquid round the system would be too great. The temperature drop of the liquid between the pump and the specimen being only about 20° C., random fluctuations can only be a small fraction of this, and on trial the specimen temperature was maintained constant to within 1/2° C. over long periods.

To measure the temperature in the pump and at the specimen, copper-constantan thermocouples are used. These have nearly linear characteristics over the range 0° C. to 400° C. The cold junction is kept in a mixture of ice and water, and the hot junction dips into the MS 550 at the point where the temperature is to be measured. The E.M.F.'s developed by the thermocouples are measured by a potentiometer as shown in Fig. 28.

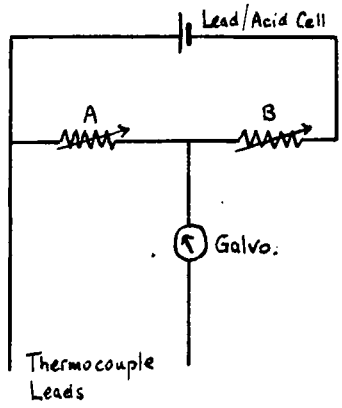

Fig. 28. The Thermocouple Potentiometer.

A is a decade resistance box giving 11,110 ohms in steps of 1 ohm. B is a box giving 100,000 ohms in steps of 10,000 ohms. To measure the thermal E.M.F.'s, B is normally set at 50,000 ohms, and the value of A in ohms is then very nearly equal to the temperature difference between the hot and cold junctions expressed in ^{o}C. The accumulator voltage is standardised against a Weston cadmium cell by replacing the thermocouple leads by the standard cell, and setting B to 10,000 ohms, when for balance A should also be nearly 10,000 ohms.

The bridge can measure temperatures to greater than 1^{o} C. accuracy. The galvanometer used is a Tinsley type with built-in lamp and scale, and changes of A of 1 ohm, corresponding to about 1^{o} C. change of temperature, cause deflections of about 3 mm. The scale can be read to better

than 1 mm.

The hot junction used to measure the specimen temperature does not actually touch the specimen. Owing to the various other considerations in the design of the specimen holder and the temperature compensator, it is necessary to carry the thermocouple leads to the compensator along the double-bore silica tube which transmits the displacements of the specimen to the extensometer condenser. The thermocouple junction rests in a small hole in the top of the aluminium cylinder (Z, fig. 19) which is in contact with the specimen. Since the whole temperature compensator is immersed in MS 550, the temperature difference between thermocouple and specimen must be very small.

The thermocouples were initially calibrated against a mercury in glass thermometer over the range 0° C. to 360° C. The hot junction of the thermocouple was bound to the bulb of the thermometer and the temperature of the MS 550 bath in which they were immersed was gradually raised. In order to check these calibrations 2 fixed temperatures were later used, the condensing temperature of water vapour (100° C.), and the condensing temperature of benzophenone (306° C.). For temperatures below 0° C. there was no thermometer available from which a continuous calibration could be made, so 3 fixed temperatures were used. They were the freezing point of mercury (-39° C.), the freezing point of carbon disulphide (-112° C.), and the temperature of liquid nitrogen

boiling at atmospheric pressure (-196° C.). Owing to the presence of impurities of oxygen in the nitrogen which tend to depress the temperature of the latter, the temperature was checked by using an oxygen vapour pressure thermometer which is very sensitive in the range 190°C. to 197°C.

2.7 APPARATUS FOR MEASUREMENT OF INTENSITY OF MAGNETIZATION.

Measurements have already been made (see Honda, Masumoto and Shirakawa) of the variation with temperature of the magnetization of single crystals of nickel. For several reasons it was considered desirable to measure this variation on the ellipsoids actually used for the present magnetostriction measurements. The specimens used by the Japanese workers were flat-ended rods, and the demagnetization field in the specimens was therefore non-uniform. The heat treatment applied to the rods was not disclosed, and the magnetic properties almost certainly differ from those of the specimens used here. No mention was made of any hysteresis effects found; this may be because there were actually no such effects, and in any case they must certainly be small. Measurements on the ellipsoids had the advantage that the specimen could be subjected to precisely the same magnetic conditions in measuring the magnetization and the magnetostriction, and the figures for variation of $\Delta l/l$ with I could

be obtained without any calculations of the demagnetizing fields.

Search coil, magnetometer and pendulum magnetometer methods have all been used for measurements on single crystals. Probably the easiest of these to use is the search coil method, and as a Grassot fluxmeter of 15,000 Maxwell-turns per division was available, this method was adopted. In the Appendix is given a theoretical calculation by the author (1954) of the flux linkage of a coil of finite dimensions with a uniformly magnetized prolate spheroid. If a coil of length $2l$, of inner radius r_1 and outer radius r_2 is placed symmetrically and coaxially round a spheroid of major axis $2a$ and minor axis $2b$, then an approximate value of the flux linkage is

$$8\pi^2 b^2 I l n_1 n_2 (r_2 - r_1)/e$$

where $e = \sqrt{(1 - b^2/a^2)}$ and n_1 and n_2 are the turns per unit length parallel to and perpendicular to the axis. For the theory to apply, l must not be greater than 1/4 of the length of the spheroid, i.e. about 0.4 cms. Since a former must encircle the specimen, the inside radius cannot be less than 0.25 cms., and to ensure a good flow of heat transfer liquid round the specimen the outside radius cannot be much greater than 0.5 cms.

The fluxmeter, when mounted with lamp and scale at 1 metre, has a sensitivity of 1.3×10^{-4} cms. per Maxwell turn. To

obtain ½% accuracy, and assuming the scale can be read to 1/2 mm., the flux-linkage required is 8×10^4 Maxwell turns. Using the maximum size of flux coil within the limitations stated above, the diameter of the wire must not be greater than about 0.022 cms.

The insulation of the wire presented problems. No enamel could be found which would withstand heating to 400° C., and a varnished glass covering which was tried was of too large diameter. A solution was found in the use of Aluminium wire with an anodised layer on its surface. This was wound on a "Duralumin" former, and the surface in contact with the wire was also anodised. The windings were wrapped in sheet mica. This method of insulation was found to hold good at 370° C., the maximum temperature at which it was tested. The increase of resistance caused by using Aluminium wire instead of Copper does not matter.

The search coil containing the specimen is mounted in a holder made of "Pyrex" glass, the holder being of similar type to the quartz specimen holder used for the magnetostriction measurements. Fig. (29) shows the arrangement of the holder. The search coil rests at the bottom of a centre tube of 1.2 cms. internal diameter, and the MS 550 liquid flows round the outside of this tube. The holder is mounted in the solenoid so that its two feed tubes dip into the pump in precisely the same way as did those of the quartz holder.

The "Duralumin" coil former is kept with its axis parallel

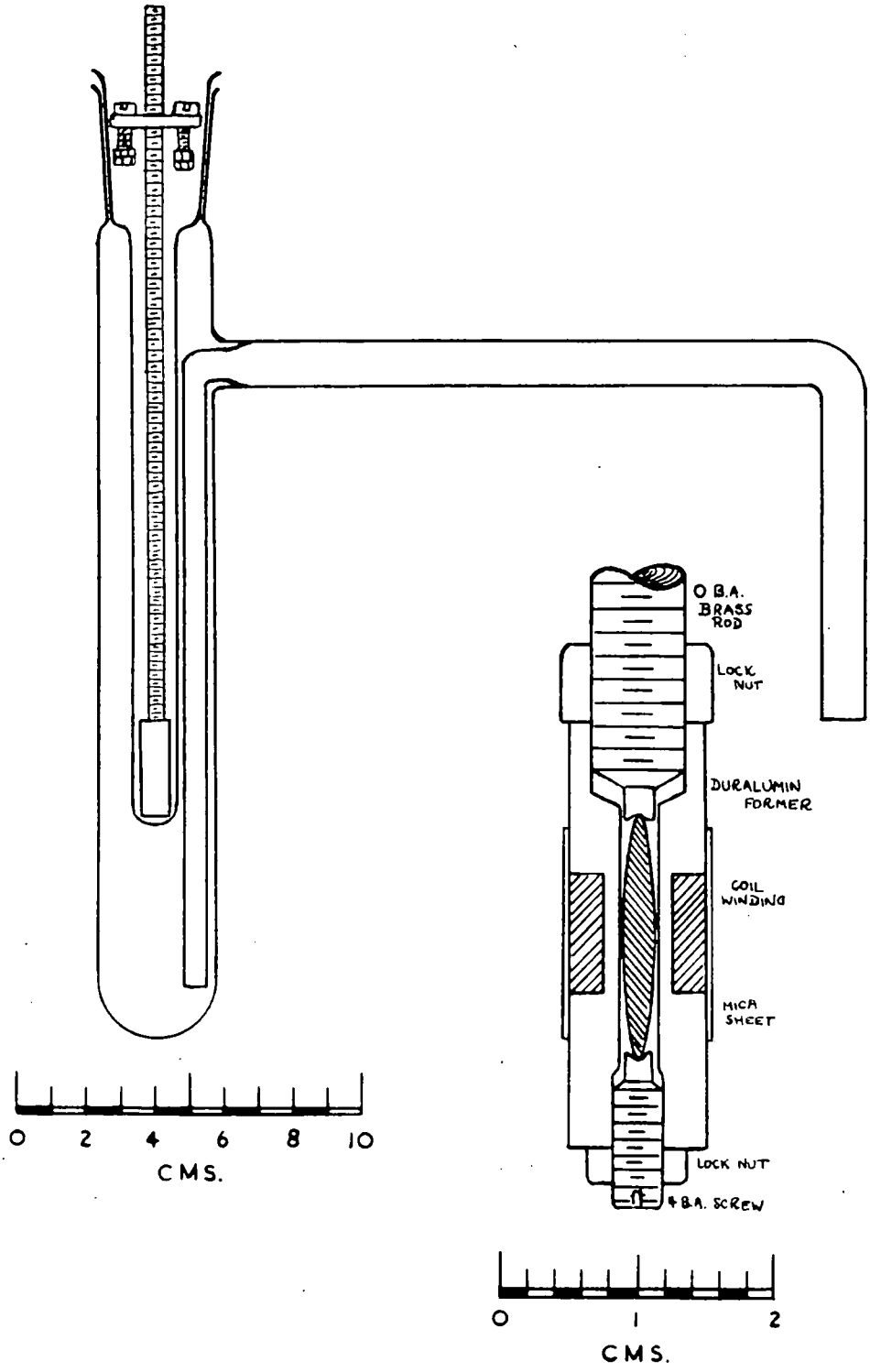

FIG.29. - The Search Coil and Specimen Holder for Magnetization Measurements.

to that of the holder and of the solenoid by the 0 B.A. brass rod screwed into its upper end. This rod has a small hole in its lower end into which fits the top of the ellipsoidal specimen, and the specimen is held in position by a similar hole in the 4 B.A. screw at its lower end. The windings of aluminium wire are in the central section of length 0.843 cms. and inner diameter 0.507 cms. There are 436 turns in 11 layers, the outer layer being flush with the former.

The windings are kept in position by a layer of sheet mica which overlaps the former as shown. This layer is held in position by a ring of copper wire. The leads from the coil are taken to two screws mounted on an asbestos disc in the neck of the holder, and ordinary twin flex connects the screws to the fluxmeter terminals. Aluminium wire being rather difficult to join, the wire was made continuous between the two screws via the flux coil.

The thermocouple used for measuring the temperature of the specimen is strapped to the former of the flux-measuring coil, and the two leads, which are glass insulated, are taken out through the asbestos disc. The thermocouple wires are of copper and constantan from the same reels as those used in the magnetostriction measurements.

The search coil used in this way measures changes in flux due to changes in both the intensity of magnetization of the specimen and the field. To compensate for the effect of the

field change, the secondary of a mutual inductance was put in series with the search coil. The primary of the inductance is in series with the solenoid, so that changes in solenoid current produce E.M.F.'s in the fluxmeter circuit proportional to the rate of change of current. By suitably adjusting the value of the inductance, the E.M.F.'s can be made equal and opposite to those due to flux-linkage of the field with the search coil. The fluxmeter deflection is then proportional to the intensity of magnetization of the specimen.

The method used for finding the absolute value of the intensity of magnetization is given in the Appendix. Due to the small size of the coil and the uncertainty of the effective radii of the windings, the value of R cannot be determined to an accuracy greater than 1%, consequently the absolute values of I will have a similar error. The values found agree well with those of previous workers.

2.8 PREPARATION OF THE SPECIMENS.

The single crystals have been supplied by the Physics Department of the University of Leeds. Both the ellipsoidal specimens used were cut from the same crystal which was in the form of a cylinder of length 3 cm., and diameter 1 cm. For orientating the crystal the back-reflection X-ray method was chosen, and the existing X-ray camera had to be modified for this work. For most purposes it was convenient to use a

6 cm. cylindrical camera; using a standard net the pictures taken could then be re-drawn as stereographic projections of the crystal faces, and after some practice the orientation of the crystal was readily determined. At a later stage in the work it became necessary to photograph the X-ray pattern reflected from the crystal embedded in a block of resin, and the crystal face could not then be set at the centre of the 6 cm. camera, so a flat plate back-reflection fitting was built onto the camera. Since the orientation had already been roughly determined, it was only necessary to determine from the flat-plate photographs any inaccuracies in the embedding of the crystal.

In order that the X-ray pictures should be sharp and clear, the surface from which the beam was reflected had to be free of strain. After the crystal had been carefully cut with a hacksaw, it was necessary to file it with a fine file, and then polish it with fine emery paper. The surface layer was then removed by electro-polishing, and the resulting surface was suitable for X-ray photography. Electro-polishing also showed any inclusions in the surface, and by polishing the whole surface of the crystal, a good idea could be obtained of any defects of the crystal. Boundaries between separate crystals were shown up best by using electro-polishing solutions with a high chlorine content, but a smooth surface was best obtained with a 50% solution of orthophosphoric acid in water.

Single crystals are very soft, and in order to avoid distortion of the structure in shaping the specimens an attempt was made to reduce the specimen to correct size by electro-removal methods, thus avoiding mechanical working. A machine was constructed using as a basis that described by Farmer and Glaysher(1953), and square-section rods were mounted in the chuck. It was found to be impossible to reduce these to circular section by using tangential streams of electrolyte since the electrolyte tended to be pulled onto the specimen by surface tension. A pad moistened with electrolyte was no more successful.

A static arrangement with a square section rod was arranged in an attempt to remove material preferentially from the corners of the rod and thereby gradually produce a circular section. It was found that removal did not take place in the manner which might have been predicted by considering the probable electrostatic fields in the electrolyte, and the experiment was not proceeded with.

Other experiments were made with the object of converting a cylindrical shaped specimen to an ellipsoid. The idea was to lower the specimen gradually into the electrolyte bath, so that the tip of the cylinder would be subject to more electro-removal than the centre. The experiment failed as no electrolyte was found which would remove nickel uniformly without pitting or bubbling at the anode. The effect of bubbling was to make it impossible to calculate the amount of

material removed, but more important, it carried the electrolyte level up the side of the specimen to an unpredictable extent. Solutions which produced no bubbling caused preferential removal in the different crystallographic directions. Various trial ellipsoids were made of polycrystalline nickel, but these were not of the accuracy considered necessary, and electrolytic methods of shaping were abandoned.

The only alternative method of shaping ellipsoidal specimens is by lathe-working. A preliminary test was made on a small single crystal of nickel to determine the depth of distortion caused by cutting with a sharp tool, each time taking a cut of 1/1000 inch. A back-reflection X-ray photograph of the worked surface was then taken, which showed none of the characteristic pattern associated with a cubic crystal, but only a series of blurred rings such as might be formed by a polycrystalline specimen. A further series of photographs was then taken between successive electro-removals of layers 2/1000 cm. thick. These showed a gradual change of structure, and below a depth of 0.015 cm. the crystal lattice was unstrained. It was decided to prepare on the lathe a specimen which, when electropolished to a depth of 0.015 cm., would be an ellipsoid of the required dimensions.

The first step in the preparation of the specimen was orientation of the lattice directions, and this was carried out by using the X-ray camera as previously described. The

crystal was then set in a block of Marco resin SB 26C, and a face cut perpendicular to the crystallographic direction which had been chosen to lie along the axis of the ellipsoid. This could only be cut roughly at first, and further photographs were then taken until the face was accurately perpendicular to the required direction. This face was then mounted against a block on the carriage of the milling machine so that four new faces could be cut perpendicular to the first face, these four faces forming a rectangle where they intersected the end face. The crystal could then be mounted in a four-jaw chuck with the chosen axis along the lathe axis. The faces cut were partly through nickel and partly through resin, since the original cylinder of nickel was set at a random angle to them.

The specimen being mounted correctly in the lathe, half of its length was turned down to $\frac{3}{8}$ inch diameter and the specimen reversed and fitted into a $\frac{3}{8}$ inch collet. By turning down half the specimen at a time to the next lowest collet size and then reversing it, the whole specimen was gradually reduced to $\frac{1}{8}$ inch diameter.

Knowing the length of specimen available, the correct shape could be calculated which, after electro-polishing, was to become an ellipsoid. This was done graphically by drawing out the shape of the ellipse, and then drawing a further line outside this ellipse at the appropriate distance from it. An optical system was fixed on the lathe so that

a profile of the specimen could be projected onto an enlarged outline shape mounted behind the lathe. The specimen was then carefully filed down until half of it fitted the outline, the final removal being with very fine emery paper. It was then reversed and fitted into a specially made collet shaped to fit the semi-ellipsoid, and the second half filed to shape.

The specimen was then electro-polished with a 50% solution of orthophosphoric acid. Owing to the non-uniform field around the specimen, more nickel was removed from the ends than from the centre, so the ends were mounted against little sheets of tin which had a shielding effect. By adjusting the proportion of time with and without the shields, the removal was made uniform over the specimen, and the specimen shape was then very nearly ellipsoidal.

From the single crystal of nickel the maximum length obtainable in the [111] direction was some 1.8 cm. In the [100] direction the length was 2.2 cms. However, since the magnetostrictive effect along the [100] is about $2\frac{1}{2}$ times that along the [111], the additional length was of little practical use, and both specimens were made to the same size. This meant that the apparatus could be used for either specimen with the minimum of modification. In their final form, both specimens have a length of 1.770 cm.

The actual shapes of the specimens after preparation are shown in Table 10. y_1 and y_2 are the diameters at distance x from each end of the specimen, y_c is the calculated diameter

for an ellipsoid with the same maximum diameter. The measurements were made with a travelling microscope having vernier scale movements in two perpendicular directions. Some of the scatter may be due to errors arising from the method of measurement, but this is not greater than .002 cm. in any reading, and the rest must be due to irregularities of the ellipsoid surface. The [100] specimen shows the greatest departure from the correct shape, being excessively pointed at its ends, while the [111] specimen is very nearly correct. For neither specimen is there much error for values of x greater that 0.2, corresponding to over 3/4 of the length of the crystal, although it is errors in the end shape that are likely to cause the greatest non-uniformity of field in the specimen.

TABLE 10.

Dimensions of the ellipsoidal specimens.

x	[100]			[111]		
	y_1	y_2	y_c	y_1	y_2	y_c
50	82	78	92	102	81	92
100	130	112	128	130	126	128
150	156	143	154	155	152	155
200	178	166	174	176	178	176
250	195	185	192	192	196	194
300	214	205	207	209	213	209
350	223	215	219	220	224	221
400	230	224	230	230	233	232
450	238	234	240	239	244	242
500	245	243	248	251	249	250
550	251	251	255	255	261	257
600	256	255	261	259	266	263
650	260	260	266	264	273	268
700	266	266	270	268	274	272
750	268	270	273	277	274	275
800	273	272	275	279	274	277
900	275	274	275	277	275	278

All dimensions cms. x 10^{-3}

Using the dimensions of the ellipsoids which best fit the measured values of y_1 and y_2 shown in Table 10, the following values of the demagnetizing factor N have been calculated:

For the [100] specimen, N = 0.491.

[111] N = 0.495.

From these values of N it was calculated that the magnetostrictive form effect was sufficiently small to be neglected.

On both specimens one or two small pits appeared during the electro-removal process. These were about 1/10 mm. deep, and of similar diameter. Their effect on the internal field is probably small.

The final stage in the preparation of the specimens was the annealing process, intended to free the crystal lattice from any strains caused by the cold working. The specimens were heated in a stream of hydrogen to a temperature of 910° C., and maintained at that temperature for two hours. They were then cooled at a rate not exceeding 100° C. per hour. This is substantially the treatment used by Bates and Wilson (1953) for specimens whose domain structures were later studied by the Bitter pattern technique. Further X-ray photographs of the ellipsoids were then taken which showed that they remained single crystals. These photographs also showed that the chosen crystallographic axis was in both cases parallel to the ellipsoid axis to an accuracy greater than 1° of arc.

Some small pieces of the crystal from which the specimens were prepared were sent to the Research Department of the Mond Nickel Company. The impurities found by their analysis are listed in Table 11, which also shows the estimated effect of each on the saturation magnetization and the saturation magnetostriction at room temperature. The magnetostriction effect is calculated for polycrystalline nickel from measurements by Schulze (1927, 1928) on iron-nickel and cobalt-nickel alloys, but it cannot be assumed

that the effect on the saturation magnetostriction along any crystallographic axis will be proportionally the same.

TABLE 11.

Impurities in the Specimens.

Element	%	Effect on I (c.g.s.u.)	Effect on λ (x 10^{-6})
Carbon	0.02		
Silicon	0.04		
Iron	0.17	2.8	0.14
Cobalt	0.29	2.7	0.24
Chromium	0.02	-1.0	
Titanium	0.02	-1.3	
Copper	0.04	-0.4	
Manganese	0.10	1.2	
Magnesium	0.02		
Total	0.62	4.0	

2.9 EXPERIMENTAL PROCEDURE.

MAGNETOSTRICTION MEASUREMENTS.

The electronic bridge circuit became sufficiently steady for accurate measurements to be made within 10 minutes of switching on, so that room temperature measurements could be made each day before the temperature of the system was raised; this provided a valuable check that the apparatus was working correctly. The heating element in the pump was then switched

on, and the pump motor started. Although with the maximum voltage applied to the heating coil the liquid in the pump soon warmed up, there was considerable time lag before the liquid was flowing freely through the system. This was because of the high viscosity of the liquid at low temperatures and the limited pressure difference which the pump could produce. Once the liquid was circulating freely, which usually took about $1\frac{1}{2}$ hours, the specimen soon reached its stable temperature. At high temperatures, however, it still required about an hour for the whole system to become stable. The quartz rod which transmitted the displacement of the end of the specimen to the condenser was thought to be the main cause of the delay. Since one of its ends was at the specimen temperature and the other was at room temperature, there was a considerable thermal gradient along the rod, and this took a long time to establish.

Stable conditions having been reached, the displacement condenser was adjusted for zero output. Correct working of the bridge was verified by switching in the 12 pF. condenser in the balance arm. Measurements were then made of the output voltage from the bridge corresponding to different currents through the solenoid. At temperatures less than about 250° C. conditions were sufficiently stable for the specimen to be gradually magnetized from an initially demagnetized state by increasing the field in steps. At temperatures higher than this, thermal drift made it necessary

to take independent readings of the change in length between the demagnetized state and the state corresponding to a certain applied field. At temperatures above about 300° C., only measurements of the saturation magnetostriction were made. Examination of hysteresis effects required very steady conditions, and it was found that reproducible results could only be obtained at room temperature.

During the time taken to make a series of measurements the temperature of the specimen could be kept constant to better than 1° C. The temperature was measured on the potentiometer circuit to the nearest 1° C.

In a complete day's observations it was usually possible to measure magnetostriction at 4 or 5 different temperatures. To make sure that the oscillator output kept constant during that time, the 12 pF. condenser in the bridge balancing arms was occasionally switched into the circuit; this produced a constant output voltage when the bridge was working correctly.

It was found impossible to keep the pump running and to maintain the liquid at high temperature overnight because of accumulation of gas in the feed pipes. This accumulation was especially severe when the MS 550 liquid was newly put into the system; after several weeks it became less but never entirely ceased. After a day of measuring the magnetostriction, the specimen holder on its frame and with the condenser still mounted had to be lifted out of the pump and the solenoid so that the gas could be sucked out. It was occasionally

necessary to suck out air that had entered the return feed pipe when the level in the pipe into which it dipped became too low. Because of the change in viscosity of the liquid with temperature, the pump speed had to be gradually reduced as the temperature rose, otherwise the difference in levels in the pump became so great that air entered the feed pipe. At high temperatures, with the aluminium lid over the pump box, the optimum pump speed was difficult to estimate, and on several occasions the motor was run too fast.

In practice the water cooling of the solenoid was not used. The actual measurements did not take more than a few minutes of continuous running, and cooling was not necessary. The solenoid did sometimes become rather hot, causing an increase in the resistance of the windings. This made the maximum applied field less than 1000 oersteds due to the limitations of the generator, and it also meant that for a a certain applied field different values of the control resistances had to be used.

MAGNETIZATION MEASUREMENTS.

Most of the considerations discussed above apply to the measurements of intensity of magnetization except that the time taken to reach steady conditions was much less. This was because it was no longer necessary to wait for the whole system to reach steady temperatures, only the specimen in the flux coil needed to be at constant temperature.

The fluxmeter was zeroed with the electrostatic zeroing device and the scale deflection noted for increasing values of the applied field. At room temperatures, magnetization measurements were taken round the complete hysteresis cycle.

2.10 ADAPTION FOR LOW TEMPERATURE WORK.

Of the apparatus for high temperature measurements described in sections 2.3 to 2.7, only the pumping system and the solenoid required modification for low temperature work. Although the pump had been constructed in such a way that adaptation for use below room temperature was not difficult, it was decided to experiment with a simpler arrangement. In this, a Dewar flask of liquid nitrogen was gradually raised so that the bottom of the specimen holder dipped into it. The heat conducting liquid in the specimen holder caused the temperature along the latter to decrease until finally a steady temperature gradient was established along the holder. By adjustment of the height of the liquid nitrogen round the holder, the temperature of the specimen could be adjusted from room temperature to a little above that of liquid nitrogen.

The Dewar flask previously used as a thermal insulator between the specimen holder and the solenoid was not suitable since the small gap between its inner wall and the specimen holder prevented sufficient liquid nitrogen being contained

in it. A flask of inner diameter 50 mm. was therefore used, its outer diameter being the maximum which could be raised inside the solenoid. The water cooling system on the inside of the solenoid was discarded, and in order that the Dewar flask could be readily raised into position, the solenoid was mounted on an aluminium frame so that the base of the solenoid was some 80 cm. above the top of the galvanometer pillar. On this frame was fixed an arrangement by which the Dewar flask could be adjusted to the desired height. The specimen holder and the differential condenser were mounted on the frame N (fig. 18) as before, consequently the side tubes on the specimen holder were much higher than before and did not dip into the pump.

The main tube of the specimen holder was filled with heat conducting liquid and the side tubes closed with rubber bungs, one of which was pierced to allow for thermal expansion of the liquid. The liquid used was iso-pentane which boils at 26° C. and is stated to have a melting point of -159° C. When tested, however, it did not become solid at a very definite temperature, but was very viscous when the temperature was lowered to -165° C.

Using this arrangement the temperature of the specimen could be maintained at a remarkably steady value. The lowest temperature obtained was -186° C., at which point variations were less than $\frac{1}{2}^{\circ}$ C., and at higher temperatures the steadiness was even better. A disadvantage found was that it

was impossible to lower the temperature during magnetization measurements to the same extent as during magnetostriction measurements. This was because the heat conduction along the brass rod supporting the flux coil was greater than along the quartz displacement rod. The small loss of temperature range due to this did not justify further modifications to the apparatus.

Modification to the solenoid was necessary since at temperatures below -50° C. the increase in the negative value of the anisotropy constant K_4 prevented the original maximum applied field of 1000 oersteds from magnetizing the [100] specimen to saturation. It was decided that at these high fields the compensating coils could be dispensed with, which allowed an increase of maximum field when driven from the D.C. generator, although the uniformity of field was necessarily reduced. Calibration by search coil and flux-meter showed that 1310 oersteds could be produced when the solenoid without compensating coils was placed directly across the generator. The current was then 4.3 amps, but due to the large heat dissipation, it could only be maintained at that value for short periods.

To increase the field still further, all the available lead-acid accumulators were collected and put in series with the generator. The maximum current then obtainable was 5.5 amps which produced a field of 1680 oersteds. As will be seen in Part 3 of the thesis, this was insufficient to

magnetize the [100] specimen to saturation.

Procedure during experimental runs was much the same as that described in section 2.9. The Dewar flask containing the liquid nitrogen was gradually raised inside the solenoid until the specimen was at approximately the desired temperature. After about 1/4 hour, conditions were usually sufficiently steady for readings to be taken. It was found that conditions became steady much more quickly than with the high temperature system, so that observations at several temperatures could be made within one day.

At the lowest temperatures there was no suitable liquid which could be put into the thimble of the temperature compensator as a lubricant, but at temperatures above about -130° C. iso-pentane was used. A minor disadvantage found with the apparatus when working at low temperatures was that water from the atmosphere tended to freeze onto the quartz displacement rod which was at much lower temperature than the surroundings, which resulted in water collecting in the thimble when the system was allowed to warm up to room temperature again. When the temperature was again lowered, the specimen was frozen solid into the thimble, and magnetostriction measurements could not be made until the thimble was cleaned.

PART 3.

RESULTS

3.1 RESULTS.

The measurements obtained were initially in the form of values of the change in length from the demagnetized state corresponding to various applied fields at certain fixed temperatures, and values of the intensity of magnetization I corresponding to various applied fields at certain other fixed temperatures. These measurements, as such, are difficult to interpret, and it was necessary to change them into corresponding figures of I, $\Delta l/l$ and the true field H for various temperatures. The method adopted was to prepare graphs of I against temperature for fixed values of the applied field. Smooth curves were drawn through the experimental points; owing to the very small amount of scatter of the points these curves were considered accurate to better than 1%. The values of I were read off from the curves corresponding to the temperature and the applied field at which values of $\Delta l/l$ had been recorded. Knowing the values of the demagnetizing factor, the applied field, and the intensity of magnetization, the true field in the specimens could be calculated.

The figures obtained in this way are shown in Table 12 for the [100] specimen and in Table 13 for the [111] specimen. It will be noticed that in each case at the lowest temperature the values of I and H are not quoted. This is because the I measurements were not made below -170° C., and it was considered unwise to extrapolate the I - T curves.

TABLE 12.

Magnetostriction. [100] Specimen.

H_{APP}	-186° $-\frac{\Delta l}{l}$	I	H	-161° $-\frac{\Delta l}{l}$	I	H	-143° $-\frac{\Delta l}{l}$	I	H
100	0			0.6	196	4	0.6	196	4
200	2.1			3.7	314	46	3.7	315	46
300	4.9			7.6	332	137	7.9	336	135
400	7.9			11.6	350	228	11.8	356	225
500	11.0			15.8	368	319	16.8	376	315
600	14.0			17.7	388	409	19.5	396	406
700	16.4			22.0	404	502	24.4	412	498
800	18.7			25.0	420	594	28.7	430	589
900	21.4			28.7	434	687	33.4	446	681
1000	24.1			31.1	446	781	36.0	458	776
1310	31.1			39.1	482	1074	48.5	493	1068
1680	35.4			45.7	499	1425	50.7	510	1420

H_{APP}	-130° $-\frac{\Delta l}{l}$	I	H	-120° $-\frac{\Delta l}{l}$	I	H	-113° $-\frac{\Delta l}{l}$	I	H
100	0.3	196	4				0.6	196	4
200	3.7	316	45				4.9	317	44
300	8.5	338	134				11.0	344	131
400	13.4	361	223				15.2	368	219
500	18.6	381	313				20.8	389	309
600	22.0	401	403				25.6	410	398
700	27.5	419	495				30.5	430	488
800	31.1	438	585				35.1	450	579
900	35.4	454	677				40.6	465	672
1000	39.2	466	771	43.3	473	768	44.0	477	766
1310	51.0	500	1064	53.4	505	1062	52.5	506	1062
1680	54.4	515	1417	55.0	519	1415	54.4	519	1415

TABLE 12.

Magnetostriction. [100] Specimen.

	-100°			-93°			-74°		
H_{app}	$-\frac{\Delta l}{l}$	I	H	$-\frac{\Delta l}{l}$	I	H	$-\frac{\Delta l}{l}$	I	H
100	0.6	196	4	0.6	196	4	0.6	196	4
200	5.2	319	43	5.5	320	43	6.1	325	41
300	11.0	348	129	12.5	352	127	14.0	359	124
400	17.2	374	216	18.6	378	214	20.8	389	209
500	23.8	397	305	24.4	402	303	28.7	416	290
600	29.9	418	395	29.9	424	392	34.2	440	384
700	34.8	440	484	36.0	446	481	40.8	464	472
800	40.8	462	573	40.8	466	571	46.5	484	563
900	47.0	475	667	45.7	481	664	51.0	499	655
1000	50.0	487	761	50.0	492	759	53.1	508	750
1310	53.7	512	1059	54.4	512	1059	54.0	512	1059
1680	54.8	518	1415	55.0	517	1418	54.4	514	1417

	-65°			-60°			-43°		
H_{app}	$-\frac{\Delta l}{l}$	I	H	$-\frac{\Delta l}{l}$	I	H	$-\frac{\Delta l}{l}$	I	H
100	0.9	196	4				1.5	196	4
200	7.9	326	40				8.5	331	38
300	15.8	363	122				20.8	374	117
400	23.2	395	206				31.1	411	198
500	32.4	423	292				39.6	442	283
600	39.1	448	380				46.5	467	371
700	45.2	472	468				50.7	490	459
800	50.1	491	559				52.5	502	554
900	53.1	506	652				53.1	506	652
1000	53.7	510	750	54.0	510	750	53.7	508	758
1310	54.0	512	1059	54.4	512	1059	53.7	508	1061
1680	54.4	512	1419	54.4	512	1419			

TABLE 12.

Magnetostriction. [100] Specimen

	-21°			-11°			0°		
H_{APP}	$-\frac{\Delta L}{L}$	I	H	$-\frac{\Delta L}{L}$	I	H	$-\frac{\Delta L}{L}$	I	H
50							0.6	100	1
100	1.2	196	4	1.2	196	4	1.2	197	3
150							5.5	284	11
200	11.0	337	35	10.4	341	33	13.4	344	31
300	24.4	386	111	25.9	396	106	30.5	402	103
400	36.6	429	189	39.2	438	185	40.8	448	180
500	46.7	464	272	47.0	470	269	47.8	476	266
600	51.0	484	362	50.7	487	361	51.0	488	361
700	52.8	493	458	51.8	495	457	51.8	494	457
800	53.1	502	554	52.5	502	554	52.2	499	555
900	53.1	504	653	52.8	502	654	52.5	499	655
1000	53.1	504	753	52.8	502	754	52.5	499	755

	19°			36°			43°		
H_{APP}	$-\frac{\Delta L}{L}$	I	H	$-\frac{\Delta L}{L}$	I	H	$-\frac{\Delta L}{L}$	I	H
50	0.6	100	1						
100	1.8	197	3	1.8	197	3	2.4	198	3
150	5.6	284	11						
200	16.1	350	28	18.4	357	25	18.7	359	24
300	35.4	421	93	39.2	438	85	40.0	444	82
400	46.5	463	172	47.5	470	169	46.8	472	168
500	50.5	480	264	49.5	480	264	48.2	480	264
600	51.3	488	361	49.7	485	362	48.4	484	362
800	51.6	493	558				48.6	485	462
1000	51.8	493	758	50.2	488	760	48.9	485	762

TABLE 12.

Magnetostriction. [100] Specimen.

	76°			105°			136°		
H_{APP}	$-\frac{\Delta l}{l}$	I	H	$-\frac{\Delta l}{l}$	I	H	$-\frac{\Delta l}{l}$	I	H
50	0.9	100	1						
100	3.4	198	3	2.4	199	4			
150	10.3	291	7						
200	21.9	367	20	20.9	369	19			
300	39.9	455	76	38.4	452	78	36.7	440	84
400	44.1	469	170	40.3	455	176	37.6	442	183
500	44.7	470	269	40.8	457	276			
600	45.0	471	369	41.0	459	375	38.1	442	383
1000	45.0	472	769						

	151°			155°			191°		
H_{APP}	$-\frac{\Delta l}{l}$	I	H	$-\frac{\Delta l}{l}$	I	H	$-\frac{\Delta l}{l}$	I	H
50				0.9	100	1	0.9	100	1
100				4.6	199	4	4.6	199	4
150				9.7	292	7	10.6	291	7
200				23.1	369	19	21.1	365	21
300	34.5	434	87	33.7	431	88	28.4	406	101
400	36.0	434	187	34.2	431	188	29.0	406	201
600	36.4	434	387	34.7	431	388	29.5	406	401

Saturation Magnetostriction for H_{APP} = 1000 oersteds,

At 50°C, $-\lambda = 48.4 \times 10^{-6}$

At 64°C, $-\lambda = 46.4 \times 10^{-6}$

Saturation Magnetostriction for H_{APP} = 600 oersteds,

At 170°C, $-\lambda = 32.9 \times 10^{-6}$.

TABLE 12.

Magnetostriction. [100] Specimen

	196°			232°			265°		
H_{app}	$-\frac{\Delta l}{l}$	I	H	$-\frac{\Delta l}{l}$	I	H	$-\frac{\Delta l}{l}$	I	H
50	0.9	100	1	1.0	100	1	1.0	100	1
100	4.7	199	4	3.1	199	4	4.2	199	4
150	10.8	291	7	9.8	287	9	12.2	280	13
200	21.6	364	21	17.9	351	28	16.9	330	38
300	28.2	402	103	22.8	371	118	16.9	336	135
400	28.2	402	203	22.8	371	218			

Saturation I_s and λ for H_{app} = 300 oersteds:

Temp.	$-\lambda$	I_s
218°C	25.4	383
248	20.7	355
282	15.6	313
285	14.6	309
294	13.5	294
308	10.8	267
324	8.4	214
335	5.5	190
336	4.7	187
345	3.3	152
354	0.9	92
357	0	30

TABLE 13.

Magnetostriction. [111] Specimen

H_{APP}	-182° $-\frac{\Delta L}{L}$	I	H	-154° $-\frac{\Delta L}{L}$	I	H	-135° $-\frac{\Delta L}{L}$	I	H
50	0.7			0.8	102	0	0.6	102	0
100	3.0			2.8	203	0	3.0	203	0
150	7.0			6.8	300	2	7.0	300	2
200	13.0			12.6	398	3	13.2	398	3
250	18.0			18.0	495	5	18.6	494	6
300	20.4			20.3	514	46	20.2	514	46
400	20.8			20.9	517	144	20.6	517	144
600	21.4			21.7	521	342	21.2	520	342
800	21.8						21.8		
1000	22.1			22.3	523	741	22.2	522	741

H_{APP}	-108° $-\frac{\Delta L}{L}$	I	H	-102° $-\frac{\Delta L}{L}$	I	H	-77° $-\frac{\Delta L}{L}$	I	H
50	0.6	102	0				0.7	102	0
100	2.8	203	0				3.0	202	0
150	6.8	300	2	7.0	300	2	7.4	299	2
200	12.8	398	3	12.6	398	3	13.2	398	3
250	18.0	494	6	17.6	494	6	18.4	492	7
300	20.2	513	46	20.2	513	46	19.8	510	48
400	20.8	515	145	20.6	515	145	20.2	512	147
600	21.4	517	344	21.3	517	344	20.8	514	346
1000	21.6	518	743	21.4	518	743	21.2	515	745

Saturation Magnetostriction at -127°C,

For H_{APP} = 1000 oersteds, $-\lambda = 22.0 \times 10^{-6}$.

TABLE 13.

Magnetostriction. [111] Specimen

	-68°			-56°			-47°		
H_{APP}	$-\frac{\Delta L}{L}$	I	H	$-\frac{\Delta L}{L}$	I	H	$-\frac{\Delta L}{L}$	I	H
50	0.6	102	0				0.8	102	0
100	2.8	202	0				2.9	202	0
150	7.0	299	2				7.0	299	2
200	11.8	397	4				12.8	397	4
250	17.2	492	7				17.9	489	8
300	19.2	508	49	19.7	507	49	19.4	505	50
400	20.0	510	148	19.9	509	148	20.2	507	149
600	20.8	513	346	20.0	511	347	20.4	509	348
1000	20.8	514	745	20.4	512	747	20.4	511	747

	-30°			-22°			-11°		
H_{APP}	$-\frac{\Delta L}{L}$	I	H	$-\frac{\Delta L}{L}$	I	H	$-\frac{\Delta L}{L}$	I	H
25				0.2	51	0			
50				0.7	102	0	0.6	102	0
75				2.0	152	0			
100				2.9	202	0	2.8	202	0
125				5.0	250	1			
150				7.0	298	3	7.0	298	3
175				10.0	348	3			
200				12.8	396	4	12.2	396	4
225				16.0	446	4			
250				17.6	486	10	17.2	484	11
300	19.4	502	51	19.2	500	52	18.8	496	54
400	20.0	504	150	19.8	502	152	19.4	498	153
1000	20.2	507	749	19.9	505	750	19.6	502	752

TABLE 13.

Magnetostriction. [111] Specimen.

	0°			21°			35°		
H_{APP}	$-\frac{\Delta L}{L}$	I	H	$-\frac{\Delta L}{L}$	I	H	$-\frac{\Delta L}{L}$	I	H
25				0.2	51	0			
50	0.5	102	0	0.6	102	0			
75				1.5	152	0			
100	2.6	202	0	2.6	202	0			
125				4.1	250	1			
150	6.6	298	3	6.5	298	3			
175				9.2	347	3			
200	11.8	395	5	12.2	395	5			
250	17.2	482	12	17.8	475	15			
300	18.8	493	56	19.1	486	60	18.3	481	62
400	19.3	495	155	19.3	489	158	19.1	484	161
1000	19.4	499	753	19.3	492	756	19.1	487	759

	48°			77°			92°		
H_{APP}	$-\frac{\Delta L}{L}$	I	H	$-\frac{\Delta L}{L}$	I	H	$-\frac{\Delta L}{L}$	I	H
25				0	51	0	0.2	51	0
50				0.6	101	0	0.6	102	0
75				1.5	152	0	1.5	152	0
100				2.6	202	0	2.4	202	0
125				3.9	250	1	4.1	250	1
150				6.2	297	3	5.8	296	4
175				8.4	346	4	8.6	345	4
200				11.4	390	7	11.8	388	8
225				14.9	428	13	14.9	424	15
250				16.4	454	25	15.7	448	28
300	18.3	477	64	17.7	464	70	17.4	458	73
400	18.7	478	164	18.1	468	168	17.8	461	175
1000	18.7	482	761	18.1	470	767	17.8	463	771

TABLE 13.

Magnetostriction. [111] Specimen

	106°			127°			171°		
H_{App}	$-\frac{\Delta l}{l}$	I	H	$-\frac{\Delta l}{l}$	I	H	$-\frac{\Delta l}{l}$	I	H
25				0.1	51	0			
50				0.9	102	0	0.9	102	0
75				1.7	152	0	1.5	152	0
100				2.8	202	0	2.4	201	0
125				4.1	248	2	3.7	246	3
150				5.8	294	5	5.0	290	7
175				8.4	342	5	7.9	338	8
200				11.0	382	11	10.8	372	16
225				13.5	412	21	12.0	392	31
250				15.1	432	30	13.1	408	48
300	17.2	452	76	16.2	440	82	14.2	415	95
400	17.4	456	174	16.6	444	180	14.4	417	194
1000				16.6	444	780	14.4	417	794

	197°			238°			260°		
H_{App}	$-\frac{\Delta l}{l}$	I	H	$-\frac{\Delta l}{l}$	I	H	$-\frac{\Delta l}{l}$	I	H
50	0.2	102	0	0.2	101	0	0.6	101	0
75	1.5	151	0	1.5	151	0			
100	2.4	200	1	2.4	200	1	2.2	200	1
125	4.1	245	4	3.9	242	5			
150	5.6	288	8	5.6	283	10	5.4	279	12
175	7.9	330	12	7.5	318	18			
200	10.6	364	20	8.4	345	29	7.9	328	37
225	11.2	377	38	8.9	350	52			
250	11.8	389	57	9.8	356	74			
300	12.9	396	104	10.4	362	121	8.6	336	134
400	12.9	398	203	10.4	362	221	8.6	336	234

TABLE 13.

Magnetostriction. [111] Specimen.

Saturation I_s and λ for H_{app} = 400 oersteds:

Temp.	$-\lambda$	I_s
139°C	15.7	437
218	11.6	381

Saturation I_s and λ for H_{app} = 300 oersteds:

Temp.	$-\lambda$	I_s
252°C	9.2	348
277	7.1	330
297	5.8	284
310	4.3	260
321	3.4	235
330	2.6	210
336	2.2	191
344	1.3	154
347	0.6	
351	0.2	
356	0	

NOTE. In Tables 12 and 13, all values of field are expressed in oersteds, all values of the intensity of magnetization in c.g.s. units, and all temperatures in degrees Centigrade.

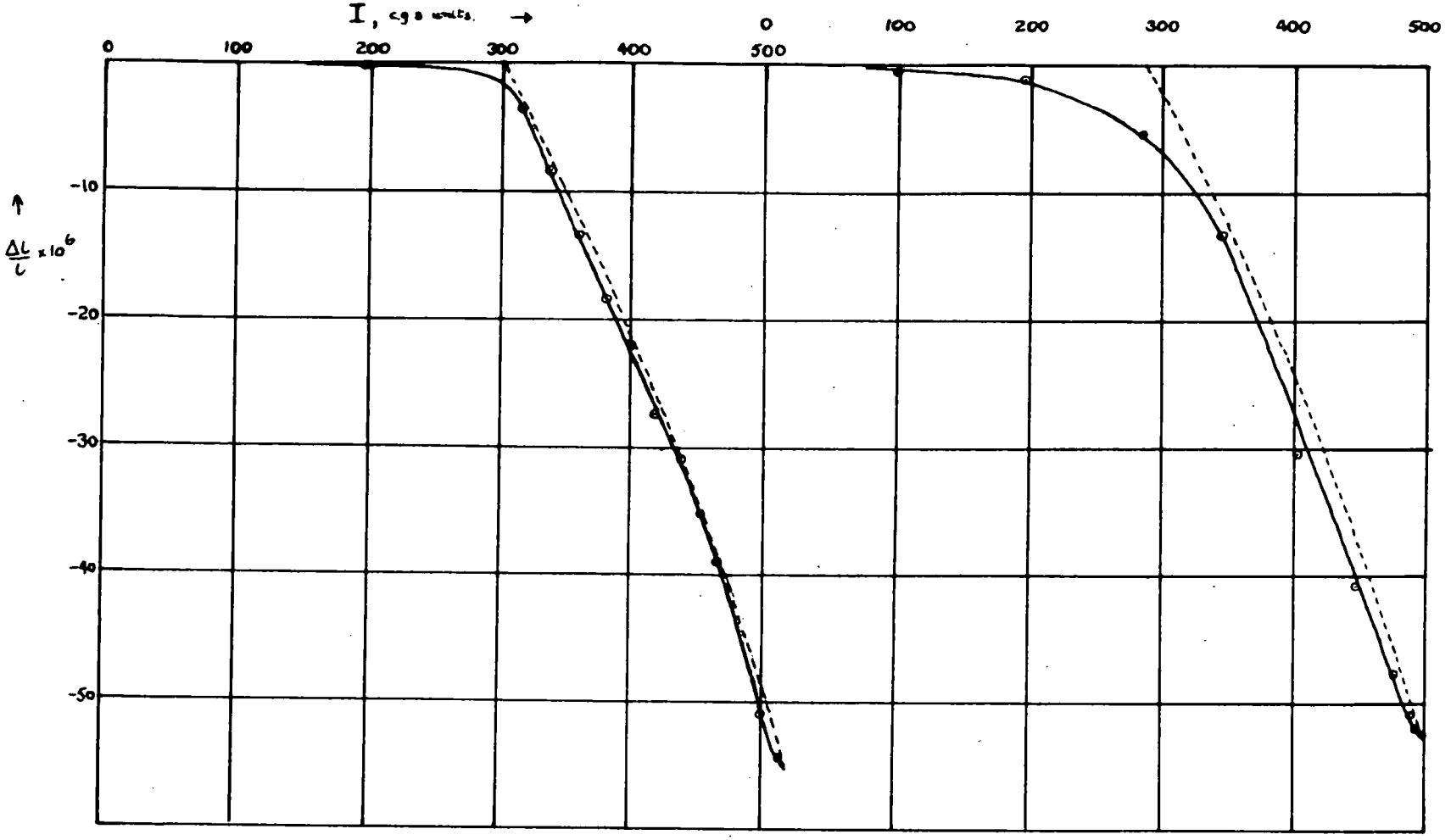

FIG. 30. - Magnetostriction as dependent on Intensity of Magnetization in the [100] direction. Left at -130°C, right at 0°C.
(dotted lines are theoretical values from Heisenberg equations)

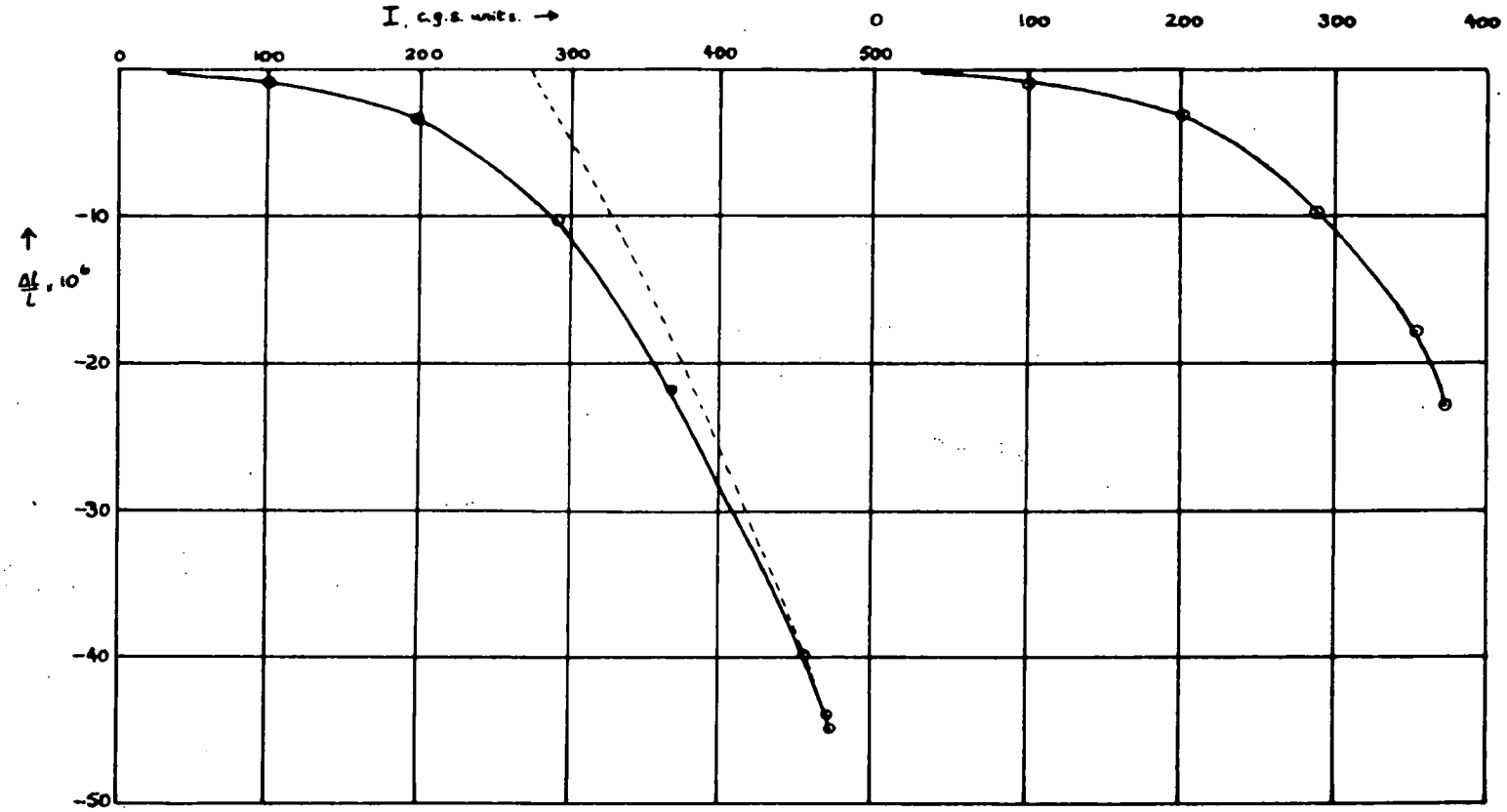

FIG. 31. – Magnetostriction as dependent on Intensity of Magnetization in the [100] direction. Left at 76°C, right at 232°C.
(dotted line is theoretical values from Heisenberg equations)

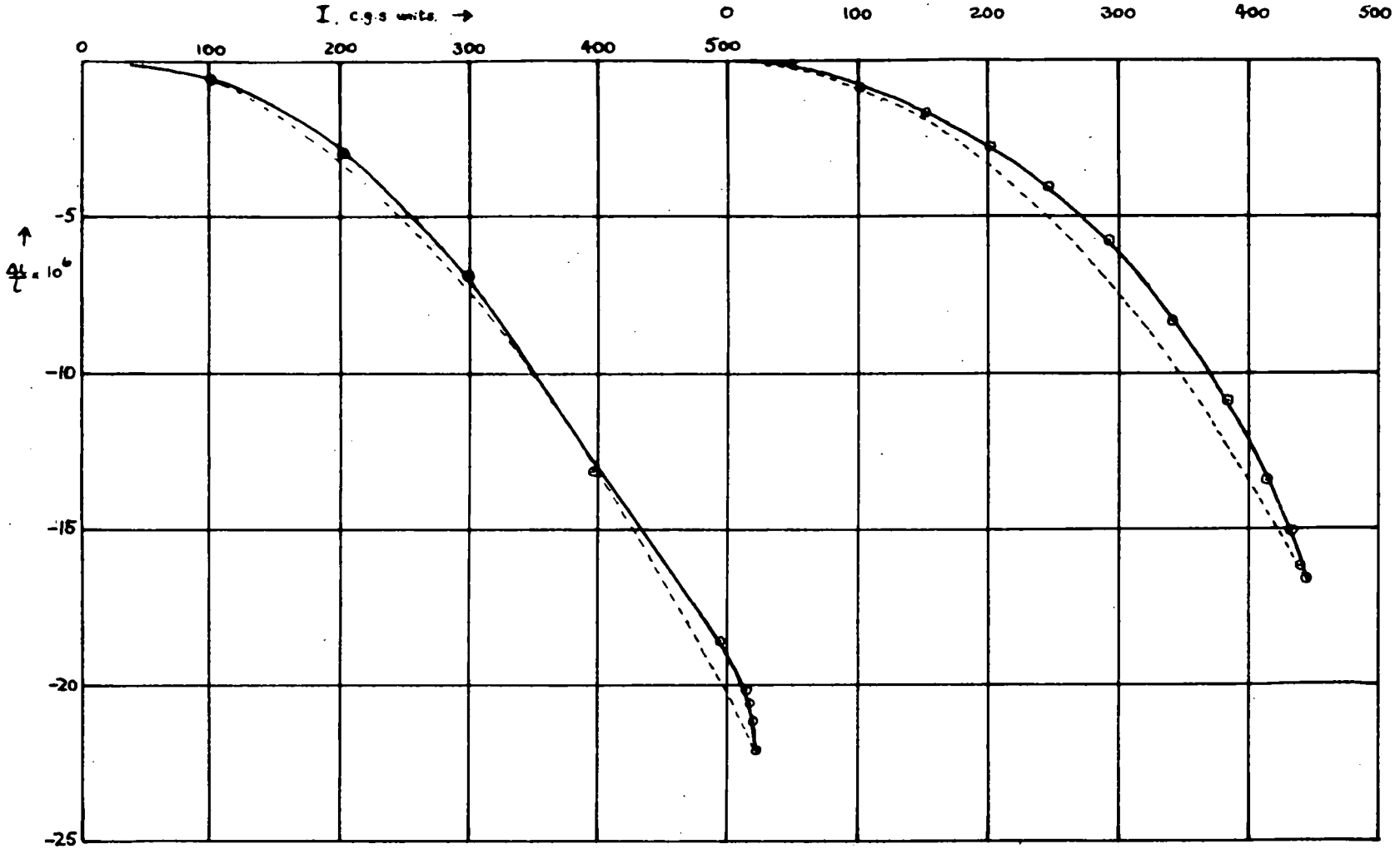

FIG. 32. – Magnetostriction as dependent on Intensity of Magnetization in the [111] direction. Left at -135°C, right at 127°C.
(dotted lines are theoretical values from Heisenberg equations)

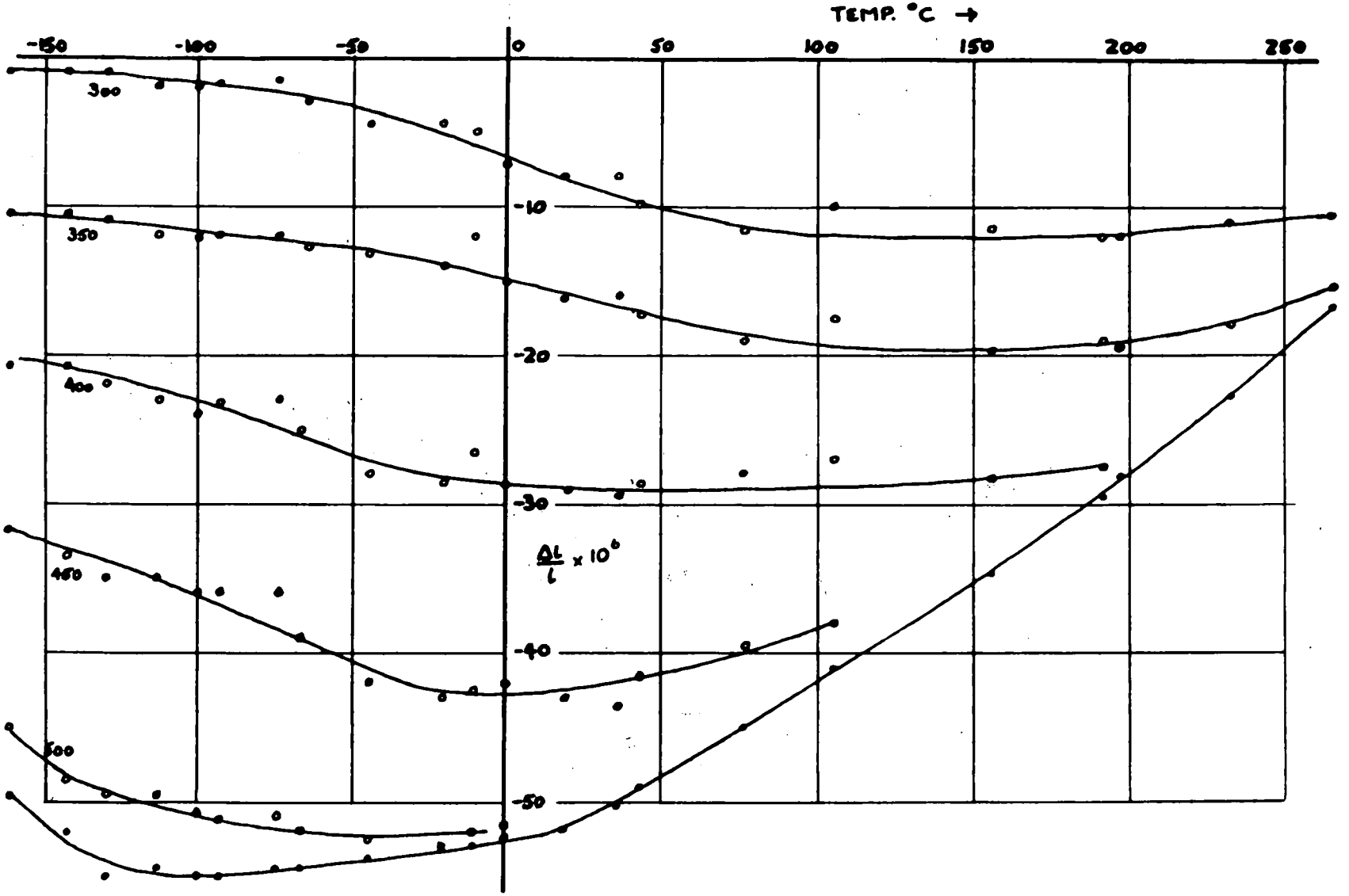

FIG.33. – Magnetostriction as dependent on Temperature in the [100] direction. Fixed values of Magnetization shown on left.

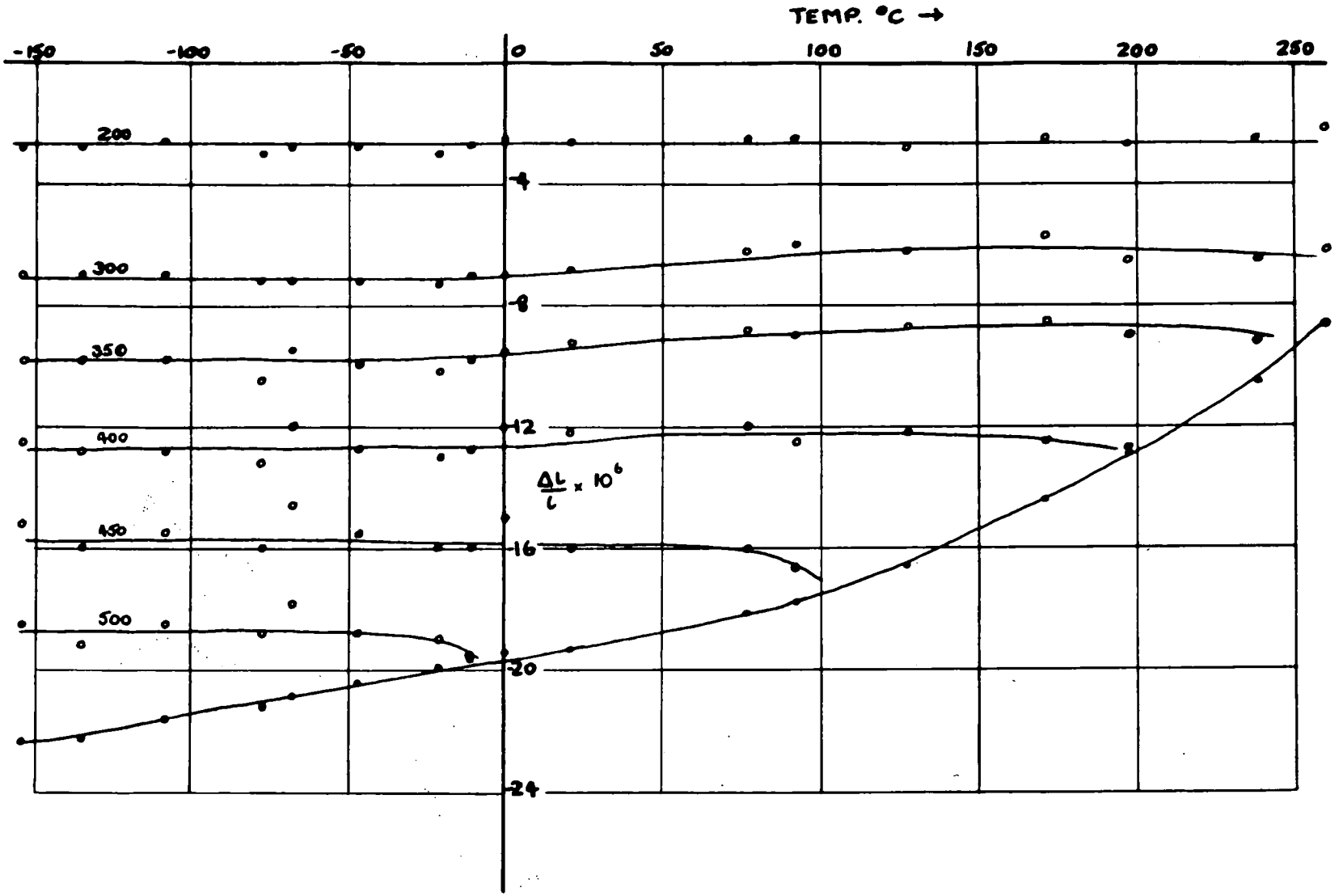

FIG. 34. – Magnetostriction as dependent on Temperature in the [111] direction. Fixed values of Magnetization shown on left.

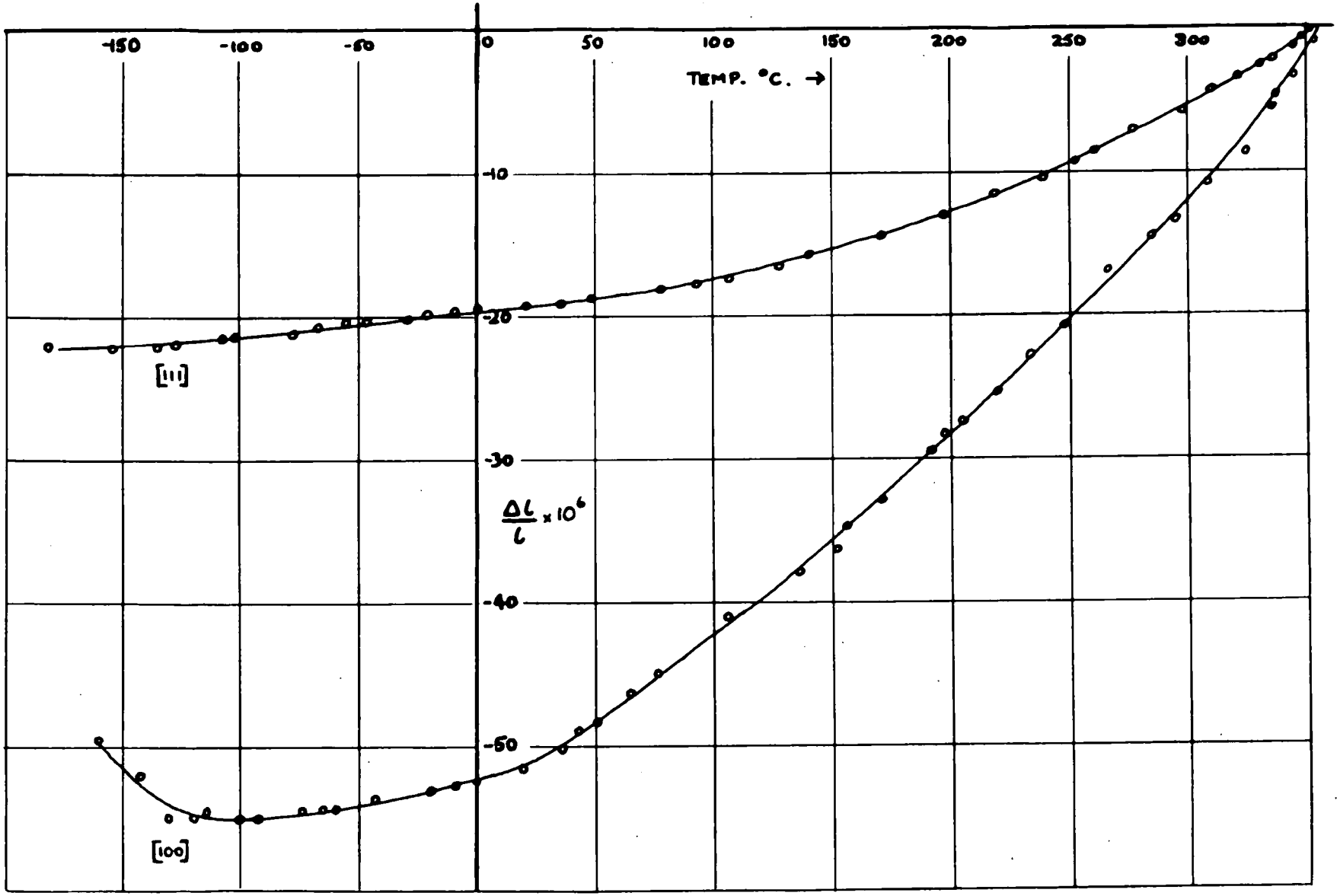

Fig. 35. - Saturation Magnetostriction as dependent on Temperature.

Curves were plotted of $\Delta l/l$ against I for fixed values of the temperature. Owing to the large number of these, only a representative selection is reproduced here in figs. (30) and (31) for the [100] direction and in fig. (32) for the [111].

From these curves the values of $\Delta l/l$ corresponding to fixed values of I could be obtained. This allowed the graphs shown in figs. (33) and (34) to be prepared; they show the variation with temperature of $\Delta l/l$ corresponding to fixed values of I. At temperatures above 260° no measurements of $\Delta l/l$ were taken apart from the saturation values, and fig. (35) shows the saturation magnetostriction plotted against the temperature for the whole range of temperatures and for both specimens. It should be pointed out here that the saturation values in the [100] direction at very low temperatures were not obtained directly as the applied field was too small to obtain saturation. The method adopted to calculate these values will now be explained.

The graphs drawn of I against temperature for various values of applied field showed that the saturation values of I for the two specimens agreed to within the experimental scatter, which was not more than 2% over the whole temperature range. It was therefore considered justifiable to use the [111] saturation value of I as the value for the [100] specimen at temperatures at which the saturation values in the latter could not be measured. Using these values of I, and

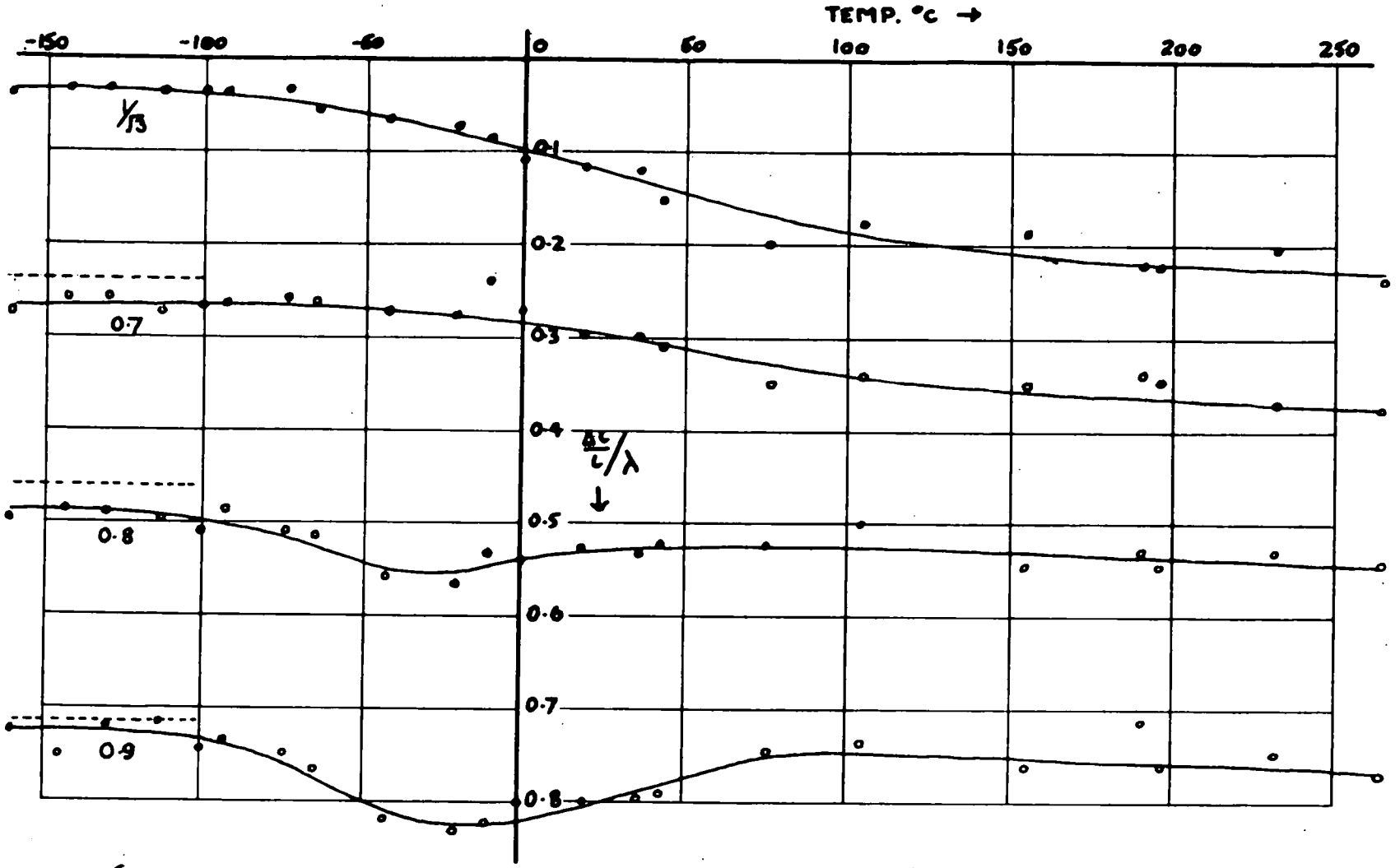

FIG. 36. - Reduced Magnetostriction : Temperature. [100] direction.
Fixed values of reduced magnetization shown on left.

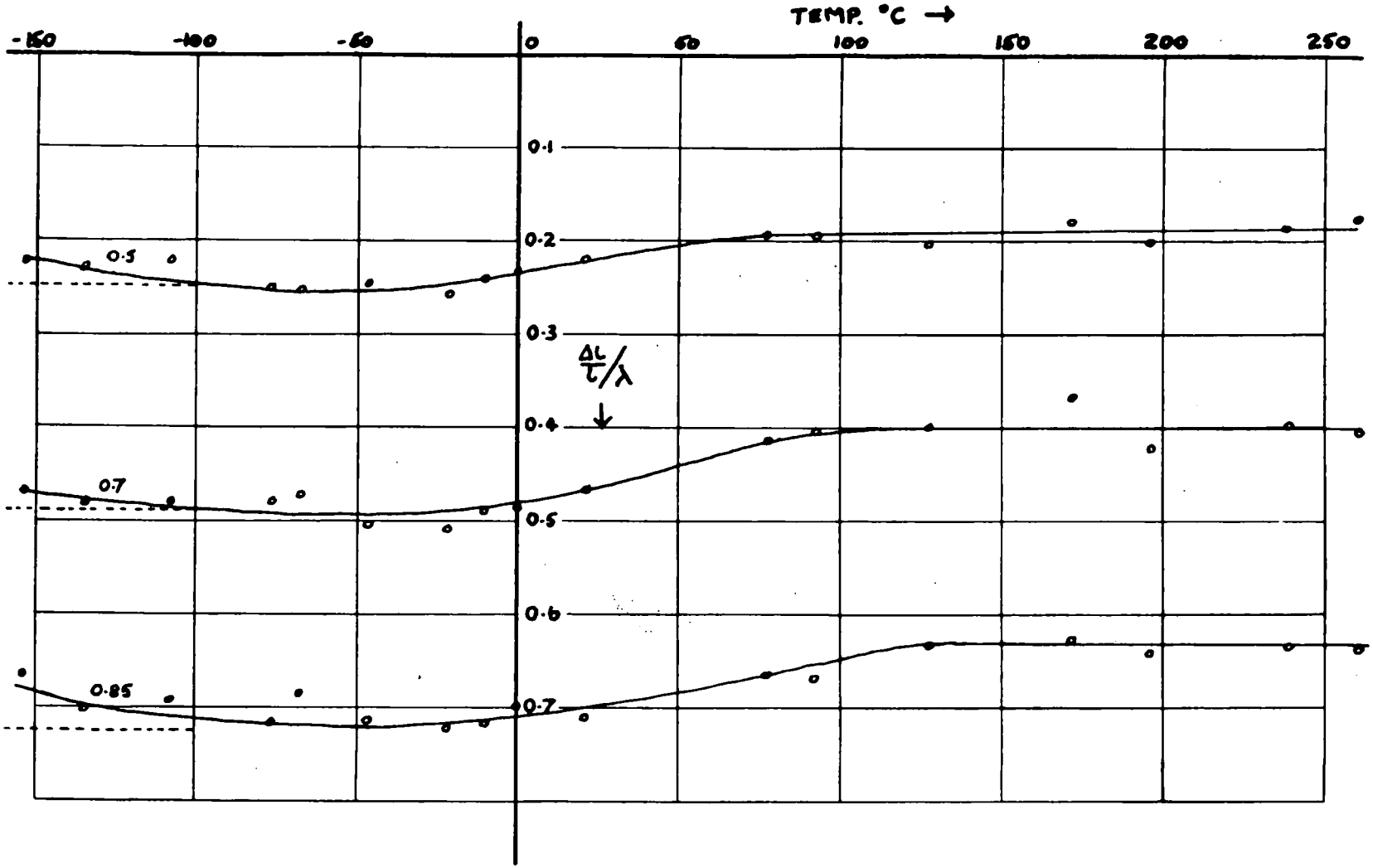

FIG. 37. – Reduced Magnetostriction : Temperature. [111] direction.
Fixed values of reduced magnetization shown on left.

extrapolating the curve of $\Delta l/l$ against I for the low temperature [100] measurements, a value of $\Delta l/l$ corresponding to saturation was obtained. It was estimated that the values obtained in this way are accurate to better than 5%.

The graphs shown in figs. (33) and (34), although valuable, are difficult to interpret. This is because there are variations of saturation magnetostriction and of the shape of the $\Delta l/l$ - I curve which both affect the shape of the $\Delta l/l$ - T curves for constant I. The variation of saturation magnetostriction is readily seen in these graphs, and it remains to show the variation of shape of the $\Delta l/l$ - I curves more effectively.

Certain values of I/I_s were chosen (I_s being the saturation magnetization), and for each of the temperatures at which a full set of $\Delta l/l$ measurements was taken, the corresponding values of I were calculated. For each of these the value of $\Delta l/l$ was read off from the graph of $\Delta l/l$ against I, and from this the corresponding value of $(\Delta l/l)/\lambda$ was calculated, λ being the saturation magnetostriction. Figs. (36) and (37) show graphs of $(\Delta l/l)/\lambda$ for fixed values of I/I_s plotted against temperature. The dotted lines on the left of these graphs indicate the values of $(\Delta l/l)/\lambda$ according to the Heisenberg theory (equations 9 and 10 of section 1.4), to which the experimental values seem to be tending at low temperatures. These curves give a representation of the variation of the shape of graphs such as in figs. (30), (31)

and (32) as the temperature is changed. Together with the graph of saturation magnetostriction shown in fig. (35) they summarize the measurements of magnetostriction over the whole range of temperature.

Measurements were also made of hysteresis effects at room temperature. Due to the limitations of the method used for measuring intensity of magnetization, no consistent and significant results could be obtained of hysteresis of this parameter. The main reason for this is that the demagnetizing field has far more influence on the intensity of magnetization for low applied fields than has the true field in the specimen. It was estimated that the coercive field in the specimens could not be greater than 1.5 oersteds. Because of this, the values of $\Delta l/l$ are quoted corresponding to certain values of the applied field, and not to the true field or to I.

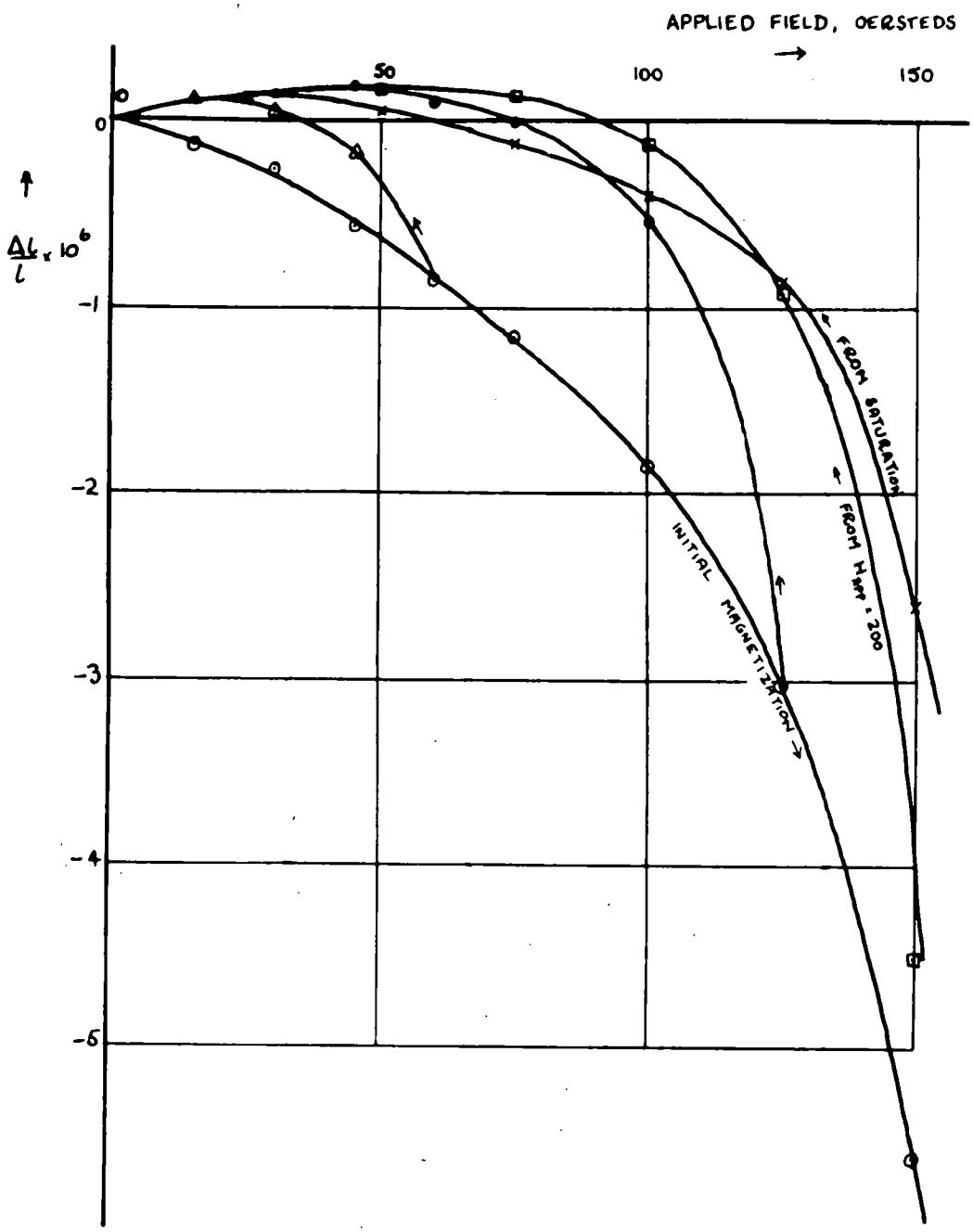

FIG. 38. - Hystersis effects in the [100] direction.

TABLE 14.

Hysteresis effect. [100] specimen. Temperature 16° C.

$H_{APP.}$	$10^6 \times \Delta l/l$, negative unless otherwise shown.				
0	0				
15	-0.11				
30	0.25				
45	0.56				
60	0.84	From Saturation			
75	1.15				
100	1.85				
125	3.02				
150	5.6				
200	16.1				
250		-15.7			
200		8.9	-16.1		
175		5.8	10.6		
150		2.6	4.5		
125		0.84	0.92	-3.02	
100		0.39	0.11	0.53	
75		0.11	+0.14	0	
60				+0.11	-0.84
50		+0.06	+0.17		
45				+0.20	0.17
30				+0.14	+0.06
25		+0.11	+0.11		
15				+0.11	+0.11
0		0	0	0	0

Table 14 and fig. (38) show results obtained with the [100] specimen. If the applied field is increased to not more than 200 oersteds, then the $\Delta l/l$ - H curves for the return to zero field all lie within the same envelope, and all pass through the origin. If the specimen is taken to saturation, then the return curve is different from those for lower maximum fields, and evidently some different domain pattern must be present, although the specimen returns to the same length which it had

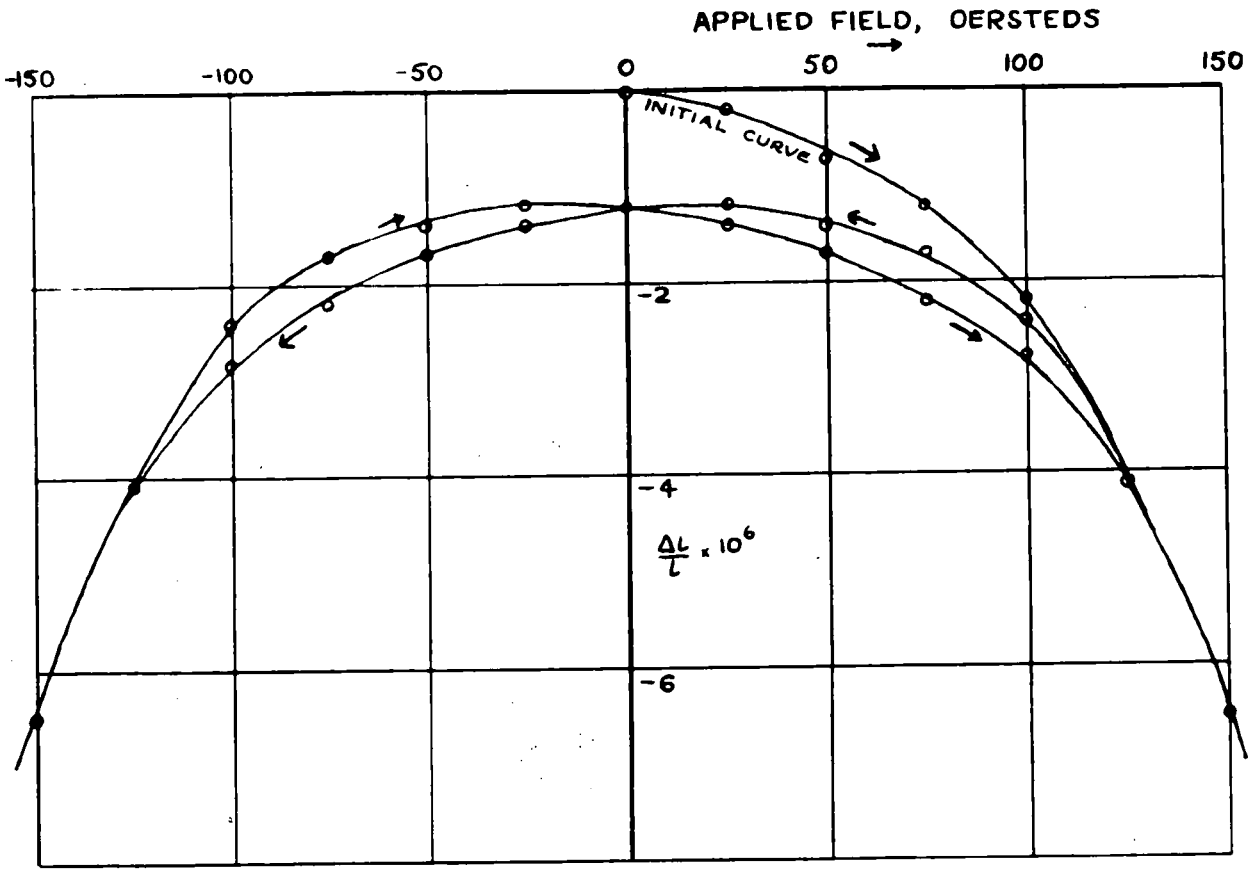

FIG. 39. – Hysteresis effects in the [111] direction.

in the initial demagnetized state. If the applied field is reduced to zero, and then re-applied in either direction, the magnetization curve corresponds to the curve found on initially magnetizing from the reference state.

TABLE 15.

Hysteresis effect. [111] specimen. Temperature 14.5° C.

H_{app}	$-\Delta l/l \times 10^6$		
	Initial	Repeated	
		Increase	Decrease
0	0	1.2	1.2
25	0.2	1.4	1.2
50	0.7	1.7	1.4
75	1.2	2.2	1.7
100	2.2	2.8	2.4
125	4.1	4.1	4.1
150	6.5	6.5	6.5

Table 15 and fig. (39) show results obtained at room temperature with the [111] specimen. It will be seen that in the state of zero applied field the specimen does not return to the same length as it had in the initial state. At field strengths greater than those shown in fig. (39), there was no detectable difference between the initial magnetization curve and those of the repeated curves. It may be remarked that because of the high susceptibility of the [111] specimen, and the consequent very small true fields corresponding to the

fields shown in fig. (39), the applied field is very nearly proportional to the intensity of magnetization, and the curves shown in fig. (39) do in fact correspond with the $\Delta l/l$ - I curves found for other materials by a number of workers, for example Masiyama (1937).

It is important that an estimate should be made of the probable accuracy of the results quoted in this section. A distinction must be drawn between the probable absolute accuracy of the complete set of measurements, and the accuracy of one measurement relative to another. The latter was readily checked by repeating measurements after the apparatus had been stripped and re-assembled. These showed that measurements of saturation magnetostriction were reproduceable to within 1% of the value at room temperature. The magnetostriction values corresponding to intermediate values of the magnetization were not reproduceable to this accuracy, and the scatter in these is within 5% of the saturation value at room temperature.

The absolute accuracy is not easy to estimate. An uncertainty in the effective length of the specimen for magnetostriction measurements, and in the angles between the crystallographic axis, the ellipsoid axis, and the solenoid axis, together with possible errors associated with the calibration beam, cause an uncertainty of not more than 5% in the absolute values. This is uncertainty in the measured change in length. Due to the demagnetized state being taken

as the reference state, there is also some uncertainty in the magnetostriction constants deduced from these measurements, and this will be discussed in the next section.

3.2 DISCUSSION OF RESULTS.

THE λ - T RELATIONSHIP.

From the graphs in fig. (35) it is at once apparent that the λ - T relationship for the two directions is of different form, and therefore that the $\lambda : I_s^2$ law found by Döring (1936) cannot in general apply to single crystal measurements. The probability that the $\lambda : I_s^2$ proportionality was fortuitous was already indicated by Takaki's measurements on iron, which showed no simple relationship between λ and I_s.

In fig. (40) is shown a graph of λ / λ_o plotted against $(I_s/I_{so})^2$, λ_o and I_{so} being the values of λ and I_s at 0° C. If the Döring relationship had held, the experimental points would have fallen on the dotted line corresponding to $\lambda/\lambda_o = (I_s/I_{so})^2$. The results for both crystallographic directions are significantly different from the dotted line. An interesting point to note is that if the polycrystalline magnetostriction is calculated from the formula

$$\lambda_{POLY} = \frac{2}{5}\lambda_{100} + \frac{3}{5}\lambda_{111}$$

as derived by Becker, then over the range of $(I_s/I_{so})^2$ from 0.7 to I.0, the polycrystalline magnetostriction is found to

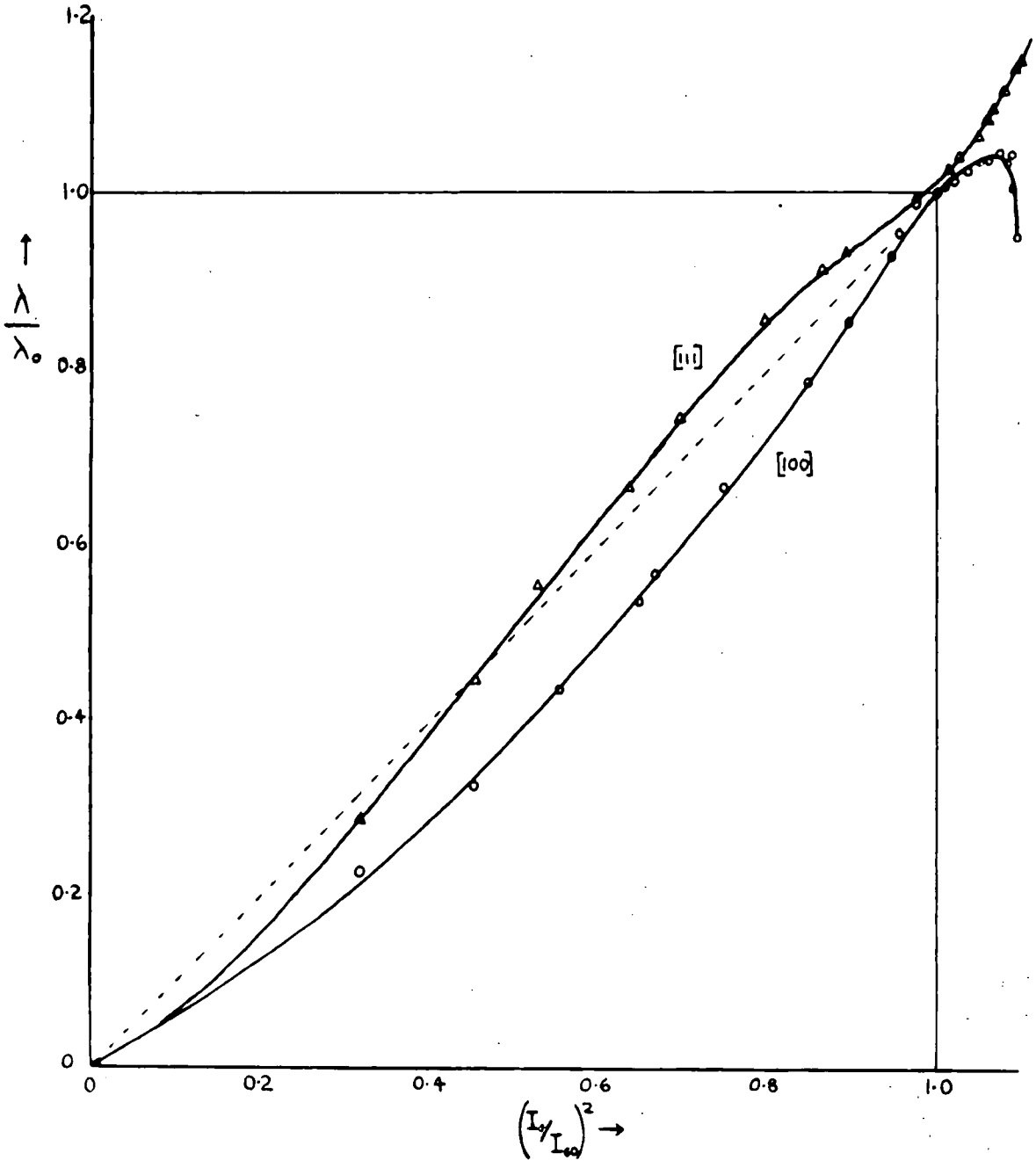

FIG.40. - Saturation Magnetostriction as a function of Saturation Magnetization. Both parameters reduced taking values at 0°C as standard.

be proportional to I_s^2, the curve lying near the dotted line of fig. (40). Below this range, the curve departs significantly from the dotted line. Doring found proportionality to I_s^2 over a greater range than this, and the calculated polycrystalline magnetostriction agrees much better with the measurements of Kirkham (1937).

The points plotted in fig. (40) are all experimental apart from those corresponding to $(I_s/I_{so})^2 = 0.32$. These are for 300° C. and are taken from the smooth curves plotted through experimental points on the λ - T and I_s - T graphs. It was considered unwise to use values found at temperatures above 300° C., since small errors in temperature measurements cause large errors in the corresponding values of λ and I_s deduced from the λ - T and I_s - T curves. The values of the Curie temperature found by the four different series of measurements are shown below.

[111] magnetostriction, 353° C.
[100] magnetostriction, 354° C.
[111] magnetization, 358° C.
[100] magnetization, 359° C.

The scatter in the experimental points is not more than 2° C. near the Curie temperature, and the difference in temperatures deduced from magnetostriction falling to zero and magnetization falling to zero is therefore more than could be accounted for by random error. The probable explanation is that the temperature distribution around the specimen was

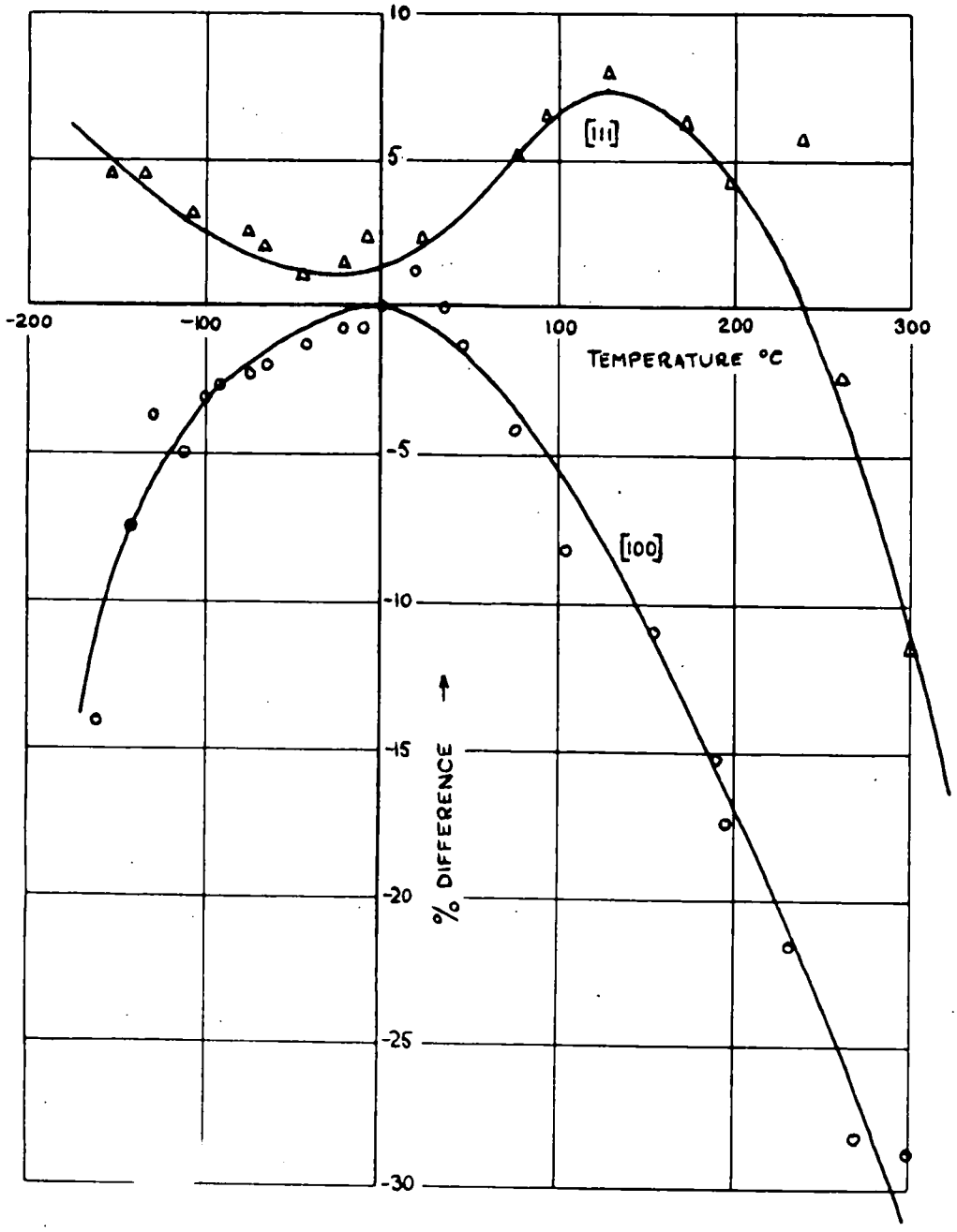

FIG.41. - Departure of Saturation Magnetostriction from proportionality to I_s^2.

different in the two series of measurements, and that the thermocouple temperature was not exactly the same as the specimen temperature. The error here is likely to be larger in the magnetization measurements than in the magnetostriction ones, since in the former the metallic thimble surrounding the specimen had no good thermal contact with bodies at room temperature, whereas in the magnetization measurements the O B.A. brass rod supporting the aluminium former formed a path along which heat could flow away from the specimen and the former.

It may be mentioned here that in neither the magnetization nor the magnetostriction measurements was there any indication of the curve tailing away as it approached the Curie temperature; on the contrary in both cases it cut the temperature axis very sharply, and at higher temperatures neither magnetostriction nor magnetization could be detected.

The results shown in fig. (40) are plotted in a different way in fig. (41). This shows $\left[\lambda/\lambda_o - \left(I_s/I_{so}\right)^2\right] \Big/ \left(I_s/I_{so}\right)^2$ expressed as a percentage, and plotted against the corresponding value of the temperature. No significance should be attached to the fact that the [111] curve does not pass through the origin; this is because although the experimental values at 0° C. on which the results were calculated do in fact give a point on the origin, the scatter of the points of which this is one is sufficiently large to make the curve lie well off.

These curves allow the points at the top end of fig. (40) to be spread out over a wider range, and they indicate more clearly the departure from the proportionality to I_s^2.

It has not been possible to find a law governing the relationship between λ and I_s, neither has a satisfactory theory been advanced to explain the fundamental mechanism of magnetostriction, and it is therefore difficult to draw any useful conclusions from the λ - T curves of fig. (35). Corresponding to a change in temperature there are changes in magnetization, lattice constant, anisotropy, elastic moduli, and almost every other physical property associated with a solid, and it appears to be impossible to separate the different effects that each of these has on the magnetostriction.

MAGNETOSTRICTION BELOW SATURATION.

The magnetization-magnetostriction relationships in the principle crystallographic directions below saturation have been calculated theoretically by Heisenberg, and the equations obtained are given in section 1.4. The relationships are based on the assumption that the anisotropy energy is sufficiently large to cause all the domain boundary movement to occur before any rotation of the direction of magnetization. Thus it would be expected that the experimental measurements would best agree with the theory at temperatures at which the anisotropy is greatest, which for nickel are the lowest temperatures. That this is so is clearly indicated in figs.

(36) and (37) where the dotted lines indicate the values of $(\Delta l/l)/\lambda$ calculated from, the Heisenberg theory.

In the [100] direction the theory predicts a zero length change when the magnetization increases from 0 to $I_s/\sqrt{3}$, corresponding to boundary wall movement or change from one easy direction to another, followed by a length change due to the rotation from the four easy directions nearest the [100] to the [100] direction. There should therefore be a sharp kink in the $\Delta l/l$: I curve at $I/I_s = 1/\sqrt{3}$. Fig. (30) shows that this kink is not obtained, but that there is a very sharp curve at approximately the correct position, and that the general agreement between theory and experiment is good.

The gradual transition from the sharp to the smooth curve as the temperature is raised is shown by figs. (30) and (31), and is reflected in the graph of fig. (36). This may be accounted for by the decrease of anisotropy energy which makes the domain configuration less dependent on the anisotropy energy and more on the energy due to the random strains and inclusions, boundary walls, and the demagnetizing field of the whole specimen. The depressions in the $I/I_s = 0.8$ and $I/I_s = 0.9$ curves at about -30° C. are a reflection of the tendency found in the range -70° C. to 50° C. for the $\Delta l/l$ - I curves to tail off near saturation as shown in fig. (30) for 0° C. These depressions are certainly significant; the scatter of points does not allow them to be removed and the scatter of points on the I - H_{App} graph from which the I values were deduced

is very small, so that little error arises in the deduction of values of I corresponding to values of the applied field.

In the [111] direction the curves seem to agree with their calculated values according to the Heisenberg theory at about -75° C., but to fall away again at lower temperatures. It will be seen from figs. (36) and (37) that in the [111] direction the experimental results are never greater than the theoretical while in the [100] direction they are never less than the theoretical. In the [100] case this is readily accounted for by the assumption that rotations are taking place before all the boundary movements are completed. However, in the [111], the reason for the departure is not easy to find since in this direction there is only movement from one easy direction to another, and no rotation. It is likely, however, that in the [111] direction the initial domain distribution does not agree with that assumed theoretically to the same degree of accuracy that it does in the [100] direction. This is because in the [111], magnetization is always along an easy direction, and apart from the effect of the demagnetizing field there is little tendency for the magnetization direction to depart from the ellipsoid axis direction in the demagnetized state. In the [100] specimen the 8 directions of easy magnetization are all equally directed with respect to the specimen axis, and therefore in the demagnetized state the chance of a domain being magnetized along any one of them is equal. This idea is supported by the measurements of hysteresis

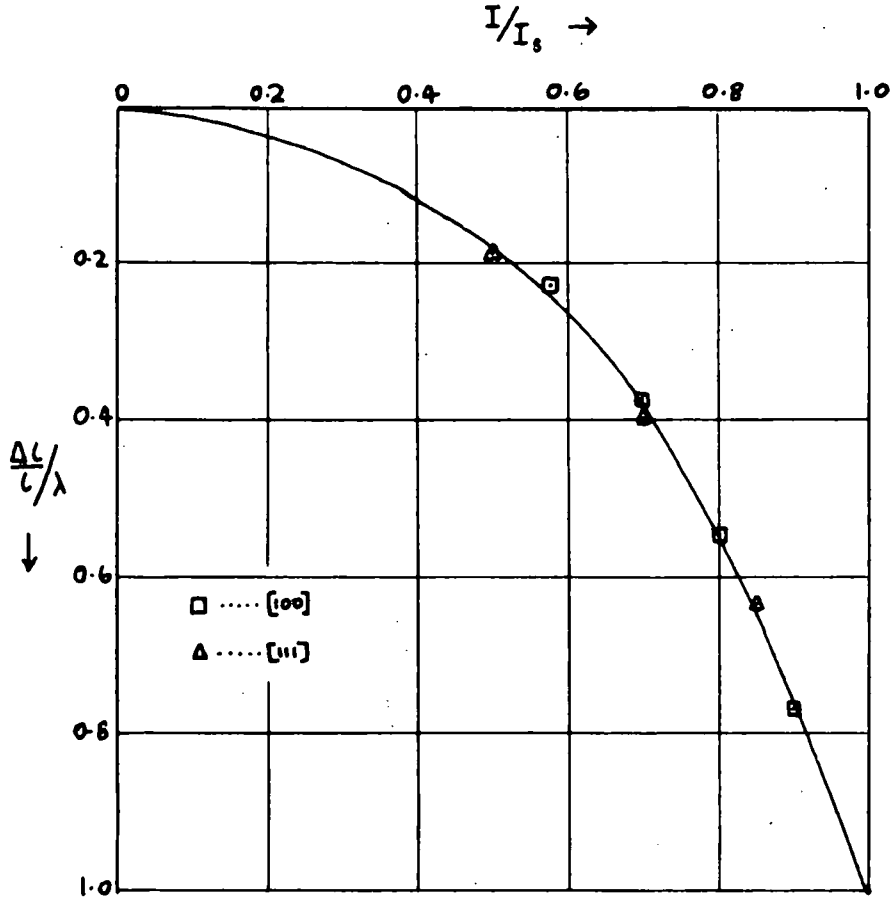

FIG.42. - Reduced Magnetostriction : Reduced Magnetization at 260°C.

at room temperatures which will be discussed later.

The experiments of Honda, Masumoto and Shirakawa (1935) show that at high temperatures there is little difference between the magnetization curves in different directions, but that the [110] is probably the direction of easy magnetization. However, since the anisotropy energy is so small, it is probable that the domain pattern is highly dependent on strains and on the specimen shape. The values of $(\Delta l/l)/\lambda$ corresponding to a temperature of 260° C. have been obtained from the smooth curves of figs. (36) and (37), and have been plotted in fig. (42). The agreement between the values obtained for the [111] and the [100] directions is remarkable. Although it is not impossible that this agreement is fortuitous, the accuracy with which both sets of points fit the smooth curve is very high, and the possibility of a chance agreement of such accuracy is remote. It is not clear why there should be the same law governing magnetostriction in both directions, for even on the assumption that at 260° C. the crystal has become magnetically isotropic, the very fact that the saturation magnetostriction in one direction is different to that in another is bound to cause different domain distributions in the two specimens. Unfortunately the mathematical equation governing the curve of fig. (42) cannot be found with any degree of certainty. Equations of the form $y = ax^2 + bx3$ and $y = ax^2 + bx^4$ can both be fitted to the curve to within the accuracy of the experimental results, and no simple mathematical

relationship other than a power law could be found which would fit the curve.

HYSTERESIS MEASUREMENTS AT ROOM TEMPERATURE.

Comparison of the magnetostriction hysteresis graphs shown in figs. (38) and (39) immediately shows one significant difference between the results obtained for the different crystallographic directions, for in the [100] direction the specimen always returns to its original length when the applied field is reduced to zero. This is probably a result of the equivalence of the 8 easy directions with respect to the direction of the applied field, as was suggested previously. The reference state is therefore almost certainly the state in which the domain directions are equally along the 8 easy directions. In the [111] direction the reference state can only be reached by continually reversing the applied field while its magnitude is gradually reduced to zero. It is probable that after a field has been applied and then reduced to zero, there is a higher proportion of the specimen magnetized in the direction of the applied field or the opposite direction than in the six other easy directions. This condition may also apply to a lesser degree in the reference state.

The hysteresis effect in both cases must be an indication that the magnetization process is not reversible. This is probably due to strains and inclusions impeding the movement

of boundary walls and thereby causing the domain configuration corresponding to increasing and decreasing applied fields to be different. The fact that the magnetostriction curves for repeated magnetizations are thus affected makes it almost certain that the initial magnetostriction is affected to some extent. It would have been desirable to carry out these measurements at low temperatures, where the increased anisotropy might be expected to reduce the hysteresis effect by making the domain configuration less dependent on strains. Unfortunately the hysteresis effects were of such small magnitude that reproduceable results could only be obtained in very steady conditions, and these conditions could not be established at other than room temperature.

CONCLUSIONS.

The results obtained indicate that at low temperatures the magnetostriction below saturation of the nickel crystal corresponded to the values predicted by Heisenberg's theory, and that with increasing temperature there was a steady departure from the theoretical values. The saturation magnetostriction depended on temperature in a way which did not correspond to any known theory.

APPENDIX.

THE FLUX LINKAGE OF THE SPECIMEN AND THE SEARCH COIL.

An expression for the flux-linkage with a search coil produced by a uniformly magnetized ellipsoid has been derived in a paper by the author (1954).

If the surface of the ellipsoidal specimen is expressed by the equation

$$\frac{x^2}{a^2} + \frac{y^2+z^2}{b^2} = 1 \quad , \quad \text{or} \quad x^2 + \frac{y^2+z^2}{1-e^2} = a^2$$

then a confocal ellipsoid is

$$\frac{x^2}{t^2} + \frac{y^2+z^2}{t^2-1} = a^2e^2$$

The flux through a loop whose axis coincides with $y = z = 0$, and points on which are defined by (x,t), is then

$$F = \pi y^2 H + \pi y^2 . 4\pi I \left(\frac{1-e^2}{e}\right)\left(\frac{t}{t^2-1} - \coth^{-1} t\right) \qquad (24)$$

where I is the intensity of magnetization of the specimen, H is the applied field. For a flux coil of finite size, this expression must be integrated with respect to x and y. In the general case the integral has not yet been solved, so a method of approximation has been developed applicable only when the search coil is less than half the ellipsoid length.

Then, for a search coil of n_1 turns per unit length, n_2 layers per unit length, internal radius r_1, external radius r_2, and length $2l$ placed symmetrically round the specimen, the flux linkage is

$$K = n_1 n_2 \int_{-l}^{l}\int_{r_1}^{r_2} F\,dx\,dy$$

$$= \pi H n_1 n_2 2l\left(\frac{r_2^3 - r_1^3}{3}\right) + 8\pi^2 b^2 I l n_1 n_2 a\left[L + M\left(\frac{L}{ae}\right)^2 + N\left(\frac{L}{ae}\right)^6\right]_{y=r_1}^{y=r_2} \qquad (25)$$

where

$$L = \frac{1}{3}\frac{y}{ae}\left[1+\left(y/ae\right)^2\right]^{1/2} + \frac{2}{3}\sinh^{-1}\left(y/ae\right) - \frac{1}{3}\left(y/ae\right)^3 \operatorname{cosech}^{-1}\left(y/ae\right)$$

$$M = \frac{-y/ae}{3\left[1+\left(y/ae\right)^2\right]^{1/2}}$$

$$N = \frac{2}{105}\left(\frac{y/ae}{\left[1+\left(y/ae\right)^2\right]^{1/2}}\right)\left(\frac{3}{\left[1+\left(y/ae\right)^2\right]^2} + \frac{4}{1+\left(y/ae\right)^2} + 8\right)$$

Suppose the search coil is now connected to a fluxmeter whose throw is proportional to the flux change through the coil. A throw Δ_H is produced by establishing a field H without the specimen in the coil, and a throw Δ_I by establishing an intensity I in the specimen with the field throw compensated.

Then

$$\frac{\Delta_I}{\Delta_H} = \frac{4\pi I}{H}\cdot\frac{3b^2 a}{r_2^3 - r_1^3}\left[L + M\left(\frac{L}{ae}\right)^2 + N\left(\frac{L}{ae}\right)^6\right]_{y=r_1}^{y=r_2} \qquad (26)$$

$$= \frac{4\pi I}{H}\cdot R$$

or

$$I = \frac{H}{4\pi R \Delta_H}\cdot\Delta_I \qquad (27)$$

where R is a dimensionless factor dependent on the shape of the specimens and the search coil.

For the [111] ellipsoid, $R = 0.114_5$, and for the [100], $R = 0.112_5$.

The value of Δ_u/H is obtained by establishing known fields in the solenoid, and noting the galvanometer deflection. This is also used to provide a check that the deflection is linear with flux change. It may be noted that a correction must be applied to deflections greater than 10 cm. to allow for the fact that the deflection on the scale is a measure of $\tan\theta$, not of θ, where θ is the galvanometer deflection.

Corrections must also be applied to the deflections to allow for thermal expansion of the flux coil and the specimen. The flux coil expansion makes the compensating flux change produced by the mutual inductance no longer equal and opposite to the flux change due to the applied field. The theoretical difference is 0.5% of the field deflection per 100° C.; this was verified experimentally. The flux coil expansion makes negligible difference to the linkage with the intensity of magnetization of the specimen. Expansion of the specimen causes an additional throw of 0.5% per 100° C.

Allowance having been made for these effects, the values of the intensity of magnetization corresponding to unit deflection are given by:

For the [111] specimen, I = 27.3 c.g.s. units per cm.

For the [100] specimen, I = 27.7 .....

REFERENCES.

Akulov, 1928	Z.Physik, 52, p.389.
Bates and Wilson, 1953	Proc.Phys.Soc.A, 64, p.691.
Becker, 1934	Z.Physik, 87, p.547.
Becker and Döring, 1939	Ferromagnetismus, Springer, Berlin.
Bitter, 1937	Introduction to Ferromagnetism, McGraw Hill, New York.
Bozorth and Hamming, 1953	Phys.Rev. 89, p.865.
Brown, 1953	Rev.mod.Phys. 25, p.131.
Döring, 1936	Z.Physik, 103, p.560
Farmer and Glaysher, 1953	J.sci.Instrum. 30, p.9.
Fowler, 1936	Statistical Mechanics, 2nd. Ed. Cambridge Univ. Press.
Heddle, 1952	Brit.J.appl.Phys. 3, p.95.
Heisenberg, 1928	Z.Physik, 49, p.619.
Honda, Masumoto and Shirakawa, 1935	Sci.Rep.Tôhoku Univ. 24, p.291.
Honda and Shimizu, 1903	Phil.Mag.(6), 6, p.392.
Hunt, 1954	Brit.J.appl.Phys. 5 (to be published)
Joule, 1847	Phil.Mag.(3), 30, pp.76,225.
Kaya, 1928	Sci.Rep.Tôhoku Univ. 17, p.639
Kaya and Takaki, 1936	Sci.Rep.Tôhoku Univ. Anniversary Volume, p.314.
Kirkham, 1937	Phys.Rev. 52, p.1162.
Kittel, 1949	Rev.mod.Phys. 21, p.541.
Langevin, 1905	Ann.Chim.Phys. 5, p.70.

Lawton and Stewart, 1948	Proc.Roy.Soc.A, 193, p.72.
Lee, 1953	Science Progress, 41, p.58.
Masiyama, 1928	Sci.Rep.Tôhoku Univ. 17, p.945.
1937	Sci.Rep.Tôhoku Univ. 26, pp.1,65.
Mason, 1951	Phys.Rev. 82, p.715.
Masumoto, 1927	Sci.Rep.Tôhoku Univ. 16, p.333.
Néel, 1932	Ann.Phys.(Paris),(10), 17, p.5.
1934	J.Phys.Radium, 5, p.104.
1944	J.Phys.Radium, 5, p.241.
Pearson, 1953	Brit.J.appl.Phys. 4, p.342.
Schulze, 1927	Z.tech.Physik, 8, p.495.
1928	Z.Physik, 50, p.448.
1931	Ann.Phys.(Leipzig), 11, p.937.
1933	Z.Physik, 82, p.674.
Stoner, 1933	Phil.Mag.(7), 15, p.1018.
1948	Rep.Progr.Phys. 11, p.43.
1950	Rep.Progr.Phys. 13, p.83.
Sucksmith, 1950	E.R.A.Technical Report N/T51.
Takaki, 1937	Z.Physik, 105, p.92.
Van Vleck, 1937	Phys.Rev. 52, p.1178.
Webster, 1925	Proc.Roy.Soc. 107, p.496.
Weiss, 1907	J.de Phys. 6, p.667.
Weiss, 1948	Phys.Rev. 74, p.1493.
Whiddington, 1920	Phil.Mag.(6), 40, p.634.